MOLECULAR GENETIC ANALYSIS OF LATTICE AND GRANULAR CORNEAL DYSTROPHIES IN INDIAN PATIENTS

Thesis submitted for the degree of
Doctor Of Philosophy

To

THE DEPARTMENT OF BIOCHEMISTRY
SCHOOL OF LIFE SCIENCES
UNIVERSITY OF HYDERABAD
HYDERABAD – 500 046
INDIA

By

S.V.V. Kalyana Chakravarthi
Hyderabad Eye Research Foundation
L. V. Prasad Eye Institute
Hyderabad – 500 034

SEPTEMBER 2008
Enrolment No: 02LBPH05

Dedicated to

Annayya

UNIVERSITY OF HYDERABAD

School of Life Sciences

Department of Biochemistry

Hyderabad - 500 046 (India)

DECLARATION

The research work embodied in this thesis entitled, "**Molecular Genetic Analysis Of Lattice And Granular corneal Dystrophies In Indian Patients**", has been carried out by me at the L V. Prasad Eye Institute, Hyderabad, under the guidance of **Dr. Chitra Kannabiran** and Prof. T. Suryanarayana I hereby declare that this work is original and has not been submitted in part or full for any other degree or diploma of any other university.

S.V.V. Kalyana Chakravarthi

Dr. Chitra Kannabiran

Supervisor,
Kallam Anji Reddy Molecular Genetics Lab,
L. V. Prasad Eye Institute,
Hyderabad.

Prof. T. Suryanarayana

Co-supervisor,
Department of Biochemistry,
School of Life Sciences,
University of Hyderabad.

UNIVERSITY OF HYDERABAD

School of Life Sciences

Department of Biochemistry

Hyderabad - 500 046 (India)

CERTIFICATE

This is to certify that this thesis entitled, **"Molecular Genetic Analysis Of Lattice And Granular Corneal Dystrophies In Indian Patients"** for the degree of **Doctor of Philosophy** to the University of Hyderabad is based on the work carried out by **S.V.V.Kalyana Chakravarthi** at the L. V. Prasad Eye Institute, Hyderabad, under our supervision. This work has not been submitted for any diploma or degree of any other University or Institution

Dr. Chitra Kannabiran

Supervisor,
Kallam Anji Reddy Molecular Genetics Lab,
L. V Prasad Eye Institute,
Hyderabad

Prof. T. Suryanarayana

Co-supervisor,
Department of Biochemistry,
School of Life Sciences,
University of Hyderabad

Head,
Department of Biochemistry,
School of Life Sciences,
University of Hyderabad.

HEAD
Dept. of Biochemistry
School of Life Science

06/09/08

Dean,
School of life sciences,
University of Hyderabad.

Dean, School of Life Science,
University of Hyderabad
Hyderabad - 500 046. (India)

06/09/08

Words cannot express my gratitude to ***Dr. Chitra Kannabiran****. I express my heartfelt thanks for her guidance and care which helped me develop professionally and personally. She paved the way for my scientific career with her valuable suggestions. I express my heartfelt thanks for her support in all high and low times.*

I extend my heartfelt gratitude to ***Prof. D. Balasubramanian*** *for his unconditional support throughout my stay at L.V. Prasad Eye Institute.*

I am thankful to ***Prof. T. Suryanarayana*** *Department of Biochemistry, School of Life Sciences, University of Hyderabad, for having agreed to be my co-supervisor.*

I would like to specially thank ***Dr. G. N. Rao*** *Chairman, L.V. Prasad Eye Institute for allowing me to work with a great organization. He has been a great source of inspiration to me.*

My special thanks to ***Dr. Geeta K. Vemuganti*** *for helping me with the histopathology portion of my work, and in general for her constant encouragement and excellent advice.*

I am very thankful to cornea consultant ***Dr. M. S. Sridhar*** *for helping me in the enrollment of patients for the present study and also for helping me to understand the clinical aspects of corneal dystrophies.*

My sincere thanks to ***Dr.Subhabrata Chakrabarti, Dr. Inderjeet Kaur*** *and* ***Dr. Yashoda Ghanekar*** *for their valuable suggestions.*

I thank CSIR for providing me the fellowship, which made my studies possible.

I thank my seniors ***Bindu*** *for his suggestion which has showed me an opportunity to work with* ***Dr. Chitra Kannabiran*** *and* ***Saroj*** *who helped me in learning techniques and good laboratory practices,* ***Geeta, Neeraja,*** *my friends* ***Ramakrishna*** *and* ***Kishore*** *who were with me during my initial days of Ph.D.*

My heartfelt thanks to my friends ***Purshotham, Venu, Soundarya, Rajeshwari, Afia, Kiran,***

CONTENTS

support. My Special thanks to all my colleagues: ***Aparna, Avid, Joveeta, Madhavi, Surya, Naresh, Sankarathi, Saritha, Nageshwar Rao, Subhash, Vidya*** *and* ***Gnaneswar.***

My special thanks to ***Smitha*** *and my friends from the University of Hyderabad*

I thank ***Ganesh, Uma, Elizabeth*** *for their help at various stages. I thank* ***Naidu*** *and* ***Sridhar*** *for their professional and personal help. I thank staff of library especially* ***Banu*** *for her support during the time of writing thesis.*

I thank staff of clinical biochemistry for helping me in collecting the blood samples. I acknowledge the help received from ***Jobi, Jagdeesh, Srinivas*** *and other staff of MRD for giving me the medical records whenever I requested.*

I thank the ISD staff for their help especially ***Koteswara Rao, Kumar, Srikanth*** *and* ***Siva*** *for helping me through many difficult situations. I acknowledge the help received from staff of LVPEI.*

I thank Mr. Mubarak Ali for providing cell lines in necessity.

It would be meaningless if I forget the support received from my ***Pedamma, Pednanna, Pinni, Babai*** *and* ***my parents,*** *without their help it would have been impossible for me to reach this stage. My Brother* ***Mahipal*** *and sister-in-law* ***Daranija*** *have always been my source of strength and encouragement and supported me a lot during all my endeavors.*

I will be failing if I don't acknowledge the support received from my wife, ***Sirisha.*** *She was there with me to bear my tantrums and temperaments with a great patience. I thank her, her parents and family members wholeheartedly for their support and encouragement.*

CONTENTS

*support. My Special thanks to all my colleagues: **Aparna**, **Avid**, **Joveeta**, **Madhavi**, **Surya**, **Naresh**, **Sankarathi**, **Saritha**, **Nageshwar Rao**, **Subhash**, **Vidya** and **Gnaneswar**.*

*My special thanks to **Smitha** and my friends from the University of Hyderabad*

*I thank **Ganesh**, **Uma**, **Elizabeth** for their help at various stages. I thank **Naidu** and **Sridhar** for their professional and personal help. I thank staff of library especially **Banu** for her support during the time of writing thesis.*

*I thank staff of clinical biochemistry for helping me in collecting the blood samples. I acknowledge the help received from **Jobi**, **Jagdeesh**, **Srinivas** and other staff of MRD for giving me the medical records whenever I requested.*

*I thank the ISD staff for their help especially **Koteswara Rao**, **Kumar**, **Srikanth** and **Siva** for helping me through many difficult situations. I acknowledge the help received from staff of LVPEI.*

I thank Mr. Mubarak Ali for providing cell lines in necessity.

*It would be meaningless if I forget the support received from my **Pedamma**, **Pednanna**, **Pinni**, **Babai** and **my parents**, without their help it would have been impossible for me to reach this stage. My Brother **Mahipal** and sister-in-law **Daranija** have always been my source of strength and encouragement and supported me a lot during all my endeavors.*

*I will be failing if I don't acknowledge the support received from my wife, **Sirisha**. She was there with me to bear my tantrums and temperaments with a great patience. I thank her, her parents and family members wholeheartedly for their support and encouragement.*

CONTENTS

Chapter 1
Introduction
&
Literature Review

1.0 INTRODUCTION AND LITERATURE REVIEW

1.1 Anatomy of the cornea

The cornea is a clear tissue present at the front of the eye as shown in Figure 1.1. It provides 85% of the refractive power of the eye. It is approximately half a millimeter (550 microns) thick and has a diameter of 12 mm. The adult human cornea measures 11 to 12 mm horizontally and 9 to 11 mm vertically. The thickness of the cornea increases from center to periphery where it is about 0.7 mm thick. It is made up of tissue similar to that of the sclera but it has no blood vessels. Absence of blood vessels and orderly arrangement of collagen fibers are responsible for corneal transparency. The mean diameter of collagen fibers and the mean distance between the collagen fibers are less than half of the wavelength of visible light (400-700 nm). Due to this orderly arrangement, the scattering of incident light by one collagen fiber is canceled by the interference from the other which allows light to pass through the cornea. The cornea consists of 3 main and 2 auxiliary layers as shown in Figure 1.2. The main layers from the surface to the inner eye are epithelium, stroma and endothelium. Bowman's membrane lies between the epithelium and the stroma and the Descemet's membrane is between the stroma and the endothelium.

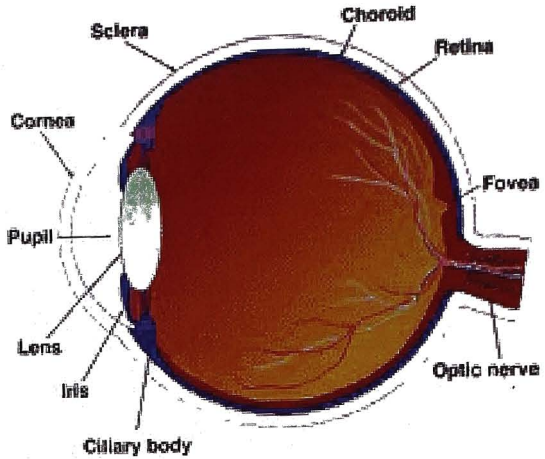

Figure 1.1: The anatomy of the human eye and major parts of the eye (www nasa gov/ . /22oct_cataracts html web site)

1.1.1 Epithelium

The corneal epithelium consists of 5-6 layers of cells (Fig 1.2), of approximately 50 μm thickness. The epithelium has three different cell types, superficial cells (2-3 layers), wing cells (2-3 layers) and a monolayer of columnar basal cells. The columnar basal cell layer helps in attaching to the Bowman's layer through numerous junctional complexes. The superficial cells are flat and polygonal in shape with a diameter of 40-60 μm and a thickness of 2-6 μm. The surface of superficial cells is covered with microvilli, which increases the surface area of each cell and helps in active uptake of oxygen and nutrients from the tear fluid. Two types of the superficial cells, large dark cells (matured) and small light cells (younger) were identified by electron microscopy studies on rabbit and cat

corneas [Pfister *et al.,* 1973]. The layer of superficial cells is followed by two to three layers of wing cells, which are named, on their characteristic wing shape. The wing cells are in an intermediate state of differentiation between the basal and superficial cells and are rich in intracellular tonofilaments comprised of keratin. Keratin expression is regulated in a manner dependent on the differentiation of corneal epithelial cells [Doran *et al.,* 1980, Sun *et al.,* 1976]. Among all the cells of the corneal epithelium mitotic activity is present only in the basal cells. The basal cells of the corneal epithelium secrete a 40-60 nm thick layer called as basement membrane which is present immediately posterior to corneal epithelium. The basal cells are cuboidal in shape and rest on the basement membrane with the help of hemidesmosomes. Laminins and the type IV collagens are major components of the basement membrane [Berman *et al.,* 1983]. The presence of the basement membrane between the epithelium and Bowman's layer fixes the polarity of epithelial cells. The epithelium together with tear film contributes to maintenance of an optically smooth surface of the cornea and provides a barrier to external biological and chemical insults. The junctions present between the corneal epithelial cells prevent the passage of chemical substances into the deeper layers of the cornea. Different types of intercellular junctions such as tight junctions (between the superficial cells), gap junctions (wing cell layer and basal cell layer), adherens and desmosomes (in all cell layers) are present in the corneal epithelium and participate in the maintenance of cell-cell and cell-matrix interactions.

1.1.2 Basement membrane

The basement membrane is secreted by the basal cells of the epithelium. The basal membrane is an electron-dense layer. It also contains heparin or heparan sulfate proteoglycans and fibrin [Berman *et al.*, 1983] The presence of the basal membrane fixes the polarity of the epithelial cells. The basement membrane provides a matrix on which cells can migrate and is thought to be important for maintenance of the stratified and well-organized corneal epithelium.

1.1.3 Bowman's layer

Bowman's layer is an acellular layer present at the interface between the corneal epithelium and stroma (Fig 1.2). It has a thickness of 12 μm and consists of randomly arranged collagen fibers and proteoglycans The collagen fibers are of type I and type III, synthesized by stromal keratocytes and they appear continuous with those in the stroma.

1.1.4 Stroma

The stroma occupies more than 90% of cornea (Fig 1.2). The anatomical properties of stroma are responsible for corneal strength and transparency. The corneal stroma consists of extracellular matrix, keratocytes (corneal fibroblasts) and nerve fibers. Two to three percent of the stroma is occupied by keratocytes and the remaining consists of collagen and glycosaminoglycans (GAGs). 70% of the corneal dry weight is made of collagen fibers.

The corneal stroma consists of type I, type III, type V, type VI collagens and they are fibers of uniform diameter (22.5–35 nm). The distances between the collagen fibers are highly uniform (41.4 ± 0.5 nm); this regular arrangement is responsible for corneal transparency. Between the collagen fibers various glycosaminoglycans are present. The most available glycosaminoglycan in the corneal stroma is keratan sulfate (65% of total glycosaminoglycan content), the other GAGs are chondroitin sulfate and dermatan sulfate. Glycosaminoglycans play a major role in regulation of hydration by absorbing and retaining water. Expression of integrins in the keratocytes suggests that keratocytes interact with extracellular matrix proteins through the integrin system. Keratocytes are the cellular component of the stroma. They are spindle-shaped cells and have a turnover rate about 2-3 years. They are similar to fibroblasts and possess an extensive intracellular cytoskeleton. The presence of cytoskeleton allows the cells to contract and may be responsible for the maintenance of corneal shape. The shape and function of keratocytes are regulated by the extracellular environment [Nishida *et al.*, 1998, Tomasek *et al.*, 1982].

1.1.5 Descemet's membrane

Descemet's membrane (DM) is a basement membrane of the endothelium, present adjacent to the corneal stroma (Fig 1.2). It is formed by the secretions of the endothelial cells and has a thickness of 3 μm at birth and 10 μm in adulthood. Type IV collagen and laminin are predominant components. Collagen fibers of stroma are continuous with Bowman's membrane but not with

Descemet's cap membrane. Descemet's reflects the changes in the corneal stroma

1.1.6 Endothelium

A single layer of cells which covers the posterior surface of the Descemet's is known as the endothelium (Fig 1.2). The endothelial cells are 5 μm thick and 20 μm wide and are polygonal (mostly hexagonal) in shape. In young adults the endothelial cell density is about 3500 cell/mm^2 [Laule *et al* 1978]. The endothelial cell density decreases with age. The ratio of hexagonal cells to other polygonal cells is termed as hexagonal value Any damage can result in decrease in the hexagonality and increase in variability of the cell area. Deviation from the hexagonality is known as pleomorphism. The anterior surface of the cells is flat and the posterior surface has microvilli and marginal folds. The marginal fold outgrowths increase the surface area, which is in contact with the aqueous humor. The endothelial cells are interdigitate and contain various junctional complexes and gap junctions. Presence of gap junctions help in movement of small molecules and electrolytes between the endothelial cells. Desmosomes are absent in corneal endothelium. The interconnected endothelial cell layer provides a leaky barrier to the aqueous humor. The endothelial cells can proliferate *in vitro* [Nayak *et al.,* 1984], and they cannot proliferate in vivo in humans, monkeys and cats but they divide in rabbits. Any damage to the corneal endothelium leads to stromal or epithelial edema. The most important physiological function of the endothelium is regulation of the water content of the

corneal stroma. The ion transport system of the endothelium counteracts the influx of water into the corneal stroma. Any disorder or disease that can alter the integrity of the corneal layers results in loss of transparency. Loss of corneal transparency in turn results in reduced visual acuity.

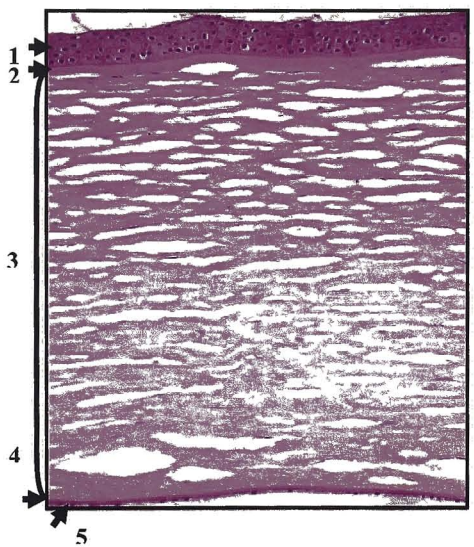

Fig 1.2: Section of normal human cornea (formalin-fixed, paraffin-embedded and stained with PAS Magnification 100X) showing the different layers 1, Epithelium, 2, Bowman's membrane, 3: Stroma, 4 Descemet's membrane, 5 Endothelium. [Picture courtesy of Dr Geeta Kashyap Vemuganti, Ophthalmic Pathology Service, LVPEI, Hyderabad].

1.2 Corneal dystrophies

Corneal dystrophies are rare, progressive, non-inflammatory, generally bilateral disorders involving the formation of opacities in the cornea. Opacities are characterized by the accumulated deposits in some of the dystrophies. On the

basis of the layer involved, they are classified as epithelial dystrophies, stromal dystrophies and endothelial dystrophies. The details of the different epithelial, Bowman's layer, stromal and endothelial dystrophies along with their mode of inheritance are given in Table 1.1.

TABLE 1.1: Corneal Dystrophies.

	Corneal Dystrophy	Inheritance
Epithelial Dystrophies	Epithelial basement membrane dystrophy (map-dot-fingerprint corneal dystrophy	Autosomal Dominant
	Band-shaped, whorled microcystic corneal dystrophy	X Linked
	Meesmann corneal dystrophy (Stocker-Holt dystrophy)	Autosomal Dominant
Bowman's Layer Dystrophies	Corneal dystrophy of Bowman layer type I (Reis-Bucklers dystrophy)	Autosomal Dominant
	Corneal dystrophy of Bowman layer type II (Thiel-Behnkedystrophy)	Autosomal Dominant
	Grayson-Wilbrandt dystrophy	Autosomal Dominant
	Subepithelial mucinous corneal dystrophy	Autosomal Dominant
Stromal Dystrophies	Amyloidosis V (Lattice corneal dystrophy typeII; Finnish-type amyloidosis [Meretoja syndrome])	Autosomal Dominant
	Central cloudy dystrophy of Francois	Autosomal Dominant
	Central crystalline dystrophy of Schnyder	Autosomal Dominant
	Central discoid corneal dystrophy	Autosomal Dominant
	Congenital hereditary stromal dystrophy	Autosomal Dominant
	Fleck corneal dystrophy (Francois-Neetens speckled corneal dystrophy)	Autosomal Dominance
	Gelatinous drop like corneal dystrophy	Autosomal Recessive

	Lattice corneal dystrophy type III	Autosomal Recessive
	Macular corneal dystrophy	Autosomal Recessive
	Macular corneal dystrophy type IA	Autosomal Recessive
	Macular corneal dystrophy type II	Autosomal Recessive
Stromal Dystrophies	Marginal crystalline corneoretinal dystrophy (Bietti dystrophy)	Autosomal Recessive
	Posterior amorphous corneal dystrophy (Pre-Descemet dystrophy with ichthyosis)	Autosomal Dominant X Linked
	Avellino corneal dystrophy (Combined granular-lattice corneal dystrophy, Granular corneal dystrophy type II)	Autosomal Dominant
	Granular corneal dystrophy type I	Autosomal Dominant
	Lattice corneal dystrophy type I (Classic lattice corneal dystrophy)	Autosomal Dominant
	Lattice corneal dystrophy type I/IIIA	Autosomal Dominant
	Lattice corneal dystrophy type IIIA	Autosomal Dominant
	Lattice corneal dystrophy type IV	Autosomal Dominant
Endothelial Dystrophies	Fuchs endothelial corneal dystrophy	Autosomal Dominant
	Congenital hereditary endothelial dystrophy type I	Autosomal Dominant
	Congenital hereditary endothelial dystrophy type II	Autosomal Dominant
	Posterior polymorphous corneal dystrophy	Autosomal Recessive
	Posterior polymorphous corneal dystrophy	Autosomal Dominant
	X-linked corneal endothelial dystrophy	X Linked

TABLE 1.1: Corneal dystrophies, their mode of inheritance and primary layer involved are shown.

1.2.1 Autosomal dominant stromal dystrophies

There are 9 corneal stromal (Table 1.1) dystrophies-amyloidosis V, central cloudy dystrophy of Francois, central crystalline dystrophy of Schnyder, central discoid corneal dystrophy, congenital hereditary stromal dystrophy, Fleck corneal dystrophy (Francois-Neetens speckled corneal dystrophy), posterior amorphous corneal dystrophy, lattice and granular corneal dystrophies and Thiel Behnke corneal dystrophy that are inherited in an autosomal dominant mode. Lattice and granular corneal dystrophies are further divided into subtypes on the basis of the age of onset, and nature of the opacities in the stroma.

1.2.2 Lattice corneal dystrophy

LCD (OMIM 122200) was reported by Biber in 1890 [Biber *et al.,* 1890] followed by Haab [Haab *et al.,* 1899] and Dimmer [Dimmer *et al.,* 1899] in 1899. Biber described the phenotype as a fine mist-like opacity, which was composed of long and short fine lines running in various directions and crossing each other. The features of lattice dystrophy include discrete ovoid or round subepithelial opacities, anterior stromal white dots, and small refractile filamentary lines that may appear in the first decade of life. The age of onset for LCD has been reported to be as early as 3 yrs [Dubord *et al.,* 1982]. The superficial location of the deposits leads to recurrent erosions. A form of LCD that differs in being a systemic form of amyloidosis was first reported by Meratoja [Meratoja *et al.,* 1973], and is due to the mutations in the gelsolin gene. The phenotype reported

by Meratoja was classified as lattice dystrophy type II. Histopathological identification by Jones & Zimmerman in 1961 [Jones *et al.,* 1961] paved the way for distinguishing between lattice and granular corneal dystrophies. The deposits in LCD were characterized as amyloid based on their Congophilic nature [Seitelberger *et al.,* 1961]. The amyloid deposits showed apple green birefringence and dichroism under polarized light.

Lattice corneal dystrophy type I:

LCD type I (OMIM # 122200) usually manifests as fine, linear network of opacities in the anterior stroma. The clinical diagnosis of lattice dystrophy depends on careful biomicroscopic observation. Typically, the branching linear opacities extend from the center to the periphery and have a somewhat radial arrangement. Usually the lines do not extend to the limbus. They may be seen rather deep in the stroma. The lines may be double contoured or appear to be filled with fine granules. The age of onset is in the first to second decades of life and they progress with age. Visual acuity may be normal in the early stages but reduces as the disease progress. Histopathologically the subepithelial and superficial stroma contains focal deposits that are Congo red positive. The deposits are autofluorescent and fluorescent when stained with acridine orange, Congo red, fluorescein, and thioflavin T. They are argyrophilic, PAS positive, metachromatic with toluidine blue and red with Masson's

trichrome stain [Klintworth *et al.,* 1967]. On haematoxylin & eosin (H&E) stained sections they appear pink in colour. Under a light microscope Congo red stained sections appear brick red in colour. Ultrastructural investigations showed irregularly shaped, electron–dense, extracellular deposits containing fine, non-branching filaments 80–100 nm in diameter that blend with adjacent collagen [McTigue *et al.,* 1964].

Lattice corneal dystrophy type III/IIIA:

Lattice corneal dystrophy type III was initially reported by Hida and co workers [Hida *et al.,* 1987a] in a Japanese family with affected individuals in one generation, and is considered to be autosomal recessive. They observed a late onset disease with thick lattice lines in the mid-stroma [Hida *et al.,* 1987b] without corneal erosions.

LCD type IIIA (OMIM # 608471) differs from LCD type III in having autosomal dominant transmission. It was first reported by Stock and his co-workers in 1991 [Stock *et al.,* 1991] and consists of thick, ropy lattice lines seen to traverse the cornea almost from limbus to limbus that were easily detected with direct illumination. Histopathological examination revealed accumulations of varying sized amyloid deposits in the stroma and ribbons of amyloid between the stroma and Bowman's layer typical of lattice corneal dystrophy type III. Even though this phenotype is similar to type III, it shows recurrent corneal erosions.

Lattice corneal dystrophy type IV:

LCD type IV is an unusual variant of lattice dystrophy, which manifests as deep stromal thick lattice lines. The onset of disease is in the sixth to seventh decades of life [Fujiki *et al.,* 1998, Munier *et al.,* 2002, Nakagawa *et al.,* 2004].

Atypical lattice corneal dystrophy:

Apart from the above-mentioned types of lattice corneal dystrophy many variant phenotypes were reported for lattice corneal dystrophy. These uncharacteristic forms of LCD have been described as having features that partly resemble a combination of LCD type I and LCD type III based on the age of onset and the nature of the opacities. This range of LCD phenotypes has been designated as "intermediate," type I/III or as atypical and they are not strictly classifiable as LCD types I, III, IIIA, or IV.

1.2.3 Granular corneal dystrophy (GCD)

Groenouw first gave a description of this disease in 1890. He described the eye disorder of two patients, and called the corneal disease nodular corneae [Groenouw *et al.,* 1890], later in 1938, Buckler re-examined both cases and diagnosed one as Groenouw type I (granular corneal dystrophy) and the second case as Groenouw type II (macular corneal dystrophy). The common feature in these 2 dystrophies was the presence of nodular deposits. The opacities in GCD were later described as granular [Mutch *et al.,* 1944].

Histopathology of granular corneal dystrophy:

Jones and Zimmerman in 1961 [Jones *et al.,* 1961] established a method of staining to differentiate stromal lesions with eosinophilic granular deposits which were not birefringent under polarized light and which give an intense red colour with Masson's trichrome stain, but no reaction with the periodic acid-Schiff (PAS) or acid polysaccharide methods. The deposits in GCD appear as rod-shaped bodies on electron microscopy [Kuwahara *et al.,* 1967, Matsuo *et al.,* 1967].

GCD type I:

GCD type I (OMIM # 121900) is the Groenouw type of GCD with numerous grayish spots in the central cornea. The opacities are located in the anterior and mid-stroma and are irregularly rounded and resemble small crumbs of dry bread. The opacities lie partly separate and partly fused into groups and streaks. When the disease progresses the opacities grow in size and number and corneal haze develops.

GCD type II:

GCD type II (OMIM # 607541) is also known as combined granular-lattice corneal dystrophy or Avellino corneal dystrophy. It was first reported by Folberg and his colleagues in 1988 [Folberg *et al.,* 1988]. They described atypical granular corneal dystrophy with histopathologic features of both granular and lattice corneal dystrophy. Four patients of 3 families from Pennsylvania, Massachusetts, and Argentina had a clinical diagnosis of granular dystrophy.

Results of pathologic examination of the corneal buttons from each patient after penetrating keratoplasty confirmed the presence of deposits that showed characteristic features of deposits seen in granular dystrophy in the anterior third of the stroma. Amyloid was also demonstrated within some of these granular deposits by Congo red staining and birefringence under polarized light. In addition to the amyloid deposits located within the granular lesions, amyloid was also present in the form of fusiform lesions in the mid-and deep stroma, as well as in areas of the superficial stroma adjacent to the granular deposits. Each of the 3 families was said to have traced its origin to Avellino in Italy. Similar ancestry to the same region of Avellino was noted in 2 other families with granular and lattice-like lesions in the cornea [Holland *et al.,* 1992]. Based on these observations, the term Avellino corneal dystrophy was proposed [Holland *et al.,* 1992]. Later studies showed the same phenotype in patients from other regions of the world as well [Akiya *et al.,* 1999, Meallet *et al.,* 2004]. In general, GCD type II shows a high degree of interfamilial and intrafamilial phenotypic variability. Granular opacities appear to develop first, with lattice lines appearing (if at all) in more advanced stages of disease [Rosenwasser *et al.,* 1993].

GCD type III:

GCD type III (OMIM # 608470) (also known as Reis–Bucklers corneal dystrophy) was first reported by Reis in 1917 [Reis *et al.,* 1917] and further reviewed by Bucklers in 1949 [Bucklers *et al.,* 1949]. They described the opacities as having a geographic pattern and involving the Bowman's layer and superficial stroma

with recurrent corneal erosions The onset of the disease is in the first decade and it progresses rapidly with age. The clinical characteristics has become known as Reis-Bucklers dystrophy are similar to and have been confused in the literature with those of another dystrophy of the Bowman's layer that was described by Thiel and Behnke in 1967. Kuchle *et al* [Kuchle *et al.,* 1995] re-evaluated cases with Bowman's layer dystrophies and proposed that CDB1 (corneal dystrophy of Bowman layer type I) is the same as Reis-Bucklers corneal dystrophy and CDBII is Thiel-Behnke corneal dystrophy. The deposits in CDBI are rod-shaped on EM as seen in GCD and stain with Masson's trichrome stain.

Thiel–Behnke dystrophy (CDB2):

CDB type II (OMIM # 602082) clinically manifests as honeycomb–shaped sub-epithelial opacities with epithelial erosions. [Behnke and Thiel, 1965]. The disorder resembles GCD type III (Reis-Bucklers dystrophy) in its clinical appearance. By histopathology, the deposits differ in that they are not Masson-positive and are distinguished by electron microscopy in which deposits have the appearance of curly fibers beneath the epithelium [Kuchle *et al.,* 1995].

TABLE 1.2: Mutations in *TGFBI* and associated phenotypes

No	Mutation in cDNA	Mutation in amino acid	Exon	Phenotype	Clinical features	Histo-pathologic features	References
1	c.367G>C	p.Asp123His	4	GCD atypical	Dot-like opacities in anterior and mid stroma	NA	Ha *et al*, [2003]
2	c.370C>T	p.Arg124Cys	4	LCD type I	Linear, branching refractile lines in anterior and mid stroma	Amyloid deposits	Munier *et al.*, [1997]
				Atypical	Protruding sub epithelial masses resembling gelatinous drop-like corneal dystrophy (GDLD) and branching	NA	Nakamura *et al.*, [2000]
				Atypical	lattice lines in the stroma as in LCD type I	No amyloid fibrils	Morishige *et al.*, [2004]
				Atypical	Translucent lattice lines and circular central epithelial opacity in both corneas	NA	Yoshida *et al*, [2004]
					Bilateral diffuse opacities with out lattice lines		
				Atypical	Sub-epithelial corneal opacities resembling Reis- Bucklers	NA	

					dystrophy with intervening lattice lines		El-Ashry *et al* , [2004]
3	c.371G>A	p.Arg124His	4	GCD type II (Avellino corneal dystrophy)	Granular and lattice Opacities	Masson + ve and amyloid deposits	Munier *et al* , [1997]
4	c.370C>A	p.Arg124Ser	4	GCD type I	Discrete granular rounded opacities in anterior to mid stroma	Masson - + ve deposits in anterior-mid-stroma, Rod shaped on EM	Stewart *et al.*, [1999]
5	c.371G>T	p.Arg124Leu	4	GCD type III (Reis-Bucklers dystrophy)	Geographic opacities in subepithelial region with recurrent erosions; early-onset	Masson-positive Deposits in epithelium and Bowman's layer	Okada *et al.*, 1998a
6	c.[371G>T; 373_378del]	p.[Arg124Leu;Thr125_Glu 126del]	4	GCD (French variant)	Snow flake-like deposits in anterior central stroma; severity intermediate	Masson +ve deposits; dense rod-shaped structures on EM	Dighiero *et al.*, [2000]
7	c.1501C>A	p.Pro501Thr	11	LCD type IIIA	Thick, ropy lattice lines in stroma, erosions	Amyloid deposits in stroma	Yamamoto *et al.*, [1998]
8	c.1514T>A	p.Val505Asp	11	LCD type1?	Lattice lines in anterior and mid-stroma, late-onset of disease	Amyloid deposits in stroma	Tian *et al.*, [2005]

9	c.1553T>G	p.Leu518Arg	11	LCD type I/III	No details available	Sub-epithelial and stromal amyloid deposits	Munier *et al.*, [2002]
10	c.1553T>C	p.Leu518Pro	11	LCD type I	Difuse anterior stromal opacity with lattice lines	NA	Endo *et al.*, [1999]
11	c.1580T>G	p.Leu527Arg	12	LCD (deep)	Deep stromal opacities with late-onset of disease	NA	Fujiki *et al.*, [1998],
12	c.1613C>G	p.Thr538Arg	12	LCD type I/III	Corneal erosions	Subepithelial amyloid Amyloid in stroma	Munier *et al.*, [2002]
13	c.1616T>A	p.Val539Asp	12	LCD type I	Lattice lines in anterior stroma	NA	Chakravarthi *et al.*, [2005]
14	c.1618_1620 del	p.Phe540 del	12	GCD type III (Reis-Bucklers dystrophy, Sardinian) LCDI/IIIA	NA	NA	Rozzo *et al.*, [1998]
15	c.1619T>C	p.Phe540Ser	12	LCD type IIIA	Subepithelial lattice lines with corneal erosions	Amyloid in subepithelial region and deep stroma	Stix *et al*, [2005]
16	c.1631A>G	p.Asn544Ser	12	LCD type I/III	Thick ropy lattice lines, late onset (4fourth	Amyloid in deep stroma	Mashima *et al.*, [2000]

					decade)		
17	c.1636G>A	p.Ala546Thr	12	LCD type IIIA	Late-onset, opacities in deep stroma, lack of corneal erosions	Amyloid in superficial and deep stroma	Dighiero et al. [2000]
18	c.1637C>A	p.Ala546Asp	12	Polymorphic corneal amyloidosis	Thick lattice lines with recurrent erosions	Amyloid in deep central stroma	Aldave *et al.*, [2004]
19	c.1637G>A 1652C>A	p.[Ala546Asp p.Pro551Gln]	12	LCD type I	Polymorphic, polygonal, refractile corneal opacities	Amyloid deposits in superficial stroma	Klintworth *et al.*, [2004]
20	c.1640T>C	p.Phe547Ser	12	Atypical LCD	Polymorphic corneal amyloidosis	Amyloid deposits in deep stroma	Takacs *et al*, [2007]
21	c.1663C>T	p.Arg555Trp	12	GCD type I	Refractile lattice-like opacities in stroma with corneal haze, corneal erosions; onset in second to third decade	Masson's +ve deposits in Anterior to mid stroma; rod-shaped on EM	Munier *et al*, [1997]
22	c.1664G>A	p.Arg555Gln	12	Thiel-Behnke corneal dystrophy	Discrete, round granular opacities in anterior central stroma; onset first decade onward	Curly fibers"on EM; not stain with Masson trichrome or Congo red	Munier *et al.*, [1997]
23	c.1706T>G	p.Leu569Arg	13	LCD type I	Honeycomb-shaped opacities in anterior stroma; early onset	Amyloid deposits in anterior to mid	Warren *et al.*, [2003]

						stroma	
24	c.1716-1718 del	p. His572del	13	Unilateral LCD	Unilateral, late-onset lattice opacities		Aldave *et al.*, [2006]
25	c.1781G>T	p.Gly594Val	13	LCD	Pain, redness, stromal scarring, lattice lines in anterior stroma	NA	Chakravarthi *et al.*, [2005]
26	c.1856T>A	p.Met619Lys	14	Gcd type II	Age-dependent progression from central sub-epithelial needlelike deposits to polymorphic anterior stromal opacities	stromal deposits that stained with Congo red and Masson's trichrome stains	Aldave *et al.*, [2008]
27	c.1864A>C	p.Asn622His	14	LCD type I/IIIA	Late-onset, posterior stromal thick lattice lines	Amyloid in anterior and midstroma	Stewart *et al.*, [1999]
28	c.1866T>G	p.Asn622Lys	14	LCD type IIIA	Late-onset, asymmetric progression	Amyloid deposits in anterior stroma	Munier *et al.*, [2002]
29	c.1866T>A	p.Asn622Lys	14	LCD type IIIA	Late-onset , recurrent erosions, ropy lattice lines in anterior stroma	Amyloid deposits in anterior stroma	Munier *et al.*, [2002]
30	c.1868G>A	p.Gly623Asp	14	LCD type I/IIIA GCD type III (Reis-Bucklers corneal dystrophy	Pain, redness, photophobia with corneal erosions Subepithelial linear opacities Pain, recurrent erosions; onset in childhood; subepithelial "geographic"opacities	NA Hyaline deposits insubepithelial region; not	Munier *et al.*, [2002] Afshari *et al.*, [2001]

				Atypical LCD?	Opacities in Bowman's layer and stromal lattice lines	Masson or Congo Red + ve NA	Aldave *et al.*, [2005]
31	c.1870G>A	p.Val624Met	14	Atypical LCD	Unilateral thick ropy linear opacities	Amyloid	Afshari *et al.*, [2004]
32	c.1874T>A	p.Val625Asp	14	LCD type I	Branching refractile thin lattice lines	NA	Tian X *et al*, [2007]
33	c.1870_1875 del	p.Val624_ Val625del	14	LCD (atypical)	Stromal opacity with scarring; no evident lattice lines	Amyloid in anterior stroma	Chakravarthi *et al.*, [2005]
34	c.1877A>G	p.His626Arg	14	LCD type I/III (asymmetric)	Late-onset, asymmetric progression	Amyloid in anterior and mid stroma	Stewart *et al*, [1999]
35	c.1877A>C	p.His626Pro	14	LCD type I/III Reis-Bucklers corneal dystrophy	Lattice lines with corneal haze Opacities at the level of Bowman's layer forming geographic patterns of irregular density extending to the limbus. No lattice lines on retro-	Amyloid deposits in stroma Congo red positive Masson's negative subepithelial and superficial stromal amyloid deposits	Munier *et al*, [2002] Liskova *et al.*, [2008]

					illumination		
36	c.1879delG	p.Val627S.fs	14	LCD type IIIA	Late-onset, recurrent erosions, ropy lattice lines in anterior stroma	NA	Munier *et al* , [2002]
37	c.1887_1888ins9	p.Thr629_Asn630ins;AsnValPro	14	LCD type I/IIIA	Lattice lines in anterior stroma with corneal haze, erosions; onset in second decade	NA	Schmitt-Bernard *et al.*, [2000]
38	c.1892T>A	p.Val631Asp	14	LCD (deep stromal)	Late-onset with posterior Stromal opacities progressing anteriorly	NA	Munier *et al.*, [2002]

TABLE 1.2: *TGFBI* mutations, their associated phenotypes and references for the same are shown The *TGFBI* mRNA sequence (GenBank NM_000358 1) is numbered starting with the ATG codon First reports of the respective mutations are cited in the table EM – transmission electron microscopy; +ve, positive; -ve, negative, NA, not available

1.2.4 Genetics of GCD and LCD

Lattice and granular corneal dystrophies are autosomal dominant disorders that were mapped to chromosome 5q31 [Stone *et al.,* 1994]. LCD type I, GCD type I and GCD type II were mapped by Stone and coworkers. GCD type III was also mapped to chromosome 5q31 by Small *et al.,* [1996]. Mutations in the transforming growth factor beta induced gene (*TGFBI*) are responsible for these dystrophies [Munier *et al.,* 1997].

Transforming growth factor*beta*-induced gene (*TGFBI, BIGH3*):

The *TGFBI* cDNA was first isolated by Skonier [Skonier *et al.,* 1992] in an adenocarcinoma cell line in response to induction by *TGFβ1*. It was found to be expressed in several cell types including human lung adenocarcinoma, melanoma, keratinocytes, and fibroblasts by induction with *TGFβ1*. The gene was initially designated as beta-igh3 (*BIGH3;* TGF-beta inducible human clone 3) [Skonier *et al.,* 1992]. The organization of the *TGFBI* gene is shown in Figure 1 3. The gene has 34,883 bp. Truncation analyses identified the nucleotide region from -336 bp to -1 bp as having high promoter activity in A549 (adinocarcinoma) cells. The region from -1000 bp to -646 bp contained negative regulatory elements [Yuan *et al.,* 2004]. The *TGFBI*-responsive element was found to be located at –1000 bp to –336 bp upstream of the transcription start site [Yuan *et al.,* 2004].

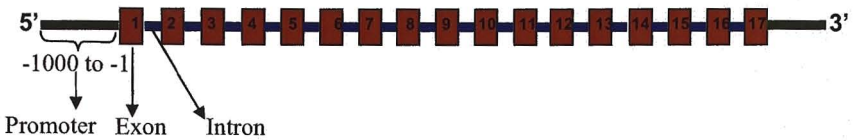

Fig 1.3: The *TGFBI* gene structure showing promoter, non-coding (introns), and coding regions (exons). Exons (numbered 1-17) are represented by orange boxes

The *TGFBI* gene codes for a 68.3 kDa extracellular matrix protein (TGFBIp) alternatively known as Arg-Gly-Asp (RGD)-collagen associated protein (RGD-CAP) [Hashimoto *et al.,* 1997], MP78/70 (a component of elastin-associated microfibrils) [Gibson *et al.,* 1996], or kerato-epithelin [Munier *et al.,* 1997]. The latter name was based on its high level of expression in the corneal epithelium. As is evident from various studies [Skonier *et al.,* 1992], *TGFBI* is also expressed in other tissues apart from cornea. For convenience the gene is designated here as *TGFBI* and the protein as TGFBIp

Expression of TGFBIp:

TGFBIp was identified in bovine tissue extracts and designated as MP78/70, and was localized to collagen fibers in tissues such as developing nuchal ligament, aorta, lung and mature cornea to reticular fibers in fetal spleen and to capsule and tubule basement membranes in the developing kidney [Gibson *et al.,* 1997]. It was associated with collagen type VI and the staining pattern in most tissues showed association with type VI collagen [Gibson *et al.,* 1997].

TGFBI expression is prevalent in different tissues during embryonic development in mouse [Schorderet *et al.,* 2000] and throughout embryogenesis

in zebrafish [Hirate *et al.*, 2003]. Escribano *et al.*, [1994] showed the expression of TGFBIp (protein) in the epithelium of rabbit cornea but at lower levels in the stroma as well. Its expression is restricted in the adult cornea to the epithelium and in corneal wound healing and in the rabbit foetal cornea, expression of *TGFBI* mRNA is detectable in the corneal stroma as well. [Rawe *et al.*, 1997]. However, despite the broad tissue distribution of *TGFBI* during vertebrate embryonic development, its function is still poorly understood.

TGFBIp structure:

The TGFBIp appears to undergo partial processing at the carboxyl terminal end to yield a 68–70 kDa isoform [Skonier *et al.*, 1994]. It contains a secretory signal (1–24 amino acids at the N-terminus), four internal tandem repeat domains that have homology to *FAS1* (fasciclin I) of drosophila and a carboxy-terminal domain with the RGD sequence (residues 642-644). The *FAS1* domain represents an ancient cell adhesion domain homologous to fasciclin I protein in *Drosophila.* Since the identification of the prototypic *Drosophila* protein fasciclin I [Bastiani, *et al.*, 1987], other proteins having homology are the fasciclin I protein of grasshopper [Snow *et al.*, 1988] and MBP70 (*Mycobacterium bovus* protein). The inter-domain homologies range from 31% (between domains 2 and 4) to 16% (between domains 1 and 3). Domain 3 is the more divergent of the 4 domains [Skonier *et al.*, 1992]. Conserved region analysis in rabbit, mouse and human TGFBIp/*BIGH3* revealed three highly conserved amino acid stretches, with 9 of 10 amino acids conserved at the N-terminal end, a second with 6 of 8

amino acids conserved about 30 residues from the N-terminal end and a third region near the carboxyl end with 12 of 16 amino acids conserved [Skonier *et al.*, 1992]. There are no predictive sites for N-linked glycosylation. The deduced amino acid sequence of TGFBIp of rabbit was 92% homologous to the corresponding proteins in human and mouse. It also has 43% homology with osteoblast specific factor-2 (OSF-2) [Rawe *et al.*, 1997]. To date, no isoforms have been reported for TGFBIp and it is encoded by a single gene [Schorderet *et al.*, 2000].

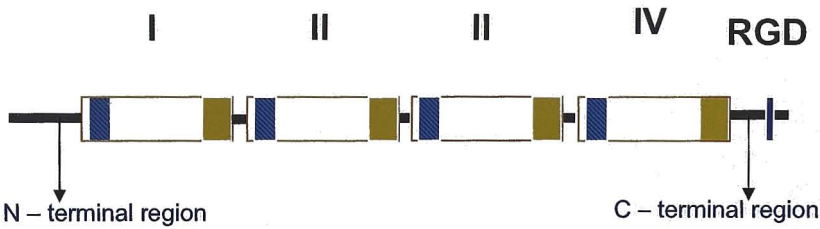

Figure 1.4: Diagram of TGFBIp showing 4 Fas1 repeat domains, integrin recognition sequence (RGD), N-terminal and C-terminal regions.

Interaction with extracellular matrix proteins:

TGFBIp has been shown to bind in vitro to a number of other extracellular matrix components including fibronectin, laminin, and collagens type I, type II, type IV and type VI [Hashimoto *et al.,* 1997; Rawe *et al.,* 1997; Billings *et al.,* 2002]. In addition, TGFBIp has multiple cell adhesion motifs within the fasciclin-like domains [Skonier *et al.,* 1994; LeBaron *et al.,* 1995; Kim *et al.,* 2003] that can mediate interactions with a variety of cell types via integrin $\alpha 3\beta 1$. Cell adhesion activity of TGFBIp was prevented by antibodies against the integrin $\alpha 3$ subunit only. The $\alpha 3$ subunit of integrin heterodimerizes with the $\beta 1$ subunit, hence antibodies against $\beta 1$ also prevented adhesion of HCE cells to TGFBIp- coated matrix [Kim *et al.,* 2000, Bae *et al.,* 2002]. TGFBIp interacts with other integrins such as $\alpha 1\beta 1$ [Ohno *et al.,* 1999], $\alpha V\beta 5$ [Kim *et al.,* 2002a] and $\alpha V\beta 3$. The motifs for interaction with $\alpha 3\beta 1$ integrin have been mapped to highly conserved aspartic acid and isoleucine residues in the second and fourth *FAS1* domains of TGFBIp [Kim *et al.,* 2000]. The structural analysis of pentapeptides, NKDIL (2^{nd} FAS1 domain) and EPDIM (4^{th} FAS1 domain) showed that they can adopt a β-turn structure similar to the RGD peptide and suggested that the NKDIL and EPDIM could interact with integrin in membranes [Park *et al.,* 2004]. The interactions with integrins $\alpha V\beta 3$ and $\alpha V\beta 5$ require at least 18 amino acids, including highly conserved tyrosine and leucine residues, which are denoted YH18 peptide consisting of amino acids 563 and 580 of TGFBIp [Kim *et al.,* 2002a, Nam *et al.,* 2003].

Functions of TGFBIp:

The precise functions of TGFBIp are unknown, but it has been proposed that it may act as a cell adhesion molecule [Kim *et al.,* 2002a] and as a bifunctional linker protein interconnecting different matrix molecules to each other and to cells [Gibson *et al.,* 1997, Billing *et al.,* 2002]. However, there is paucity of data on signaling and adaptor molecules that are recruited by TGFBIp during adhesion and migration of cells. As part of intracellular signaling, TGFBIp supports the actin stress fiber formation in adhering fibroblast cells [Billings *et al.,* 2002]. The phosphorylation of Akt, extracellular signal regulated kinases (Erk), Focal adhesion kinase (FAK) and paxillin are reported during $\alpha 6\beta 3$ and $\alpha v\beta 5$ integrin-mediated adhesion of U87 and vascular smooth cells [Kim *et al.,* 2003, Lee *et al.,* 2006]. Recent evidence suggests that TGFBIp may be important in endothelial cell-matrix interactions during vascular remodeling and angiogenesis [Aitkenhead *et al.,* 2002] and that the protein functions as a negative regulator of mineralization during cartilage differentiation and osteogenesis [Ohno *et al.,* 2002, Kim *et al.,* 2000]. Downregulation of TGFBIp was linked to tumor suppressor function of the protein but the effect of upregulation in some tumors is yet to be understood [Sasaki *et al.,* 2002, Hourihan *et al.,* 2003]. To date, the corneal stromal dystrophies represent the only known pathological manifestation so far identified for gene mutations in *TGFBI*.

***TGFBI* gene mutations in LCD:**

A mutation of c.370C>T (Arg124Cys) was first reported for LCD and is found in LCD type I [Munier *et al.,* 1997]. Other mutations including c.1514T>A (Val505Asp), c.1553T>G (Leu518pro), C.1616T>A (Val539Asp), c.1637C>A (Ala546Asp), c.1652C>A (Pro551Gln), c.1706T>G (Leu569Arg), were reported to cause the LCD type I [Tian *et al.,* 2005, Endo *et al.,* 1999, Dighiero *et al.,* 2000a, Klintworth *et al.,* 2004, Warren *et al.,* 2003]. Among the various mutations, Arg124Cys mutation is predominant in various populations studied from Hungary [Takacs *et al.,* 2007], Japan [Yamamoto *et al.,* 2000, Mashima *et al.,* 2000, Fujiki *et al.,* 2000] and Ukraine [Pampukha *et al.,* 2004] and in Western populations [Munier *et al.,* 1997, Korvatska *et al.,* 1998, Afshari *et al.,* 2001]. Various phenotypes associated with mutation of Arg124Cys are shown in Table 1.2. The first *TGFBI* mutation identified for the LCD type IIIA was c.1501C>A (Pro501Thr), found in patients having late-onset, ropy lattice lines, and recurrent corneal erosions [Yamamoto *et al.,* 1998]. Other mutations associated with the LCD type IIIA phenotype are c.1866T>G (Asn622Lys), a deletion of G at position 1879 with a predicted frameshift at Val627 and subsequent termination (c.1879delG; Val6274fs) [Munier *et al.,* 2002], c.1636G>A (Ala546Thr) [Dighiero *et al.,* 2000b], and c.1619T>C (Phe540Ser) [Stix *et al.,* 2005]. The mutations associated with LCD type IV are c.1580T>G (Leu527Arg) [Fujiki *et al.,* 1998] and c 1631A>G (Asn544Ser) [Nakagawa Asahina *et al.,* 2004], found in Japanese patients; c.1892T>A (Val631Asp), found in an Italian patient [Munier *et al.,*

2002]. Various mutations reported for different types of LCD and their phenotypes were given in Table 1.2.

***TGFBI* gene mutations in GCD:**

GCD type I was first reported to arise from a mutation of c.1663C>T (Arg555Trp) in a family with 22 affected members [Munier *et al.,* 1997]. Mutation of c.370C>A (Arg124Ser) was also reported in two families with GCD type I phenotype [Stewart *et al.,* 1999b]. Arg555Trp mutation was identified in homozygous patients [Okada *et al.,* 1998b, Mashima *et al.,* 1998]. In patients with homozygous Arg555Trp mutation the phenotype was severe and the age of onset was early. [Okada *et al.,* 1998b]

The *TGFBI* mutation linked with GCD type II is c.371G>A (Arg124His), first reported by Munier in 1997 [Munier *et al.,* 1997], and then by Korvatska and co-workers [Korvatska *et al.,* 1999]. This mutation was identified as a frequent mutation in Japanese patients [Mashima *et al.,* 2000], Fujiki *et al.,* 2000]. Due to its higher prevalence in Japan, families with homozygous Arg124His have been described in 4 reports [Mashima *et al.,* 1998, Fujiki *et al.,* 1998, Tsujikawa *et al.,* 2006]. In contrast to patients with heterozygous Arg124His mutations, patients from the same family who were homozygous for mutation of Arg124His have a severe phenotype with an early onset of the disease (within the first decade) [Mashima *et al.,* 1998]. Light and electron microscopic analysis of corneal sections from two severely affected patients aged 37 yrs and 31 yrs showed deposits in the superficial stromal layers that stained with Luxol fast blue and

Masson trichrome. The deep stromal layers were normal and none of the stromal layers were stained with Congo red. Electron microscopy showed an accumulation of rod shaped electron-dense material in the corneas of individuals with the homozygous mutation. The minimum age reported for the severe phenotype in homozygous individuals is 2 yrs [Mashima *et al.,* 1998].

A mutation of c.371G>T (Arg124Leu) was identified in *TGFBI* gene in patients with GCD type III or CDB1 [Okada *et al.,* 1998a; Mashima *et al.,* 1999]. This mutation was reported first in Japanese patients [Okada *et al.,* 1998a; Mashima *et al.,* 1999] and also in various regions including United Kingdom [Stewart *et al.,* 1999a] and China [Yu *et al.,* 2003]. The variants of GCD, their clinical features and mutations responsible were given in Table 1.2.

Genetically, Thiel-Behnke corneal dystrophy (TBCD; CDB2) is linked to 2 different loci. A mutation of C.1664G>A (Arg555Gln) in *TGFBI* is associated with this dystrophy [Munier *et al.,* 1997]. Apart from the *TGFBI* gene, CDB2 was also mapped to chromosome 10 (10q23–10q24) [Yee *et al.,* 1997]. The gene has not yet been identified at this locus.

1.3 AIM OF THE STUDY

The aim of this work was to characterize the mutational spectrum and look for genotype-phenotype correlations in Indian patients with granular and lattice corneal dystrophies. No data existed in Indian populations with these disorders prior to this study. We also attempted to determine the differences if any

between wild type TGFBI protein and some common mutants when expressed in cell culture.

1.4 OBJECTIVES

1. To screen patients with lattice and granular corneal dystrophies for mutations in the *TGFBI* gene.

2. To look for genotype-phenotype correlations.

3. To investigate the differences between wild type and mutant proteins of *TGFBI* by expression in suitable cell lines.

Chapter 2
Materials & Methods

2.0 MATERIALS AND METHODS

2.1 Patients and controls

Probands with granular or lattice corneal dystrophy presenting at the cornea clinic of L.V. Prasad Eye Institute and available family members were included in the study after approval of the protocol by the Institutional Review Board. Diagnosis was made after clinical evaluation by slit lamp biomicroscopy to detect the presence of corneal opacities, and testing of visual acuity, intraocular pressure, and fundus examination. Unaffected relatives of probands were also clinically examined. Inclusion and exclusion criteria are as listed below.

2.1.1 Inclusion criteria

1 Bilateral involvement.

2 Clinically evident stromal opacities consistent with lattice corneal dystrophy (LCD) or granular corneal dystrophy (GCD).

3 Histopathological criteria: Positive staining of deposits with Congo red followed by apple green birefringence under polarized light is a confirmatory test for amyloid and was used for diagnosis of LCD. Positive staining of deposits with Masson's trichrome to give brick red color is indicative of GCD.

2.1.2 Exclusion criteria

Patients with unilateral disease were excluded from the study.

A total of 60 probands were recruited in the study. In addition, 100 unrelated controls who were free of corneal disease were included. 4 ml of the blood was collected in heparinized vacutainers. Blood samples were stored at –20°C.

2.2 DNA Isolation

Isolation of genomic DNA from peripheral blood leukocytes was performed by a standard method involving phenol-chloroform extraction. Frozen blood samples were thawed at room temperature, lysis of red blood cells (RBC) was carried out by mixing with an equal volume of 1X phosphate buffered saline (PBS) followed by centrifugation at 4500 rpm to obtain a leukocyte pellet. The supernatant was discarded, and pellet of white blood cells was treated with Proteinase K in 7.5 ml of buffer (0.01M Tris pH 8.0, 0.1M EDTA pH 8.0, 0.5% SDS, 20mg/ml proteinase K (Bangalore Genei, Bangalore, India)) 35 µl and 10 mg/ml RNase A 17.5 µl (Bangalore Genei, Bangalore, India) by incubating overnight at 37°C. The lysate was extracted with equal volume of buffered phenol (equilibrated with 1 M Tris pH 8.0 and maintained in 0.5 M Tris, pH 8.0). The upper aqueous layer was transferred to a fresh tube and mixed with an equal (1:1) volume of phenol-chloroform. This was followed by extraction with equal volume of chloroform. DNA from the aqueous phase was precipitated with 2.0 M ammonium acetate

(one-fifth volume of 10M stock solution) and 2 volumes of ethanol. The DNA was spooled on to a 1ml pipet tip and washed with 70% ethanol. The DNA pellet was air-dried to remove residual ethanol. The DNA pellet was then dissolved in 500 µl of de-ionized water. Isolated DNA was quantified by measuring the absorbance at 260 and at 280 nm. The ratio of absorbance 260/280 was used to determine the quality of the isolated DNA.The concentration was calculated using the following formula:

Concentration of the DNA = OD_{260} X 50 X dilution factor = µg of DNA /ml

Quantified DNA was diluted to 50 ng/µl and used for polymerase chain reaction (PCR).

2.3 Polymerase chain reaction

Polymerase chain reaction was performed using primers that were complementary to flanking intronic sequences of each exon. Primer sequences are in Table 2.1. Primers were commercially obtained (Sigma-Aldrich, USA). The primers were designed so as to generate amplified products of 300bp or less for single strand conformation polymorphism (SSCP) analysis. All the primers designed were 20 base pairs or more in length with a GC content in the range of 40-80%. Tm was calculated according to the formula Tm (°C) = 2(A+T) + 4(G+C)-5. The annealing temperature for each pair of PCR primers was optimized experimentally. Details of PCR conditions for each primer pair are mentioned in the Table 2.1.

PCR amplification was carried out with following reaction parameters

dNTPs	200 µM
PCR reaction buffer	1X
Magnesium chloride	1.5 -2.5 mM
Primer (forward)	10 pmoles
Primer (reverse)	10 pmoles
Template DNA	50 ng
Taq DNA polymerase (Bangalore Genei, Bangalore, India)	1U

The final reaction volume was 25 µl. Dimethyl sulfoxide (DMSO) was used at a concentration of 5% to 10% for GC-rich templates.

The cycling conditions used were as follows

1. Initial denaturation	94°C, 2 min
2. Denaturation	94°C, 45 sec
3. Annealing	55-70°C, 30sec
4. Elongation	72°C, 45 sec
5. Final elongation	72°C, 5-7 min
Cycles (steps 2-4)	35

TABLE 2.1: PCR primers used for *TGFBI* exons

Primers	Primer Sequence	No.Of Bases	Genomic DNA Position	Product Size (bp)	Annealing Temp	Restriction Enzyme
1F	CCCTCCCGCTCGCAGCTTAC	20	5			
1R	CGCTCCGAGCCCCGACTACC	20	312	308	62°C	*BglI*
2F	TGGGGTGGACGTGCTGATCATC	22	4778			
2R	GGGGAACTGCAGCCAGCGTG	20	4984	206	60°C	
3F	TGAAGCCCTGCCTAACACAAT	21	15082			
3R	CACCATTCCCTTCCACCCAC	20	15239	157	60°C	
4F	AGGGTGTGGTTGGGCTGGAC	20	17340			
4R	CCTCGGGGAAGTAAGGCAGTTC	22	17620	281	60°C	
5F	TGCAGCCCCTAACTGACACCCT	22	17880			
5R	ACACATGGAACAGAAATGGG	20	18148	268	60°C	
6F	CTTTGGGACTATGCCTCTGTTG	22	18282			
6R	GCAATGTGTCCCAAGCCTGG	20	18530	248	58°C	
7F	GGGAGTGCCAGAGTCTTCAGGG	22	20454			
7R	GCAGGTCTTGGGCTCAATCTAG	22	20708	254	58°C	
8F	CCTGAGGTTATCGTGGAGTGGAC	23	23917			
8R	AGATGGTGGGCCAGGCAGG	19	24230	313	70°C	*MspI*
9F	ATGCCCTGGGGTGGATGAATGA	22	24934			
9R	ACAGGGGTGGGGAAGCTGCC	20	25204	270	58°C	
10F	GCACATCTCTCTGGACCTAAC	22	25742			
10R	GTAAGGAGCTTCCCAGGAGC	20	25969	227	58°C	
11F	GGAGGCCCCTCGTGGAAGTA	20	26687			

11R	GGAAGGTCGCAGCAGTGCAC	20	27018	331	58°C	*SmaI*
12F	TCAGCGTGGTGAGGTATTTAAGG	23	27662			
12R	GGGCCCTGAGGGATCACTAC	20	27918	259	58°C	
13F	CCCTCCTTGACCAGGCTAATTA	22	30089			
13R	GATATGTCCTGGAGCCCTGC	20	30341	253	58°C	
14F	GCGACAAGATTGAAACTCCATCT CA	25	31752			
14R	TTCTTCTCTCCACCAACTGCCA	22	32071	319	62°C	*HinfI*
15F	GTTTCACTCTGGTCAAACCTGC	22	32525			
15R	CCAAACAGAGGACCTGAGGC	20	32700	175	58°C	
16F	AGCAGTTGCAGGTATAACTTTCA C	24	33672			
16R	CTTGGGGGTAAGGCCTAAAC	20	33808	136	58°C	
17F	GACATGGGGAGATCTGCACC	20	34201			
17R	TCTCATTATGGTGCGGCCCA	20	34423	222	60°C	

TABLE 2.1: Primer sequences, product sizes, annealing temperatures and the restriction enzymes used for digestion of PCR products greater than 300 bp Numbers 1 to 17 refer to *TGFBI* exons, F&R denote forward and reverse, respectively

2.4 Agarose gel electrophoresis

0.8 to1.5% agarose gels were prepared by melting the required quantity of agarose in 1X Tris-Acetate-EDTA (50X stock solution: 2 M Tris, 57.1 ml glacial acetic acid, 100 mM Na_2EDTA) (1X final concentration) electrophoresis buffer by heating in a microwave oven, followed by addition of ethidium bromide to a final concentration of 0.25 µg/ml. The agarose was poured into a gel tray containing a comb, allowed to cool and solidify, and then placed in electrophoresis tank and submerged in 1X TAE buffer. DNA samples were mixed with 6X gel loading buffer (0.25% bromophenol blue, 0.25% xylene cyanol 40% w/v sucrose). Samples were loaded on the gel along with DNA size standards. Horizontal electrophoresis was carried out at approximately 80-100V. The gel was photographed under UV light using the UVIDoc gel documentation system (UVITec, Cambridge, England).

2.5 PCR-RFLP (Restriction fragment length polymorphism)

PCR-RFLP was used to detect sequence variations that are known to result in either gain or loss of a recognition sequence of the particular restriction endonuclease. The method includes PCR-amplification of the relevant DNA fragment followed by the digestion with the respective restriction enzyme (details in Table 2.2) at the optimum temperatures as mentioned in the table. Digested products were subjected to agarose and polyacrylamide gel electrophoresis.

TABLE 2.2: Details of PCR-RFLP for *TGFBI* mutations.

Exon	Mutation	Restriction Enzyme	Product Size			Temp
			Normal	Homozygous	Heterozygous	
4	R124C,R124H, R124L, R124S	*Cpo1*	129, 152	281	281, 129, 152	37°C
12	V539D*	*Taal*	135,124	259	259, 135, 124	65°C
12	R555W	*Bstxl*	259	182, 77	259,182, 77	55°C
13	G594V*	*HincII*	253	170, 83	253,170, 83	37°C

TABLE 2.2: Mutations in different exons, restriction enzymes used for RFLP, digestion pattern and incubation temperatures.

TABLE 2.3: Primers for cloning of *TGFBI* cDNA

S. No	Primer Name	Primer Sequence	Location	PCR Product Size
1	BIGSFI1F	5'GCGGGCCATGGAGGCCATGGCGCTCTTCGT GCGGCTGCTG-3'	1 bp	
2	BIGNOTRHIS	5'GGGGCGGCCGCCTAGTGATGGTGGTGGTG ATGATGCTTCATCCTCTAATAACTTTTGATA-3'	2020 bp	2097

TABLE 2.3: cDNA specific primers and the size of the PCR products are shown. Red colored nucleotide sequence in forward primer is *SfiI* site. Blue colored nucleotide sequence in reverse primer is *NotI* site. Green colored nucleotide sequence in reverse primer is 6 – X – His tag.

2.6 Polyacrylamide gel electrophoresis

Polyacrylamide gels were prepared at a final concentration of 8% by mixing 13.3 ml of 30% acrylamide stock solution (29:1 acrylamide:bis), 5 ml of 10X Tris borate-EDTA (890 mM Tris, 890 mM boric acid 20 mM) (1X final conc), and de-ionized water to a total volume of 50 ml. Polymerization was initiated by addition of 300 µl of ammonium persulphate (0.06%) and 30 µl of TEMED (GE Healthcare UK Ltd Buckinghamshire England) Gels were prepared at a size of 16X16 cms and a thickness of 1.5 mm. Electrophoresis was performed in 1X TBE at 75 volts for 2-3 hrs. Gels were visualized by staining with ethidium bromide and photographed on a UVIDoc gel documentation (UVITec, Cambridge, England) system over UV light.

2.7 Single strand conformation polymorphism (SSCP)

Single-strand conformation polymorphism (SSCP) analysis is a mutation detection technique, which has a sensitivity range of 60% to 80% for fragments less than 300 bp in size but decreases with increase in fragment size [Hayashi and Yandell, 1993]. The principle of SSCP is based on the conformation of single strands due to intra-strand base-pairing following denaturation and self-annealing. A single base substitution can potentially alter the conformation of the fragment and result in differential migration under conditions of non-denaturing electrophoresis. Therefore DNA samples having wild type (normal) and altered (variant) sequences display different mobility patterns.

For SSCP analysis, 2 μl of PCR product was mixed with 4 μl of 95% formamide containing bromophenol blue and xylene cyanol. Samples were denatured at 95°C for 5 minutes and chilled immediately on ice. Samples were then separated on 8% polyacrylamide gel (19.5:0.5 acrylamide to bisacrylamide) containing 0.5X TBE and 5% glycerol. All samples were electrophorized at room temperature and at 4°C. Gels were run at constant voltage of 75 V at room temperature and 120V at 4°C. Gels were stained with 0.2 % silver nitrate for the detection of DNA. This was done by fixing the gels in 10% ethanol: 0.5% acetic acid for 45 minutes. Gels were then washed three times with de-ionized water followed by staining in 0.2% silver nitrate. They were then washed, developed in a solution of 1.5% sodium hydroxide and 0.4% formaldehyde until bands were visible at the desired intensity. Gels were washed in de-ionized water and photographed using UVIDoc gel documentation system over white light (UVITec, Cambridge, England). Fragments showing altered mobility relative to controls were sequenced directly.

2.8 RNA isolation and preparation of *TGFBI* cDNA

Human cadaveric corneas were collected from the Ramayamma International Eye Bank, L.V. Prasad Eye institute, Hyderabad, India. RNA was isolated from the blood, limbal cells (collected from Sudhakar & Srikanth Ravi stem

cell laboratory, L V Prasad Eye Institute) and corneal tissue by using Trizol reagent (Invitrogen).

A starting volume of 0.25 ml of blood or 10^6 blood leukocytes or 100 mg of tissue was taken in a sterile 2 ml microfuge tube, diluted with 0.25 ml of sterile water and mixed with 1.5 ml of Trizol reagent. Cells were lysed with repeated pipetting. Homogenized samples were made into two aliquots, each of 1ml and incubated for 5 min at room temperature. After 5 min of incubation, 0.2 ml of chloroform was added to each tube and mixed vigorously. After mixing, the tubes were left at room temperature for 15 min to separate the organic and aqueous layer. The samples were then centrifuged at 13,000 rpm for 15 minutes at 2-8°C in a microfuge. Clear aqueous phase obtained after centrifugation was transferred to a fresh microfuge tube and RNA was precipitated by adding 0.5 ml of isopropanol. Precipitated RNA was left at room temperature for 10 minutes and centrifuged at 13000 rpm for 10 minutes. The pellet was washed with 75% ethanol and centrifuged at 8,000 rpm for 10 minutes. The RNA pellet was air-dried and resuspended in 50 μl of autoclaved de-ionized water and kept on ice for 30 minutes until it dissolved completely. Dissolved RNA was quantified by measuring absorbance at 260 nm on a UV spectrophotometer. Concentration of RNA was calculated by taking 1 OD unit equal to 40 μg RNA.

RNA quality was checked by electrophoresis on 1% agarose gel containing 2.2 M formaldehyde in IX MOPS buffer. (0.2 M MOPS pH 7.0, 20

mM sodium acetate and 10 mM EDTA pH 8.0). RNA samples were loaded by preparing a mix of 2 µl of the sample, 2 µl of the 10X MOPS buffer, 4.0 µl formaldehyde, 10 µl of formamide and ethidium bromide to a final concentration of 0.25 µg/ml. Denatured at 55°C in water bath for 10 min and placed on ice. To the denatured sample 2 µl of the 10X formaldehyde-loading buffer (50% glycerol, 10 mM EDTA pH 8.0, 0.25% bromophenol blue, 0.25% xylene cyanol) was added and samples were loaded onto the agarose gel, which was submerged in 1X MOPS buffer. Electrophoresis was performed at 4 to 5 V/cm and RNA was visualized in UV light using the UVIDoc gel documentation system.

Reverse transcription PCR (RT-PCR)

Reverse transcription of cDNA from the RNA preparation was performed using a mix of 4 µl (1 µg) of the RNA and 1 µl (50 pmols) oligo dT primer (previously denatured at 60°C for 10 minutes and chilled on ice), 10 µl of 5X RT-buffer, 5 µl of 10 mM dNTP, 1µl (200 U/µl) MMLV-RT enzyme (MBI-Fermentas Inc, Maryland, USA) and 29 µl of sterile, de-ionized water. The cDNA preparation was subjected to PCR amplification using primers specific for the human *TGFBI* cDNA (shown in Table 2.3).

The reaction was incubated at 25°C for 10 minutes for primer annealing, 42°C for 1 hour for reverse transcription and heated at 70°C for 10 minutes to inactivate the enzyme. The following conditions were used to amplify the cDNA

with Taq DNA Polymerase- one cycle at 94°C for 5 minutes, followed by 35 cycles of 94°C for 1 minute, 56°C for 1 minute, and 72°C for 3 minutes, followed by one cycle at 72°C for 10 minutes.

2.9 Preparation of Competent E.coli cells and transformation

Bacterial culture of E.coli DH5α was revived from a glycerol stock by streaking cells onto antibiotic-free LB agar plates to obtain isolated colonies. A single colony was picked and grown in LB medium overnight. 1ml of overnight culture was added to 100 ml of fresh LB medium with out antibiotic for preparing competent cells [Sambrook et al., 1989].

Transformations were performed with DNA (up to a volume of 5 µl) and 100 µl of competent DH5α cells in each tube. The cells with DNA was Incubated on ice for 20 min, cells were heat-shocked in a water bath at 42°C for 90 sec, and immediately placed on ice. 400 µl of LB medium was added to the cells and they were then incubated at 37°C for 45 min to allow for recovery of cells. A volume of 200 µl of the culture was spread on LB agar plates with 50 µg/ml ampicillin. The plates were incubated for 16 hrs at 37°C.

2.10 Isolation of plasmid DNA

Alkaline lysis method was used for the isolation of plasmid from bacterial cells. The method used was as described in cloning manual (Sambrook *et al.*, 1989). Plasmid mini preps were made from 1.5 ml of overnight culture. Briefly, cells were pelleted and cell pellets from 1.5 ml cultures were resuspended in 100 µl of Glucose-Tris-EDTA (GTE) solution (Glucose 50 mM, Tris pH 7.5, 25 mM, EDTA 10 mM), incubated on ice followed by lysis in 200 µl of a solution containing 0.2N NaOH and 1% sodium dodecyl sulphate (SDS) and mixed by gentle inversion. The cell lysates were treated with 150 µl of 5M potassium acetate (pH 5.8) on ice and then centrifuged at 13,000 rpm for 10 min. The supernatants were removed and DNA was precipitated with 800 µl of ethanol. Isolated plasmid DNA was then washed with 75% ethanol and air-dried. The pellet was resuspended in 30 µl of autoclaved de-ionized water containing 10 µg/ml RNase A.

2.11 Cloning of wild type *TGFBI* c. DNA

Cloning of wild type *TGFBI* cDNA was performed in following steps

A) Cloning into TA vector

B) Sub-cloning into pCMV-HA vector

C) Insertion of C-terminal 6X-Histidine tag into *TGFBI* cDNA clone

D) Sub-cloning of 6X-His tagged cDNA into pcDNA 3.1 (-) *Neo* vector

A) Cloning into TA vector

A TA cloning vector, pTZ57R/T (Cat# k1213, MBI-Fermentas Inc, Maryland USA) was used in the initial step to clone the PCR-amplified *TGFBI* cDNA. This method depends on the property of *Taq* polymerase of a non-templated addition of A at the 3'end of the amplified product. The PCR product can be directly inserted into the vector pTZ57R/T which has dT at both ends as shown in the Figure 2.1. The specific primers shown in Table 2.3 for amplification of *TGFBI* cDNA were designed such that the 5' end of the forward and reverse primers have recognition sites for *Sfil* and *Not1* enzymes respectively (Table 2.3). The sites were inserted to enable cloning into the multiple cloning site (MCS) of the mammalian expression vector pCMV-HA (Clontech Laboratories, Inc, Mountain View, CA 94043 U.S.A).

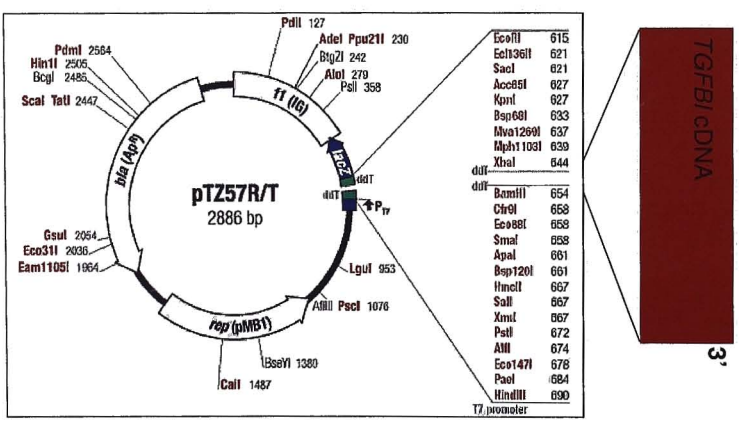

Fig 2.1: pTZ57R/T vector with multiple cloning site and the location of the insert.

Ligation procedure

Vector pTZ57R/T, (0.165 µg, 0.18 pmol ends. specified in protocol for kit-InsTA clone™ PCR Cloning Kit, cat # 1213)) - 3µl

Purified PCR fragment	–4 µl
5X Ligation Buffer	–6 µl
De-ionized Water	–6 µl
T4 DNA Ligase	–1µl (conc 5U/1µl)

The reaction was incubated at 22°C overnight. The ligation mix was transformed into competent DH5α (*E.coli)* cells. A ligation reaction with vector only was also set up to assess the extent of self-ligation of vector.

B) Sub-cloning of *TGFBI* cDNA into pCMV-HA vector

The insert was released from the pTZ57R/T- *TGFBI* clone by using *SfiI* and *NotI* enzymes and inserted into pCMV-HA vector digested with the same enzymes.

C) Insertion of C-terminal 6X-Histidine (6X-His) tag

The 6X-His tag sequence was inserted into the reverse primer used for amplifying the *TGFBI* cDNA. The full length cDNA was amplified using a forward primer BIGSFII and a reverse primer BIGNOTRHIS containing 18 nucleotides upstream of the stop codon and having the coding sequence for 6 histidine

residues in frame with the *TGFBI* sequence (Table 2.3). The PCR reaction was performed by using pCMV-HA-*TGFBI* as a template. The region amplified by the two primers consists of 2097 bp of the wild type cDNA with the 6X His tag. This PCR product (size 2097 bp) was cut with *PdiI* and *NotI* enzymes (location of RE sites shown in Figure 2.2). The fragment was ligated into pCMV-HA-*TGFBI* clone which was also digested with the same enzymes as mentioned above. The resultant clone had an N-terminal-HA (hemagglutinin) tag and a C- terminal 6X-His tag.

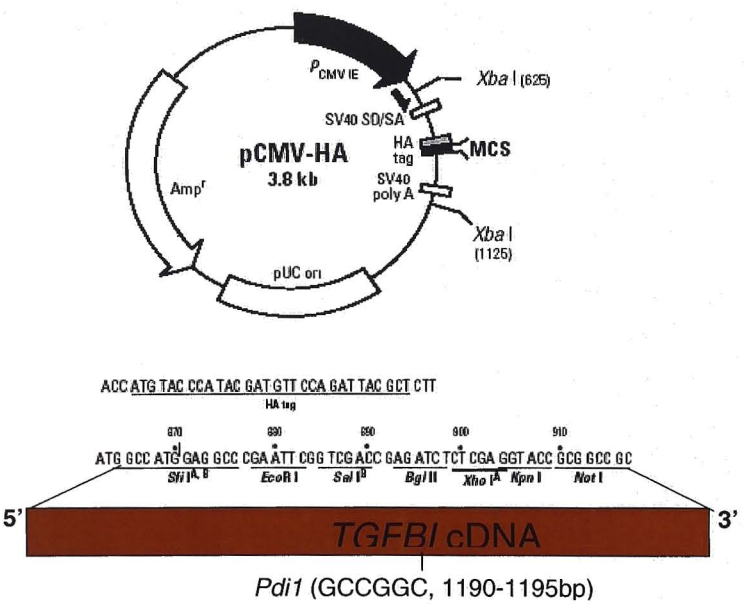

Fig 2.2: Vector map of pCMV-HA showing multiple cloning sites, HA tag sequence and the location of the insertion sites in the pCMV-HA vector

D) Sub cloning of *TGFBI* cDNA into pcDNA3.1 (-) Neo vector:

The *TGFBI* cDNAs were cloned into the pcDNA Neo plasmid in order to enable neomycin selection of the transfected cells so as to generate stable transformants. The *TGFBI* cDNA was released from the pTZ57R/T-*TGFBI* with *XbaI* and *NotI* enzymes and ligated into pcDNA3.1 Neo cut with *XbaI* and *NotI* enzymes as shown in Figure 2.3. The released product from the pTZ57R/T-*TGFBI* had 3 bp (AGA) additional to the insert before ATG. The 6X-His tag was inserted in frame with *TGFBI* as mentioned in 2.11c.

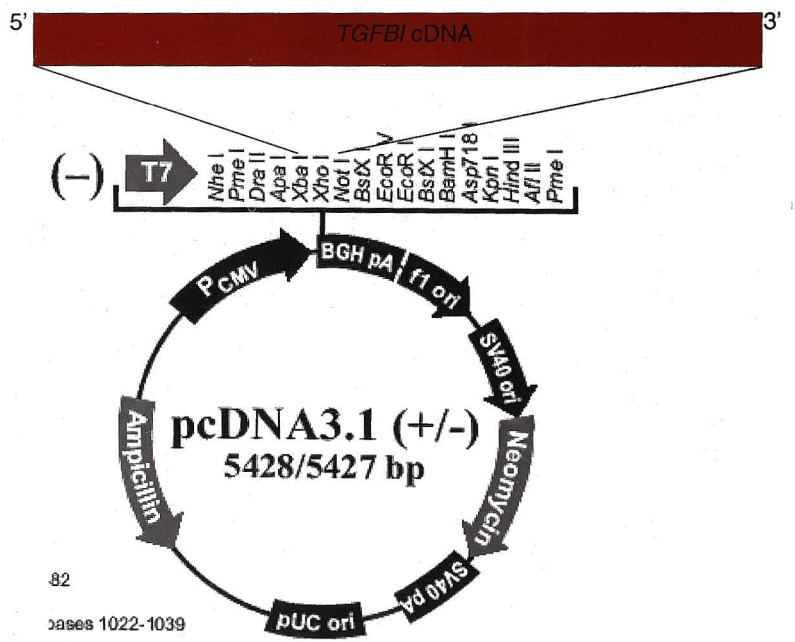

Fig 2.3: pcDNA3.1 (-) vector map along with the multiple cloning site and the location of insert

2.12 Construction of mutant clones

Mutants of *TGFBI* were generated in the wild type cDNA by megaprimer-based site-directed mutagenesis (Fig 2.4). Primers spanning the sites of the desired mutation, and designed to contain the mutant base at the appropriate position in the primer sequence, were used (Table 2.4). The primer containing the mutation was used for amplification of a part of the cDNA to obtain a PCR product containing the mutation. For creating the cDNAs (c.370C>T, c.371G>A, c.371G>T) corresponding to Arg124Cys, Arg124His, Arg124Leu mutations, different mutation-containing primers (spanning residues 360 to 380 of the *TGFBI* cDNA with respect to the first base of the ATG codon) were used as reverse primers along with a forward primer at complementary to positions 1 to 24 of the cDNA. The mutant bases (T, A and T were located at positions 11 and 10 of the reverse primers, shown in Table 2.4). For the c.1653C>T mutation corresponding to mutation of Arg555Trp, a mutant primer (spanning positions 1643 to 1663 bp of the *TGFBI* cDNA) was used as the forward primer with a reverse primer at residues 2030 to 2049 of the cDNA (Table 2.4). The mutant PCR products were 396 bp in length for mutations Arg124His, Arg124Cys, and Arg124Leu and 428bp in length for mutant Arg555Trp. PCR products were purified by agarose gel electrophoresis. These products were used as megaprimers for a second round of PCR to amplify full-length sequence. The complementary primers used for the 2nd round of amplification

were designed from the 3' end of the coding region (at residues 2021 to 2049) and at the 5' end of the coding region (at residues 1 to 24 bp) for the PCR products coding for Arg124 mutations or Arg555 mutations respectively. The final PCR product was 2097 bp long and contained the full-length cDNA sequence of *TGFBI*. The mutant cDNA for Arg124 mutations were cloned into the pCMVHA expression vector by using *SfiI* restriction enzyme present at 5' end of the PCR product (4 to 17 bp) and *PdiI* restriction enzyme, which cuts the insert at cDNA position 1192 bp. The product (1192 bp) of *SfiI* and *PdiI* digestion was ligated into the pCMVHA-*TGFBI* wt and pcDNA3.1 (-) - Neo*TGFBI* wt clones after digesting both the plasmids with the same restriction enzymes and purifying the vectors. The Arg555Trp mutant-encoding PCR product was digested with *PdiI* and *NotI*. The product (887bp) of *PdiI* and *NotI* digest was ligated into the wild type cDNA clones, pCMVHA-*TGFBI* wt and pcDNA3.1 (-) - Neo*TGFBI* wt -*TGFBI* clones after digesting with the same restriction enzymes and purifying the vectors. Transformants were screened by *CpoI* and *BstXI* digestion of Arg124 and Arg555 mutant plasmids respectively to identify the desired clones. Positive clones were isolated and sequence of the mutants was confirmed by direct sequencing.

The above-described constructs of wild type and mutant *TGFBI* cDNAs in pCMVHA vector had the HA (hemagglutinin) tag at the N-terminus and 6X-His tag at the C-terminus of the *TGFBI* cDNA. The wild type and mutant pcDNA3.1 (-) Neo-*TGFBI* cDNA clones had the 6X-His tag at C-terminus.

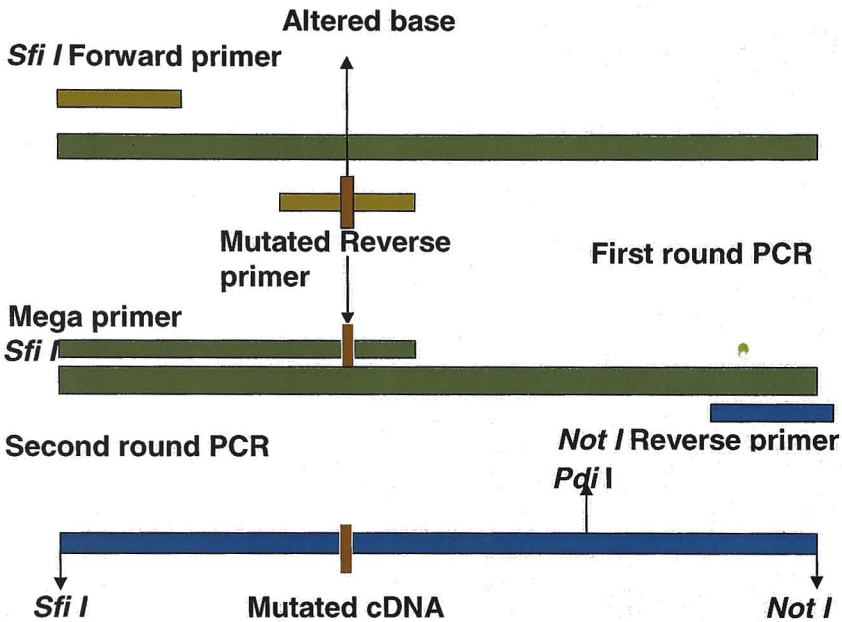

Fig 2.4: Megaprimer-based method for creating mutants in *TGFBI* cDNA

S.No	Primer Name	Primer Sequence	Location in cDNA	Mega Primer Size
1	BIGSFI1F	5'GCGGGCCATGGAGGCCATGGCGCTCTTCGTGCGGCTGCTG-3'	1	
2	R124CR	5'-TTCTCCGTGCAGTCCGTGTA -3'	360 bp	396 bp
3	R124HR	5'-TTCTCCGTGTGGTCCGTGTA-3'	360 bp	396 bp
4	R124LR	5'-TTCTCCGTGAGGTCCGTGTA -3'	360 bp	396 bp
5	R555WF	5'-CCAAGAGAATGGAGCAGACT-3'	1653 bp	
6	*BIGNOTRHIS*	5'GGGGCGGCCGCCTAGTGATGGTGGTGGTGATGATGCTTCATCCTCTAATAACTTTTGATA-3'	2030 bp	428 bp

TABLE 2.4: Shown are the details of primers used for site directed mutagenesis and amplicons size (mega primer). Location in cDNA is shown with respect to ATG.

2.13 Cell culture

HeLa and Cos1 cell lines were cultured in T25 culture flasks (Nunc, Rochester, New York. USA) with Dulbecco's modified Eagles medium (DMEM, Sigma-Aldrich, USA) and 10% fetal bovine serum (FBS, Sigma-Aldrich, USA). The human corneal epithelial cell line (HCE) was cultured in HCE medium (3.98 g of minimal essential medium (MEM) (Sigma-Aldrich, USA) & 6.66 g of Hams F12 in 824 ml of autoclaved de-ionized water, with addition of 1.38 g sodium bicarbonate, 5 mg bovine insulin, 150 mg penicillin, 100 mg streptomycin, 2.5 mg amphotericin-B, 4 mg gentamycin (100 µl, 40 mg/ml), The medium was sterilized by passing through 0.2 µm filter. To the sterilized medium 100 µl of epidermal growth factor (EGF, 0.1 mg/ml) was added. Cells were incubated at 37°C with 5% CO_2. DMEM was prepared from 13.4 g of powder in 1 litre of autoclaved de-ionized water, with addition of 3.7 g sodium bicarbonate, 150 mg penicillin, 100 mg streptomycin, 2.5 mg amphotericin B, and 4 mg gentamycin (100 µl of 40 mg/ml) (Sigma-Aldrich, USA). The medium was sterilized by passing through 0.2 µm filter.

Cells were sub-cultured at 80% confluence by trypsin treatment. Medium from the flask was removed and cells were washed with sterile 1X PBS (0.8 g sodium chloride (NaCl), 0.02 g potassium chloride (KCl), 0.012 g, potassium dihydrogen phosphate (KH_2PO_4), 0.091g disodium hydrogen phosphate (Na_2HPO_4) in 100 ml autoclaved de-ionized water. 1 ml trypsin (0.125 g, (0.125%) trypsin, 0.02 g (0.02% EDTA in 100 ml of autoclaved de-ionized

water) was added to cells, incubated for 2-3 mins and trypsin was then inactivated by addition of 1 ml of FBS. The cells were collected by repeated pipetting. Detached cells were seeded in a ratio of 1:3 on to fresh flasks containing 4 ml of medium with 10% FBS.

2.14 Transfection of cells

Transfection was carried out using the Lipofectamine method as described by the manufacturer (Invitrogen Corporation, Carlsbad, California, USA).

For transfection, cells were seeded at 30,000-40,000 cells on a 22 mm cover slip or 75,000-80,000 cells per 35 mm well of a 6 well plate to achieve a cell density of 70-80% at the time of transfection. Prior to seeding, cells were trypsinized and an aliquot was counted by using Neubauer's chamber Cells were grown in 2 ml of culture medium for each well in 6-well plate with 10% FBS.

Lipofectamine method

Seeded cells were grown on cover slips or 6 well dishes for 16-18 hrs. Before transfection cells were washed with 1X PBS and medium was replaced by the serum-free and antibiotic-free medium. Transfection medium that was serum-free and antibiotic-free cell culture medium was used while carrying out lipofectamine-based transfection. Transfection was performed as described in the user manual provided by manufacturer. Reaction mixes 1 and 2 containing 2 μl of lipofectamine in 100 μl of transfection medium and 0.5–2 μg of plasmid

in 100 µl of transfection medium respectively, were pooled. The mix was incubated at room temperature for 30 min and added to the cells, which were overlaid with 800 µl of transfection medium, drop by drop to cover the entire surface of the culture dish. After addition of transfection mix, the cells were incubated at 37°C with 5% CO_2 After 6-8 hrs incubation, 1ml of medium with10% FBS and antibiotics was added to the cells and incubation was continued.

Transfection procedure was optimized using pEGFP plasmid, expressing green fluorescent protein, which can be detected by fluorescence microscopy upon exposure to blue light. Parameters that were optimized included amount of DNA (range tested, 0.25 to 2.0 microgram per 35 mm dish), volume of lipid (1 to 4 µl per 35 mm dish), cell density at transfection (40-80% confluence) and time period from transfection until harvesting of cells (from 6 hrs until 48 hrs).

2.15 Immunofluorescence assay

Cells grown on cover slips were washed with I X PBS twice and fixed with 3% formaldehyde for 25 min at room temperature. After fixation, cells were washed 3 times with 1 X PBS and permeabilized with 0.5% Triton X 100 and 0.05% Tween 20 for 10 min. followed by three washes with 1 X PBS. Cells were treated with 4% BSA for 30 min at room temperature to prevent non-specific binding of antibody. 100 µl primary antibody diluted 1:25 (4 µg/ml) was placed on a parafilm, on which cover slips were placed in an inverted position. Cells

were incubated in primary antibody for 2 hrs at room temperature. After incubation cells were washed three times with 1XPBS and incubated with secondary antibody, FITC (fluorescein isothiocyanate)-conjugated anti-mouse IgG diluted 1:100 After 2 hrs of incubation with secondary antibody, cells were washed three times with 1X PBS, treated with propidium iodide (PI) for 1 to 2 min, washed once with 1X PBS and mounted on cover slips containing cells with 1:1 ratio of glycerol and 1X PBS. Mounted slides were kept in a moisturizing chamber to avoid drying. The slides were observed under a confocal microscope (Zeiss, Axiocam 510, Germany) at excitation wavelength of 490 nm and emission wavelength 530 nm.

2.16 Preparation of protein extracts for Western blotting

Detection of TGFBI protein secreted into the medium was performed by Western blotting of precipitated protein from culture medium. Protein from medium was precipitated with 10% tri-chloro acetic acid (TCA) and 80% ice cold acetone. 200 µl of absolute TCA was added to 2 ml of culture medium and the contents were mixed by inverting the tubes and left at room temp for 10 min. After 10 min the tubes were centrifuged at 13000 rpm for 10 min to separate the precipitated protein. Supernatant was discarded and the pellet was resuspended in 40 µl of 2X Laemmli buffer (250 mM Tris; 40% glycerol; 5% SDS, 0.05% Bromophenol Blue). Transfected cells were harvested at 12, 24, 48, and 72 hrs after transfection, Extracts from untransfected cells was prepared as a control. The cells were washed with 1 X PBS, scraped with

disposable cell scraper and collected in 100 µl of cell lysis buffer (Brij buffer) which contains 0.1M Tris, 2mM EDTA, 0.5 M NaCl, 1% Brij 96, 1% NP40, 3 µg/ml Aprotinin, 1mM PMSF. 50 µl of 2x loading (Laemmli's) buffer was added to the lysates. The samples were denatured for 5 min at 94°C placed on ice, and loaded onto SDS-polyacrylamide gels.

2.17 SDS PAGE

Discontinuous SDS polyacrylamide gel electrophoresis (gel size, height x width, 10 x 10) was performed with separating and stacking gels of 8% and 5% acrylamide respectively on a vertical electrophoresis system (Hoefer, AP Biotech UK Ltd, Buckinghamshire, England). Separating and stacking gels were made up as shown below.

De-ionized water	- 4.6 ml
30% (29:1) acrylamide	- 2.7 ml (8% final)
I.5M (4X) Tris pH 8.8	- 2.5 ml (1X final)
10% SDS	- 100 µl (0.1% final)
10% APS	- 100 µl (0.1% final)
TEMED	- 6 µl
	10.06

Stacking gel:	
De-ionized water	-1.72 ml
30% (29:1) acrylamide	- 0.50 ml (5% final)
0.5M (4X) Tris pH 6.3	- 0.75 ml (1X final)
10% SDS	- 30 µl (0.1% final)
10% APS	- 30 µl (0.1% final)
TEMED	- 3 µl
	3.06 ml

40 µl of cell lysate (corresponding to about 1/3rd of a T-25 culture dish) and 20 µl protein extract from culture medium (about half of total volume of extract from 35 mm dish) were loaded on the gel and electrophoresis was performed with 1X Tris-glycine SDS buffer (0.25 M Tris, 19.2 mM glycine and 0.01% SDS) at a constant current (25 mAmps) for 1 hour 30 min. After electrophoresis the gel was kept in transfer buffer (1Xtris- glycine-SDS with 20% methanol) for 15 min. The proteins were transferred on to nitrocellulose membrane by using semi-dry transfer unit (TE70, GE Healthcare UK Ltd Buckinghamshire England).

2.18 Western blot

Nitrocellulose membrane and 6 filter papers (Whatman no1) were cut to the same size as the gel and soaked in 1X transfer buffer (0.25 M Tris, 19.2 mM glycine and 0.01% SDS with 20% methanol) for 15 min. The transfer set-up was made by placing from bottom to top, 3 filter papers, nitrocellulose

membrane, gel and 3 filter papers on one another, in the same order on the lower lid of the apparatus. Air bubbles were removed by rolling a glass tube on top of the transfer setup. Upper lid was placed and transfer was made with a constant voltage, of 15V for 1 hr. The membrane was stained with Ponceau red stain to visualize the transferred protein and wells were marked. Membrane was de-stained and used for immuno- detection.

Immuno-detection of TGFBI protein was carried out by first placing the membrane in blocking buffer (1X PBS, 5% non fat milk and 0.05% Tween 20) for 2 hrs at room temperature, followed by incubation with primary antibody at a dilution of 1:25 for 2 hrs at room temperature. Membrane was then washed 3X with PBS containing 0.05% Tween 20) and incubated with secondary antibody (anti-mouse IgG) conjugated with horseradish peroxidase (Sigma-Aldrich, USA), at a dilution of 1:6000 for 2 hrs at room temperature. The membrane was washed three times with PBS-Tween 20 (0.05%). Detection was done by enhanced chemiluminescence method. 1 ml of solution 1 (0.45 mM Coumaric acid, 2.5 mM luminol, 100 mM Tris pH 8.5) was mixed with 1 ml of solution 2 (5 mM H_2O_2, 100 mM Tris pH 8.5) before pouring on to the membrane. Signal was detected by exposing the blot to an X-Ray film in an autoradiography cassette, following development of the film using X–ray film developer and fixer.

Chapter 3

Results

3.0 RESULTS

3.1 Mutation screening and genotype-phenotype correlations

A total of 60 families, 29 families with LCD and 31 families with GCD were screened for *TGFBI* gene mutations. Both familial (35) as well as sporadic (25) cases were included in this study. Mutations were found in 25 families with LCD and 31 families with GCD. The mutations identified were not present in any of the control individuals.

3.1.1 Mutation analysis of patients with LCD

Probands from 29 families with LCD were included in mutational analysis. A total of 40 affected and 27 unaffected individuals were available from 29 families. Diagnosis of LCD was based on clinical evaluation for 29 and confirmed by histopathology of corneal sections for 18 patients.

The mutations identified in patients with LCD are given in Table 3.1. PCR-amplified products of all exons and flanking regions of *TGFBI* obtained from genomic DNA of LCD patients were screened for mutations by single strand conformation polymorphism (SSCP) and sequencing. Mutations that were previously reported in patients from other populations were identified in 18 patients (summarized in Table 3.1). These included a sequence change c.370C>T in exon 4, leading to substitution of arginine-124 to cysteine in 16

probands, and c.1877A>G corresponding to change of histidine-626 to arginine found in 2 probands (sequence data in Figure 3.1).

TABLE 3.1: Summary of the *TGFBI* mutations in patients with LCD

Probands (n)	Mutation in *TGFBI*		Exon	Detection method	RE site change	Co-segregation tested in relatives
	cDNA	Amino Acid				
16	c.370C>T	Arg124Cys	4	SSCP, Sequencing	- *Cpo1* (Abolition)	25 affected, 3 unaffected
2	c.1877A>G	His626Arg	14	SSCP, Sequencing		3 affected
1	c.1616T>A	Val539Asp	12	SSCP, Sequencing PCR-RFLP	- *Taa1* (Abolition)	1 affected, 9 unaffected
2	c.1781G>T	Gly594Val	13	SSCP, Sequencing PCR-RFLP	+ *HincII* (Creation)	2 affected, 9 unaffected
1	c.1870_75del	Val624_ Val625del	14	SSCP, Sequencing		3 affected, 3 unaffected
3	c.1867G>A	Gly623Ser	14	SSCP, Sequencing		3 affected, 3 unaffected

TABLE 3.1: Restriction enzyme sites altered are shown as loss (Abolition) or gain (Creation) of the site due to mutation

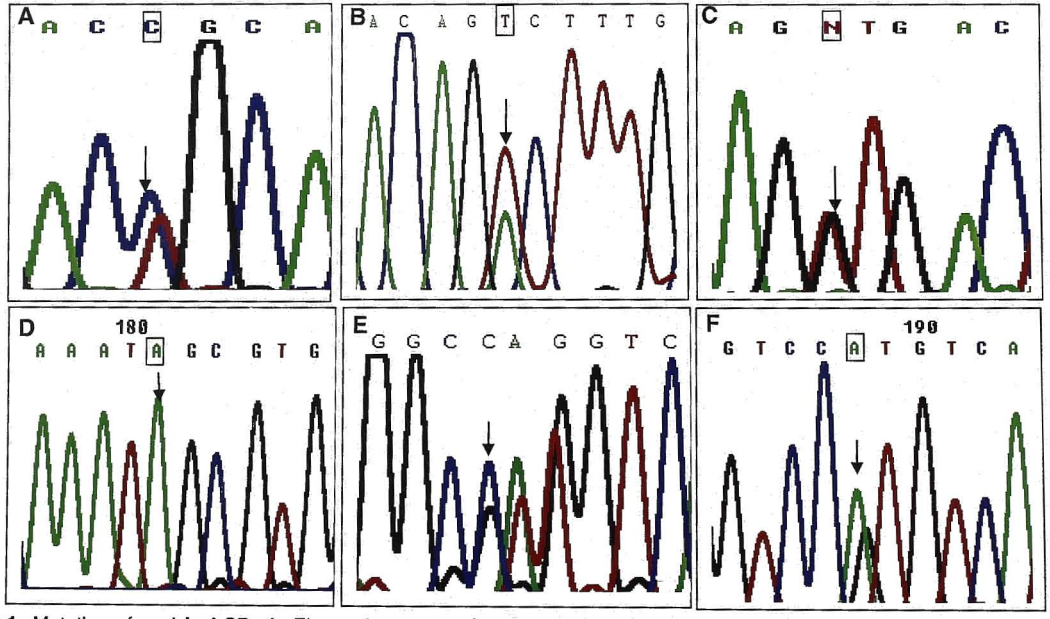

Fig 3.1: Mutations found **in LCD.** A. Electropherogram of c.370C>T (Arg124Cys) mutation B. Electropherogram of c.1616T>A (Val539Asp) C. Electropherogram of c.1781G>T (Gly594Val) mutation D. Electropherogram of c.1867G>A (Gly623Ser) mutation E. Electropherogram of c.1870_75del (Val624-Val625del) and F. Electropherogram of c.1877A>G (His626Arg) mutation.

Co-segregation of the above 2 mutations could be tested in 8 families for the Arg124Cys mutation and 1 family for the His626Arg mutation, in which relatives (13 affected and 3 unaffected) of the probands were available for testing. This was done by PCR-RFLP methods using *Cpo 1* enzyme for c.370C>T (Arg124Cys) (details in Chapter 2). The results of RFLP analysis with *Cpo1* for family LCD-4 are shown in Fig 3.2A. As shown in the figure, the presence of two fragments (lane 4) of 129 bp and 152 bp indicates 2 normal alleles and the presence of an uncut fragment of 281 bp along with the *Cpo1* digested 129 bp and 152 bp fragments indicates one normal and one mutant allele (Lanes 2 & 3). For the c.1877A>G/His626Arg mutation, co-segregation was assessed by sequencing of the relevant PCR product from 2 affected individuals of a family. Both these mutations were absent in 100 unrelated normal controls tested by the above methods.

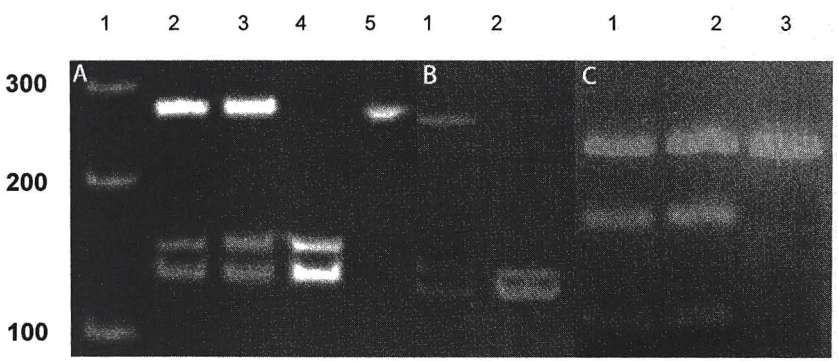

Fig 3.2: A. *Cpo1* digestion of PCR-amplified fragment of exon 4 for family LCD–4. Lane 1·100 bp DNA size standard. Digests of PCR-amplified exon 4 are shown for the proband (lane 2), offspring of proband (lane 3), and normal control individual (lane 4) Lane 5 shows undigested DNA. B. *Taa1* digestion of PCR product of exon 12 for family LCD-13 Lane 1 proband, lane 2

normal control C *Hinc II* digestion of PCR-amplified exon 13 product for the family LCD-6 Lane 1 proband (I 1 Fig 3 4), Lane 2 offspring (II 3 Fig 3 4), Lane 3- normal control

In addition to the reported mutations, we also identified four novel sequence changes in 7 families, which were further confirmed as pathogenic mutations (Table 3.1). Change of T>A at c.1616 (located in exon 12 of the gene) leading to an amino acid substitution of valine-539 to aspartic acid (Val539Asp) was found in 1 family. PCR-RFLP analysis with *Taa 1* enzyme (details in Chapter 2) was used to test for co-segregation of this mutation and for its presence/absence in normal, unrelated controls. The c.1616 T>A change results in the abolition of the site for *Taa 1.* Upon digestion with *Taa 1*, the exon 12 PCR-amplified product from a normal control showed fragments of 135 bp and 124 bp (Fig 3 2B, lane 2) fragments corresponding to a normal sequence, whereas DNA from a heterozygous individual showed fragments of 259 bp, 135 bp and 124 bp (Fig 3.2B, lane 1) This change was not found in 100 unrelated normal individuals suggesting that it is pathogenic. When we looked for the co-segregation of this mutation in the family, shown in the pedigree (Fig 3.3.), the proband's older son (II.1 in pedigree), aged 34 yrs, was heterozygous for the mutation but had a normal phenotype. This suggests that either the mutation is not fully penetrant or that it is associated with a late-onset disease, which is not yet evident in this individual. Late onset of disease was observed in the proband who developed signs of disease at about 65 yrs.

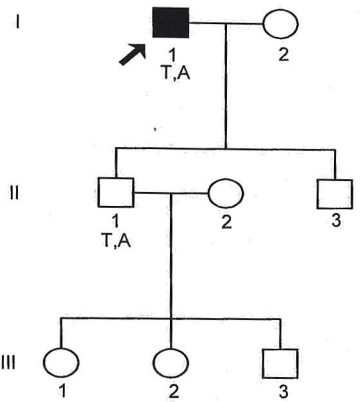

Fig 3.3: Pedigree of the family LCD-13 showing affected and unaffected individuals Genotypes of individuals tested are indicated below each symbol

The second novel change identified was c.1782G>T, in exon 13 of the *TGFBI* gene leading to substitution of glycine-594 for valine (Gly594Val). PCR-RFLP with *Hinc II* was used for co-segregation analysis and to test for the presence of the mutation in controls. A c.1781G>T results in the creation of a site for *Hinc II* enzyme. Upon digestion with *Hinc II,* the exon 13 PCR amplified product from a normal individual showed a 253 bp fragment corresponding to uncut PCR product (Fig 3.2C, lane 3) whereas DNA from a heterozygous individual showed fragments of 253 bp, 170 bp and 83 bp (Fig 3.2C lane 1 and 2). c.1781G>T/Gly594Val mutation was not found in 200 chromosomes of 100 unrelated normal controls. Co-segregation analysis of the available family members (1 affected and 8 unaffected) is shown in Fig 3.4. The offspring of the proband Fig (3.4) aged 44 (II.3) and 40 (II.6) years were both heterozygous for Gly594Val and yet asymptomatic and clinically unaffected.

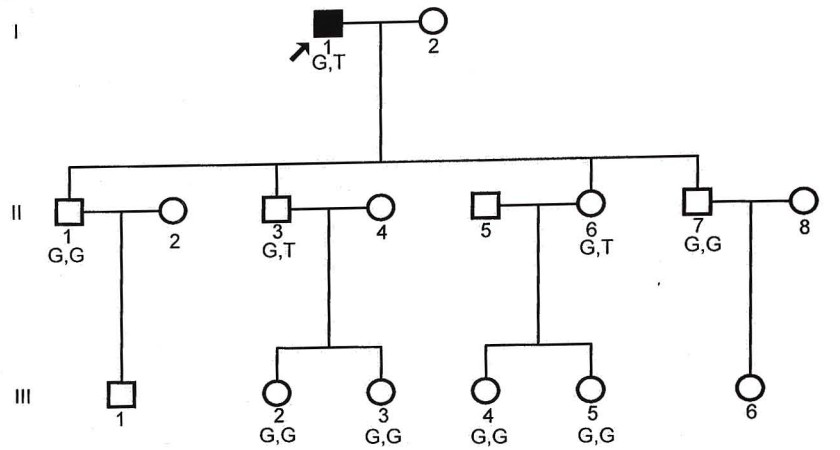

Fig 3.4: Pedigree of the family LCD–6 shows affected and unaffected individuals Genotypes of individuals tested are indicated below each symbol

The 3rd novel change observed was c.1867G>A in exon 14, that results in substitution of glycine-623 for serine. Direct sequencing of exon 14 in 100 normal controls did not show the presence of c.1867G>A in any of them. This mutation was homozygous in probands of two families (families LCD-7 & LCD-20; Fig 3.5) and heterozygous in one family (LCD-22). Co-segregation analysis of the available family members from the family LCD-7 is shown in Fig 3.5a. The offspring (III.1, III.2, and III.3) of the proband were in their 1st decade at the time of evaluation and his mother (I.2) was in her 7th decade. They were all heterozygous and had no history of corneal disease.

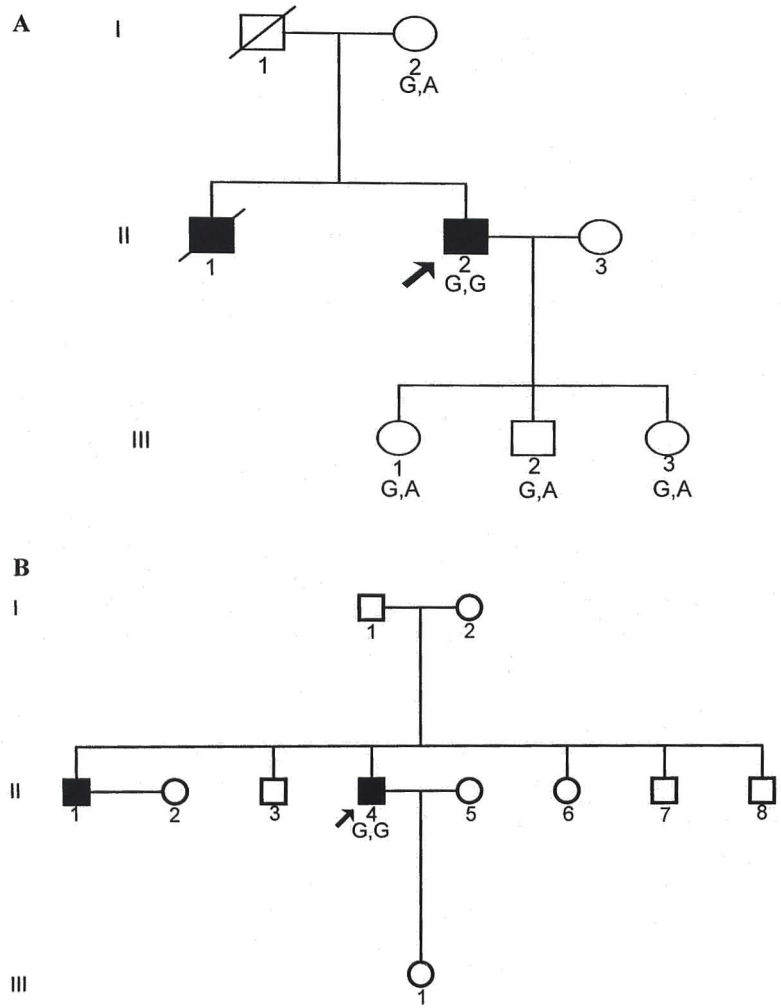

Fig 3.5: Pedigrees of the families LCD–7 (A) and LCD–20 (B) showing affected and unaffected individuals. Genotypes of individuals tested are indicated below each symbol.

The 4th novel mutation identified was c.1870_1875del/Val624_Val625 del located in exon 14, predicting a deletion of 2 amino acids, valine-624 and valine-

625. Sequencing of exon 14 in normal controls did not show Val624_Val625del change. Co-segregation of this mutation is shown in the pedigree (Fig 3.6). 6 members (3 affected and 3 unaffected) were tested for co-segregation. The proband, his older brother (II.1 in pedigree) and brother's daughter (III.1 in pedigree) were affected, heterozygous for the mutation and the other three members (III.2, III.3, and III.4) were unaffected and had 2 normal alleles.

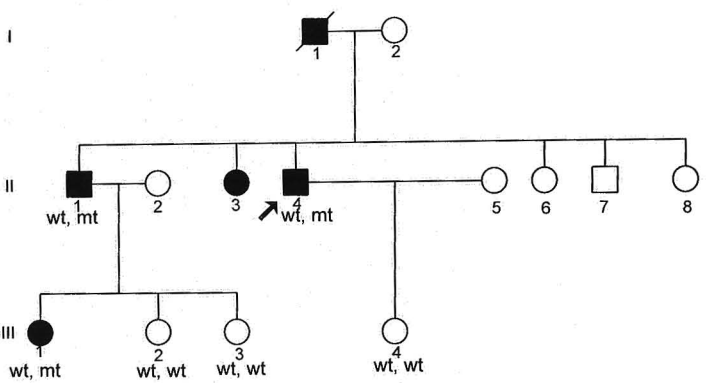

Fig 3.6: Pedigree of the family LCD–18 showing affected and unaffected individuals Genotypes of individuals tested are indicated below each symbol

The frequency of the detected mutations was 87% in families with LCD. The mutations identified were located in either the N-terminal region (exon 4) or in the fourth fasciclin-like domain of the protein. 16 of the 29 families with LCD had mutations at hotspot aminoacid, Arg124. This is similar to data obtained on other populations such as those from Japan [Mashima *et al.,* 2000, Fujiki *et al.,* 2000], Hungary [Takacs *et al.,* 2007], Ukraine [Pampukha *et al.,* 2004], and in Western populations [Munier *et al.,* 1997, Korvatska 1998, Afshari *et al.,* 2001,

Munier *et al.,* 2002]. In contrast, a study on Vietnamese patients with LCD found that mutation of His626Arg may be more frequent [Chau *et al.,* 2003]. Along with the reported mutations we also identified 4 novel mutations (T>A at c.1616/Val539Asp, c.1781G>T/Gly594Val, c.1867G>A/Gly623Ser, c.1870_1875del/Val624_Val625del) in patients with LCD.

3.1.2 Clinical and histopathological features in LCD

Among the 16 LCD patients with mutation Arg124Cys, clinical data were available for all 16 LCD patients; histopathology data were available for 9 patients. Ages of onset ranged from 20 to 58 yrs. Corneal opacities were in the form of detectable lattice lines in 13 patients. The opacities were located in the anterior to mid-stroma. Histopathologic evaluation showed the presence of amyloid deposits in 9 patients (Summarized in Table 3.2).

Variable phenotypes were found among the two probands with mutation His626Arg. One showed posterior stromal opacities (LCD-2) as shown in the Figure 3.7 and the other (LCD-10) had anterior to mid-stromal opacities. The ages of onset were 28 yrs and 40 yrs respectively.

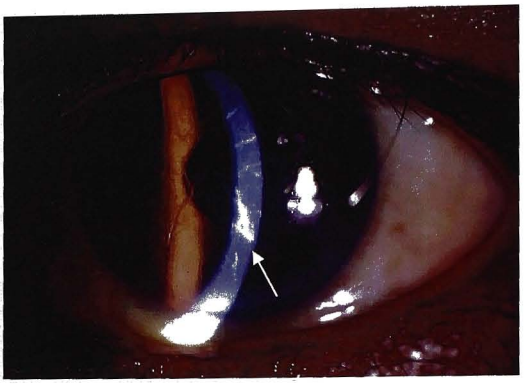

Fig 3.7: Slit lamp view of the cornea of the patient (LCD-2) with mutation His626Arg.

The previously unreported mutation of Val539Asp found in one patient in this study, was associated with opacities in the form of lattice lines (Fig 3.8) in the corneal stroma, which were confirmed as amyloid by histopathology. The onset of the disease was at the age of 65 yrs.

Fig 3.8: Slit lamp view of the cornea of the patient with mutation Val539Asp (LCD–13).

Two unrelated probands with mutation of Gly594Val (LCD-6, LCD-9), in their sixth and seventh decades of life respectively, showed posterior stromal

opacities on slit lamp examination. The opacities were in the form of thick lattice lines and extending into the limbal region of the cornea (Fig 3.9 A&B). No histopathological data was available for these patients.

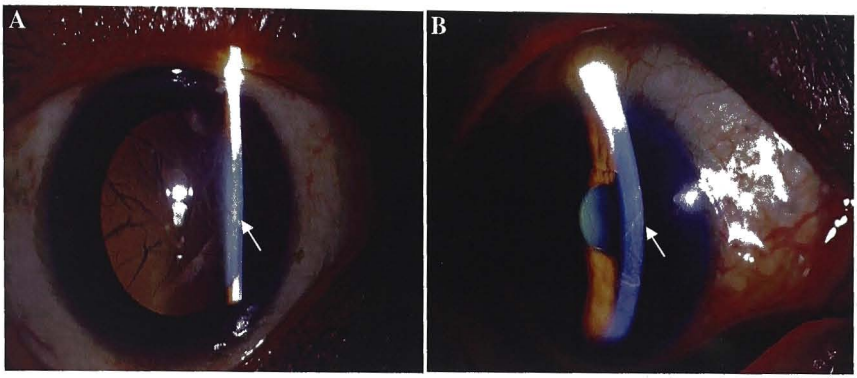

Fig 3.9: Slit lamp picture of cornea of patients LCD-6 (A) and LCD-9 (B).

The clinical manifestations in the patients with Gly594Val mutation were similar to those reported for two other mutations, Leu527Arg [Fujiki *et al.,* 1998] and Val631Asp [Munier *et al.,* 2002] and have been classified as LCD type IV. To our knowledge, this represents the third mutation causing this form of LCD. Cosegregation analysis in the family members revealed that two offspring of one of the patients carried the mutation but did not manifest disease. It is possible that the mutation carriers in this family may manifest disease at a more advanced age or that this mutation has incomplete penetrance. The high degree of conservation of the residue mutated, as well as the absence of the change in 100 unrelated control subjects support the conclusion that it is pathogenic.

One patient (family LCD-22) was heterozygous for the Gly623Ser mutation and had mild opacities in the form of lattice lines in the stroma (shown in the fig 3.10A). The patient presented to our institution in his 7th decade. The other two probands (families LCD-7 and LCD–20) were homozygous for the same mutation. The proband from family LCD-7 presented at 27 yrs of age with corneal opacities. On examination, the opacities were located in the corneal stroma and were rounded in appearance with no detectable lattice lines (shown in Fig 3.10B). The nature of his corneal dystrophy could not be diagnosed with certainty based on clinical evaluation (i.e. whether macular or granular or lattice corneal dystrophy). The patient had corneal grafts in both eyes at age 34 yrs (right eye) and 38 yrs (left eye). At presentation, he had a visual acuity of 6/9.6 in the right eye and 6/9 in the left eye. The histopathology evaluation of his corneal tissue after surgery revealed the presence of amyloid (shown in Fig 3.10C). The proband gave a history of a brother, deceased at the time of the study, who was similarly affected. Examination of his medical records revealed that he had corneal dystrophy with a similar age of onset as the proband and had undergone corneal grafting. A diagnosis of LCD was made on the basis of histopathological detection of amyloid in the cornea.

The 2nd proband (LCD-7), also homozygous for the same mutation, presented at 30 yrs of age with corneal opacities appearing as thick lattice lines as shown in Fig 3.10D. The patient had a visual acuity of 6/9 in the right eye and 6/12 in the left eye. He had a corneal graft in his left eye. Histopathology

revealed the presence of amyloid deposits. Thus, homozygous mutation of Gly623Asp showed phenotypic variability between the two families.

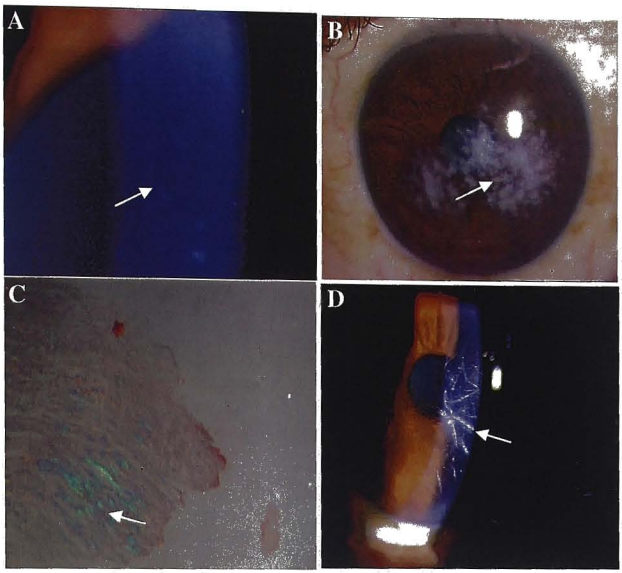

Fig 3.10: Slit lamp view of the patient LCD–22 with heterozygous mutation of Gly623Ser showing faint lattice lines (A). Slit lamp view of the proband LCD-7 with homozygous Gly623Ser mutation (B) and corneal section showing amyloid deposits (C). Slit lamp view of the second proband LCD–20 (D) with homozygous Gly623Ser mutation showing thick lattice lines.

One patient with LCD (LCD-18; II: 4 in pedigree, Fig 3.6) with mutation of Val624_Val625del had features atypical of LCD (Fig 3.11A&B). He had diffuse corneal opacities with no clear lattice lines, complained of progressive loss of vision and photophobia during his 20s and at the age of 30 yrs underwent corneal grafting. The diagnosis of LCD was based on the histopathology of the corneal button, which showed amyloid deposits in the anterior stroma (Fig

3.11C). The deposits were negative for Masson trichrome. His father and two siblings were reported to be similarly affected in their 20s. The brother of the proband, who was also examined in our institution, had corneal scarring and opacities in the superficial stroma and his cornea showed similar histopathologic findings as that of the proband.

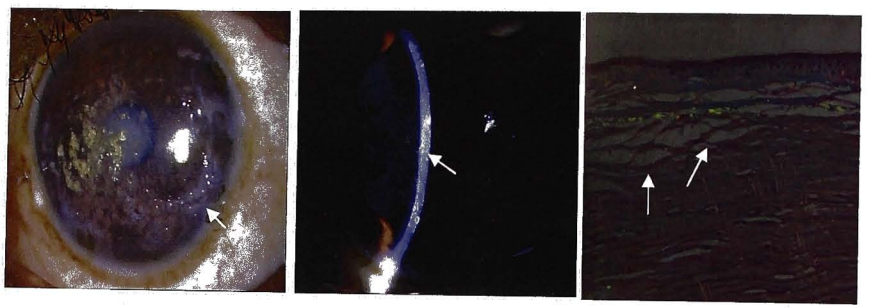

Fig 3.11: Slit lamp photographs of the cornea of proband LCD-18 showing opacities (A & B). C: Congo red-stained section of cornea of same patient showing amyloid deposits.

Table 3.2 Mutations and associated phenotypes in patients with LCD

Patient/ Family #	F/H	Sex	Age at Presen-tation	Symp-toms duration	Nature of deposits	Limbus involve-ment	Surgery	Histo Pathology	Mutation
LCD-1	Yes	M	49 yrs	3 yrs	Anterior stromal lattice lines	No	PK OS	Congo red positive	Arg124Cys
LCD-3	Yes	M	30 yrs	2 yrs	Anterior stromal lattice lines and dots	No	PK not done	-	Arg124Cys
LCD-4	Yes	F	48 yrs	5 yrs	Anterior stromal lattice lines and stromal haze	Yes OU	PTK OS	-	Arg124Cys
LCD-11	Yes	M	55 yrs	6 yrs	Anterior to mid-stromal lattice lines, stromal haze	No	PK OD	Congo red positive	Arg124Cys
LCD-14	No	F	34 yrs	4 yrs	Anterior to mid-stromal lattice lines	No	PK not done	-	Arg124Cys
LCD-15	No	F	52 yrs		Hypertrophic scaring	No	PK OD	Congo red positive	Arg124Cys
LCD-16	No	M	27 yrs	9 yrs	Anterior to mid stromal lattice lines	No	PTK OU	-	Arg124Cys
LCD-17	Yes	F	28 yrs		Lattice lines	Level not known	PK OU	Congo red positive	Arg124Cys
LCD-23	Yes	F	40 yrs	1. 6 yrs	Hypertrophic scaring	No	PK not done	Congo red positive	Arg124Cys

LCD-24	Yes	F	34 yrs	6 yrs	Pan stromal opacities	No	PK not done	-	Arg124Cys
LCD-25	No	M	50 yrs	1.5 yrs	Anterior to mid stromal thick lattice lines with Spheroidal degeneration	No	PK not done	-	Arg124Cys
LCD-26	Yes	F	38 yrs	7 yrs	Pan stromal lattice lines	No	PK OD	Congo red positive	Arg124Cys
LCD-28	Yes	F	20 yrs		Anterior stromal lattice lines	No	PK not done	-	Arg124Cys
LCD-29	Yes	M	55 yrs	31 yrs	Pan stromal lattice lines with Spheroidal degeneration	No	PK OU	Congo red positive	Arg124Cys
LCD–30	Yes	M	58 yrs	10 yrs	Pan stromal lattice lines	Yes	PK OU	Congo red positive	Arg124Cys
LCD–31	No	F	45 yrs	6 yrs	Pan stromal lattice lines	Yes	PK OS	Congo red positive	Arg124Cys
LCD-13	Yes	M	65 yrs	1 month	OU lattice lines, spheroidal degeneration	No	PK OS	Congo red positive	Val539Asp
LCD-2	Yes	M	28 yrs	1 yr	Posterior stromal lattice lines	Yes OS	PK not done	-	His626Arg
LCD-10	No	M	40 trs	7 yrs	OD anterior to mid-stromal lattice lines. Clear graft left eye	Yes OS	PK OU	Congo red positive	His626Arg

LCD-6	No	M	68 yrs	5 yrs	Mid to deep stromal thick lattice lines	Yes	PK not done	-	Gly594Val
LCD-9	No	M	72 yrs	8 months	Posterior stromal thick lattice lines	Yes OU	PK not done	-	Gly594Val
LCD-7	Yes	M	27 yrs	11 yrs	Mid to posterior stromal granular deposits, clear graft in right eye	Yes OS	PK OU	Congo red positive	Gly623Ser
LCD-20	Yes	M	30 yrs	5 yrs	Mid stromal linear opacities	No	PK OS	Congo red positive	Gly623Ser
LCD-22	No	M	60 yrs	2 yrs	Mid – deep stromal lattice lines	No	PK OD	Congo red positive	Gly623Ser
LCD-18	Yes	M	30 yrs	4 yrs	No definite lattice lines granular deposits, scaring	No	PK OD	Congo red positive	c.1917-22del
LCD-5	No	F	40 yrs		Anterior stromal lattice lines	No	PK OU	Congo red positive	None
LCD-8	No	F	60 yrs	2 months	OS clear PK OD mid stromal lattice lines, scarring	No	PK OS	Congo red positive	None
LCD-12	No	F	50 yrs	4 yrs	OU lattice lines, spheriodal degeneration	No	PK OU	Congo red positive	None
LCD-19	No	F	36 yrs	1 year	Corneal vascularity, lattice lines	No	PK OU	Congo red positive	None

Results

Patient/ Famil #	F/H	Sex	Age at Presen-tation	Symp-toms duration	Nature of deposits	Limbus involve-ment	Surgery	Histo Pathology	Mutation
LCD-1	Yes	M	49 yrs	3 yrs	Anterior stromal lattice lines	No	PK OS	Congo red ositive	Arg124Cys
LCD-3	Yes	M	30 yrs	2 yrs	Anterior stromal lattice lines and dots	No	PK not done	-	Arg124Cys
LCD-4	Yes	F	48 yrs	5 yrs	Anterior stromal lattice lines and stromal haze	Yes OU	PTK OS	-	Arg124Cys
LCD-11	Yes	M	55 yrs	6 yrs	Anterior to mid-stromal lattice lines, stromal haze	No	PK OD	Congo red positive	Arg124Cys
LCD-14	No	F	34 yrs	4 yrs	Anterior to mid-stromal lattice lines	No	PK not done	-	Arg124Cys
LCD-15	No	F	52 yrs		Hypertrophic scaring	No	PK OD	Congo red positive	Arg124Cys
LCD-16	No	M	27 yrs	9 yrs	Anterior to mid stromal lattice lines	No	PTK OU	-	Arg124Cys
LCD-17	Yes	F	28 yrs		Lattice lines	Level not known	PK· OU	Congo red ositive	Arg124Cys
LCD-23	Yes	F	40 yrs	1. 6 yrs	Hypertrophic scarin	No	PK not done	Congo red ositive	Arg124Cys
LCD-24	Yes	F	34 yrs	6 yrs	Pan stromal o acities	No	PK not done	-	Arg124Cys
LCD-25	No	M	50 rs	1.5 rs	Anterior to mid	No	PK not	-	Ar 124C s

					stromal thick lattice lines with Spheroidal degeneration		done		
LCD-26	Yes	F	38 yrs	7 yrs	Pan stromal lattice lines	No	PK OD	Congo red positive	Arg124Cys
LCD-28	Yes	F	20 yrs		Anterior stromal lattice lines	No	PK not done	-	Arg124Cys
LCD-29	Yes	M	55 yrs	31 yrs	Pan stromal lattice lines with Spheroidal degeneration	No	PK OU	Congo red positive	Arg124Cys
LCD–30	Yes	M	58 yrs	10 yrs	Pan stromal lattice lines	Yes	PK OU	Congo red positive	Arg124Cys
LCD–31	No	F	45 yrs	6 yrs	Pan stromal lattice lines	Yes	PK OS	Congo red positive	Arg124Cys
LCD-13	Yes	M	65 yrs	1 month	OU lattice lines, spheroidal degeneration	No	PK OS	Congo red positive	Val539Asp
LCD-2	Yes	M	28 yrs	1 yr	Posterior stromal lattice lines	Yes OS	PK not done	-	His626Arg
LCD-10	No	M	40 trs	7 yrs	OD anterior to mid-stromal lattice lines. Clear graft left eye	Yes OS	PK OU	Congo red positive	His626Arg
LCD-6	No	M	68 yrs	5 yrs	Mid to deep stromal thick lattice lines	Yes	PK not done	-	Gly594Val
LCD-9	No	M	72 yrs	8 months	Posterior stromal	Yes	PK not	-	Gly594Val

Results

					thick lattice lines	OU	done		
LCD-7	Yes	M	27 yrs	11 yrs	Mid to posterior stromal granular deposits, clear graft in right e e	Yes OS	PK OU	Congo red positive	Gly623Ser
LCD-20	Yes	M	30 yrs	5 yrs	Mid stromal linear o acities	No	PK OS	Congo red ositive	Gly623Ser
LCD-22	No	M	60 yrs	2 yrs	Mid – deep stromal lattice lines	No	PK OD	Congo red ositive	Gly623Ser
LCD-18	Yes	M	30 yrs	4 yrs	No definite lattice lines granular de osits, scarin	No	PK OD	Congo red positive	c.1917-22del
LCD-5	No	F	40 yrs		Anterior stromal lattice lines	No	PK OU	Congo red ositive	None
LCD-8	No	F	60 yrs	2 months	OS clear PK OD mid stromal lattice lines, scarrin	No	PK OS	Congo red positive	None
LCD-12	No	F	50 yrs	4 yrs	OU lattice lines, spheriodal de eneration	No	PK OU	Congo red positive	None
LCD-19	No	F	36 yrs	1 year	Corneal vascularity, lattice lines	No	PK OU	Congo red ositive	None

ABLE 3.2: Clinical and histopathological features of the patients with lattice corneal dystrophy. F/H - family history, PK - penetrating keratoplasty, PTK - hototherapeutic keratectomy, OD – right eye, OS - left eye, OU - both eyes.

3.1.3 Granular corneal dystrophy- Mutational screening

Probands from 31 families with GCD were included in mutational analysis. The total numbers of affected and unaffected individuals available from 31 families were 45 and 7 respectively. Diagnosis of GCD was based on clinical evaluation for 31 and confirmed by histopathology of corneal sections for 15 patients.

TABLE 3.3: summary of the *TGFBI* mutations in patients with GCD

Proba-nds (n)	Mutation in *TGFBI*		Exon	Detection method	RE site change	Co-segregation tested in relatives
	cDNA	Amino Acid				
29	c.371 G>A	Arg124 His	4	SSCP sequencing PCR-RFLP	- *Cpo1* (Abolition)	3 affected
1	c.371 G>T	Arg124 Leu	4	SSCP Sequencing PCR-RFLP	- *Cpo1* (Abolition)	2 affected
1	c.1663 C>T	Arg555 Trp	12	SSCP Sequencing PCR-RFLP	+ *Bstx1* (Creation)	40 affected, 7 unaffected

TABLE 3.3 Restriction enzyme sites altered are shown as loss (Abolition) or gain (Creation) of the site due to the mutation.

Mutations identified in GCD are summarized in Table 3.3 The most common mutation, found in 29 out of 31 families with GCD, was a change of C>T at position 1663 of the cDNA of *TGFBI* resulting in substitution of arginine-555 for tryptophan (Arg555Trp). The Arg555Trp mutation was identified as a heterozygous change in 25 families (40 affected and 7 unaffected were tested). Homozygous Arg555Trp was found in 8 affected individuals from four families

					thick lattice lines	OU	done		
LCD-7	Yes	M	27 yrs	11 yrs	Mid to posterior stromal granular deposits, clear graft in right eye	Yes OS	PK OU	Congo red positive	Gly623Ser
LCD-20	Yes	M	30 yrs	5 yrs	Mid stromal linear opacities	No	PK OS	Congo red positive	Gly623Ser
LCD-22	No	M	60 yrs	2 yrs	Mid – deep stromal lattice lines	No	PK OD	Congo red positive	Gly623Ser
LCD-18	Yes	M	30 yrs	4 yrs	No definite lattice lines granular deposits, scaring	No	PK OD	Congo red positive	c.1917-22del
LCD-5	No	F	40 yrs		Anterior stromal lattice lines	No	PK OU	Congo red positive	None
LCD-8	No	F	60 yrs	2 months	OS clear PK OD mid stromal lattice lines, scarring	No	PK OS	Congo red positive	None
LCD-12	No	F	50 yrs	4 yrs	OU lattice lines, spheriodal degeneration	No	PK OU	Congo red positive	None
LCD-19	No	F	36 yrs	1 year	Corneal vascularity, lattice lines	No	PK OU	Congo red positive	None

TABLE 3.2: Clinical and histopathological features of the patients with lattice corneal dystrophy. F/H - family history, PK - penetrating keratoplasty, PTK phototherapeutic keratectomy, OD – right eye, OS - left eye, OU - both eyes.

3.1.3 Granular corneal dystrophy- Mutational screening

Probands from 31 families with GCD were included in mutational analysis. The total numbers of affected and unaffected individuals available from 31 families were 45 and 7 respectively. Diagnosis of GCD was based on clinical evaluation for 31 and confirmed by histopathology of corneal sections for 15 patients.

TABLE 3.3: summary of the *TGFBI* mutations in patients with GCD

Proba-nds (n)	Mutation in *TGFBI*		Exon	Detection method	RE site change	Co-segregation tested in relatives
	cDNA	Amino Acid				
29	c.371 G>A	Arg124 His	4	SSCP sequencing PCR-RFLP	- *Cpo1* (Abolition)	3 affected
1	c.371 G>T	Arg124 Leu	4	SSCP Sequencing PCR-RFLP	- *Cpo1* (Abolition)	2 affected
1	c.1663 C>T	Arg555 Trp	12	SSCP Sequencing PCR-RFLP	+ *Bstx1* (Creation)	40 affected, 7 unaffected

TABLE 3.3 Restriction enzyme sites altered are shown as loss (Abolition) or gain (Creation) of the site due to the mutation

Mutations identified in GCD are summarized in Table 3.3 The most common mutation, found in 29 out of 31 families with GCD, was a change of C>T at position 1663 of the cDNA of *TGFBI* resulting in substitution of arginine-555 for tryptophan (Arg555Trp). The Arg555Trp mutation was identified as a heterozygous change in 25 families (40 affected and 7 unaffected were tested). Homozygous Arg555Trp was found in 8 affected individuals from four families

(Fig 3.12, A-D). A representative electropherogram for this sequence change is shown in Fig 3.13A.

A

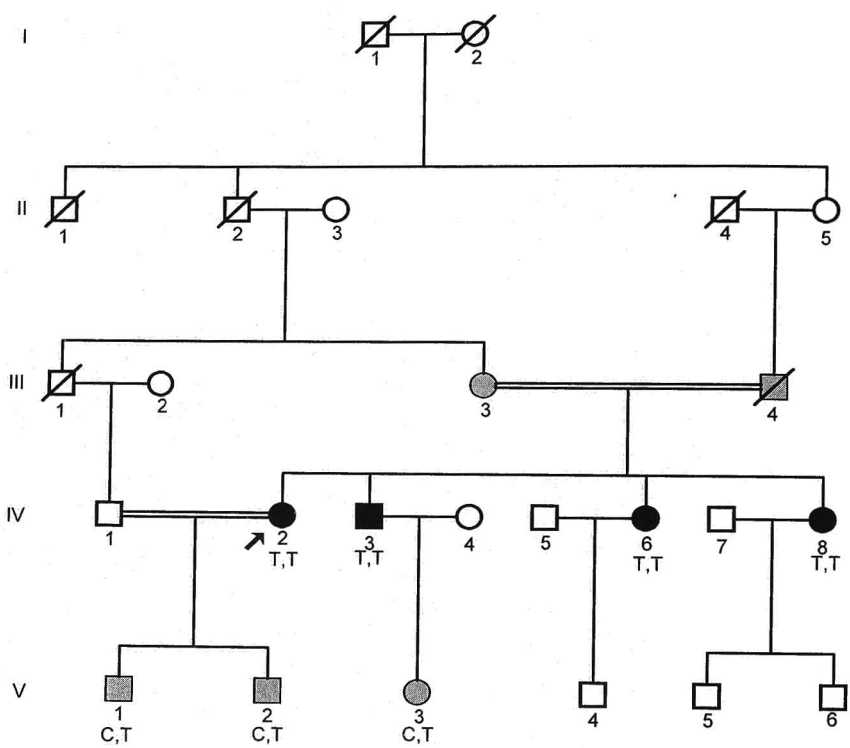

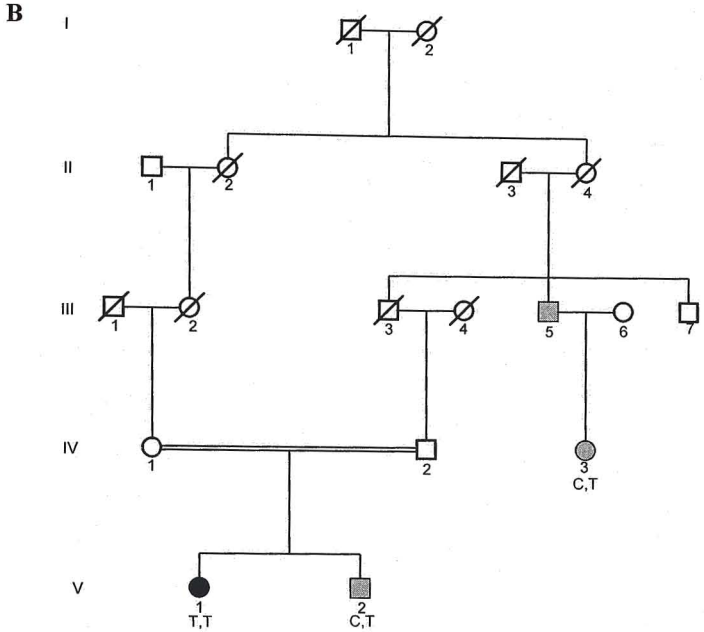
B
I
1
2
II
1
2
3
4
III
1
2
3
4
5
6
7
IV
1
2
3
C,T
V
1
T,T
2
C,T

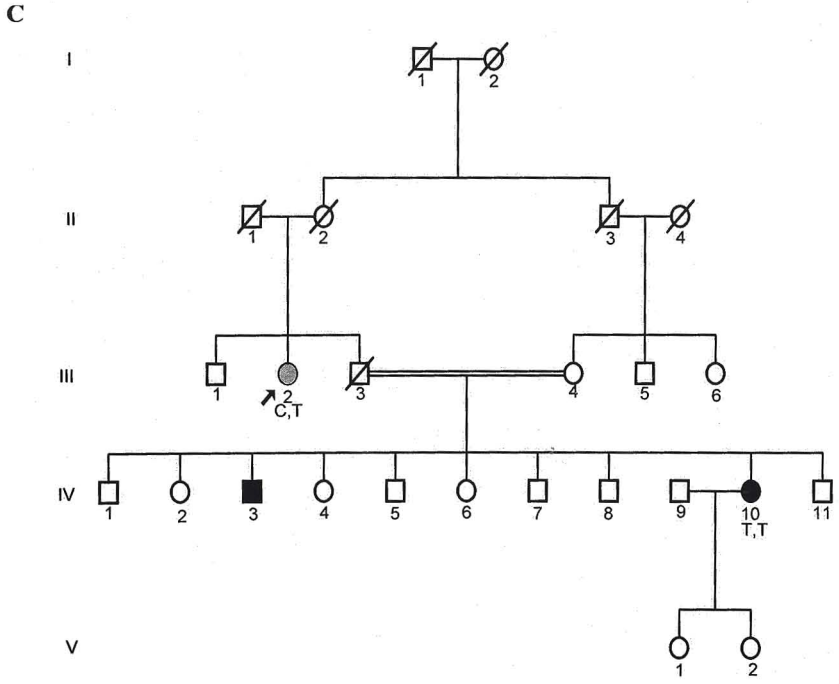
C
I
1
2
II
1
2
3
4
III
1
2
C,T
3
4
5
6
IV
1
2
3
4
5
6
7
8
9
10
T,T
11
V
1
2

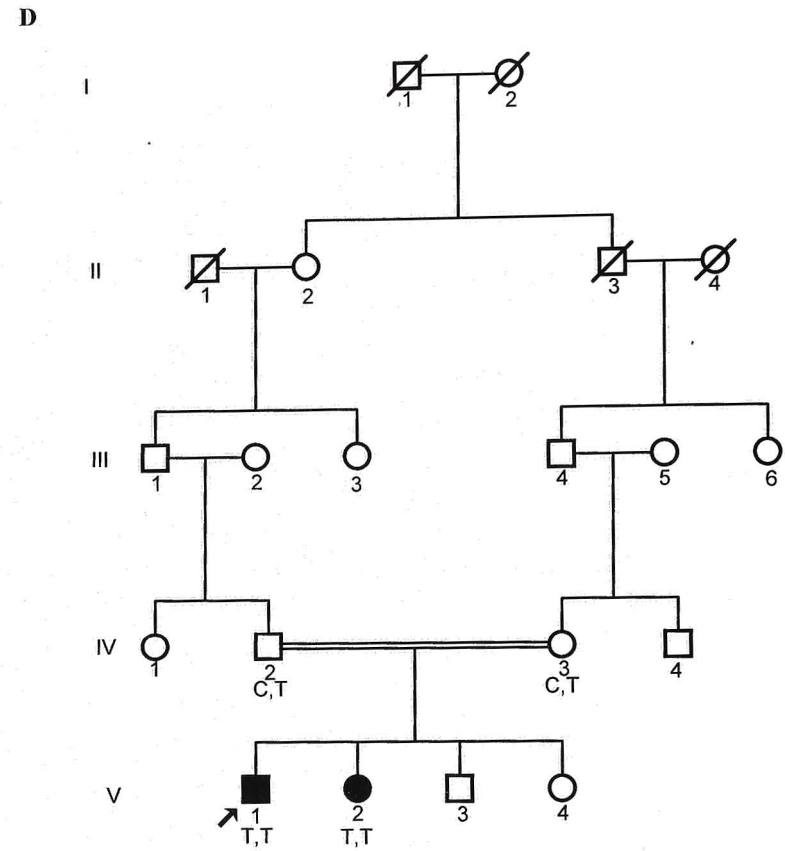

Fig 3.12: Pedigrees of families with GCD having homozygous (black symbols) and heterozygous individuals (shaded symbols). Double lines indicate consanguinity. A. Family GCD-30 B. Family GCD-28. C· Family GCD-6 D: Family GCD-29 Genotypes are indicated below each symbol.

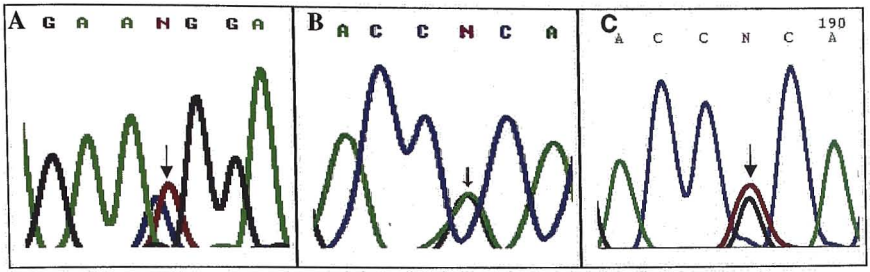

Fig 3.13: Sequence electropherograms showing mutations found in patients with GCD. A: Mutation c.1663C>T (Arg555Trp) shown for proband from family GCD-1 B: Mutation c.371G>A (Arg124His) found in family GCD-21. C: Mutation c.371G>T (Arg124Leu) found in family GCD-18.

Mutation of c.371G>A (Arg124His) (Fig 3.13B) was found in one family (Fig 3.14) (3 affected individuals tested). Digestion of the exon 4 PCR products with *Cpo 1* was used to check co-segregation of this change with disease in the family. The results are shown in Fig 3.15. This analysis showed that all the three affected members (I.2, II.2, and II.3) of the family had heterozygous mutation of Arg124His. As shown in the figure 3.15, the presence of two fragments (lane 6) of 129 bp and 152 bp indicates normal alleles and presence of an uncut fragment of 281 bp (lanes 2, 4 and 5 of Fig 3.15) along with the 129 and 152 bp fragments indicates a heterozygous mutation.

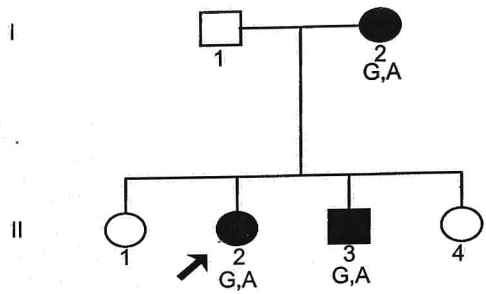

Fig 3.14: Pedigree of the family GCD–21 with Arg124His mutation showing affected and unaffected individuals. Genotypes are shown below each symbol.

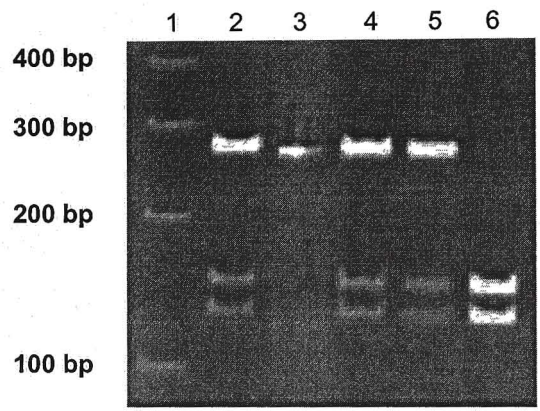

Fig 3.15: *Cpo1* restriction digestion pattern of exon 4 PCR product of family GCD-21. Lane 1:100 bp DNA size standard. Lane 2: DNA from proband (II.2 in Fig 3.14). Lane 3: undigested DNA. Lane 4: DNA from proband's mother (I.2 in Fig 3.14). Lane 5: DNA from proband's sibling (II.3 in Fig 3.14). Lane 6: DNA from normal control.

The 3rd change found in GCD was c. 371G>T (shown in Fig 3.13c) leading to mutation Arg124Leu found in one family (GCD-18) with 2 affected individuals.

The frequency of the detected mutations was 100% in patients with GCD. The mutations identified were located in either the N-terminal region (exon 4) or in the fourth fasciclin-like domain of the protein as identified in LCD. 31/31 families with GCD had mutations at either of two reported hotspots, Arg124 and Arg555. This is in contrast to data obtained from Japan and Korea where in Arg124His mutation was most prevalent [Mashima *et al.,* 2000, Fujiki *et al.,* 2000].

3.1.4 Clinical and histopathological features of patients with GCD

Mutation Arg555Trp was identified in 29 families with GCD. The patients with heterozygous Arg555Trp mutation presented with granular opacities with the extent of opacities ranging from the anterior third to the full thickness of the stroma (Table 3.4)

Four families had different individuals who were homozygous as well as heterozygous for mutation of Arg555Trp. The clinical details of these patients are shown in Table 3.4. Eight homozygous individuals from 4 families were found to have severe manifestations with an early age of onset (childhood) and dense granular opacities covering the entire cornea in the first decade of life, as shown in Fig 3.16A. Histopathology after corneal grafting of homozygotes revealed

abundant superficially located Masson-positive deposits (shown in Fig 3.16C). Eight members available for the study from these families were heterozygous for the Arg555Trp mutation. 7 of the 8 heterozygotes were found to have relatively mild phenotypes and were asymptomatic in their twenties (representative photograph shown in Figure 3.16B).

The data from 4 families with homozygous mutations showing that the two mutated alleles (homozygous) of the gene is responsible for the early occurrence of the phenotype in contrast to the phenotype resultant due to the single mutated allele (heterozygous). The onset of the phenotype in patients with two mutated alleles was early [Okada *et al.,* 1998b]. Another mutation Arg124His was also reported in families with severe phenotype [Mashima *et al.,* 1998 Fujiki *et al.,* 1998]. From our study, the data on onset of the disease, age at intervention and the recurrence period after surgery in patients with homozygous and heterozygous individuals showed that the disease onset is more severe in homozygous individuals as reported in literature, surgical intervention is required within first to second decade of life and the recurrence may be early [Okada *et al.,* 1998b]. The opacities in sub-epithelial region of the cornea may be suggestive of Reis-Bücklers corneal dystrophy, although the clinical appearance of Reis-Bücklers corneal dystrophy, which consists of fine opacities that show a geographic pattern, is different from that of the patients in our study.

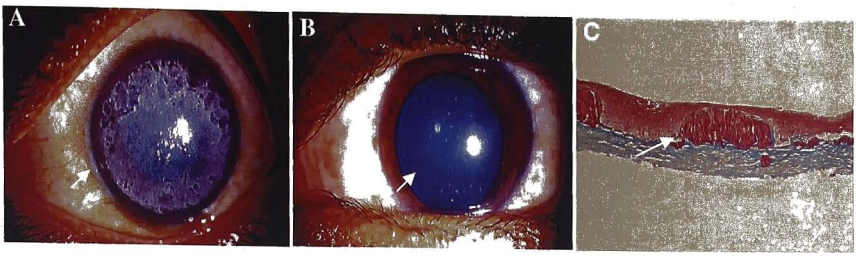

Fig 3.16: Slit lamp view of the corneas of individuals from family GCD-30 homozygous aged 40 yrs (A) and heterozygous aged 21 yrs (B) showing corneal opacities. The Masson's trichrome-stained corneal section of the patient with homozygous mutation showing sub-epithelial deposits. Arrows point to the corneal deposits.

The proband with heterozygous mutation of Arg124His (II: 2 in pedigree 3.14) had few sub-epithelial and anterior stromal grayish-white rounded opacities involving the central cornea (Fig 3.17A) at 25 yrs of age. Her mother aged 45 yrs (I:2 in pedigree) and brother aged 24 yrs (II:2 3.14), also heterozygotes, were mildly affected. Her eldest and youngest sisters (not evaluated in this study) were reported to be unaffected. The mother had an unaided visual acuity of 20/20 in both eyes. Anterior segment evaluation revealed a few anterior stromal granular opacities (Fig 3.17B) involving the central cornea. The brother of the proband (II: 3 in Fig 3.14), had no specific complaints other than refractive error. Anterior segment evaluation revealed a clear cornea in the right eye and a single granular opacity in the anterior stroma (Fig 3.17C) in the left eye.

The members of this family (pedigree 3.14) showed variable expressivity of the phenotype, with greater degree of corneal opacity in the proband (II.2 in

pedigree 3.14) who was 25 yrs old when compared to her mother who was 45 yrs old. Also, there was no evidence of co-existing lattice-like opacities in this family corresponding to a mixed granular-lattice phenotype, as has been reported in the literature in patients with the Agr124His mutation [Munier *et al.*, 1997: Korvatska *et al.*, 1999: Eifrig *et al.*, 2004].

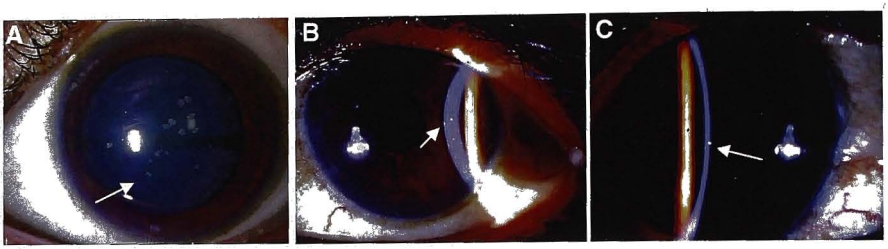

Fig 3.17: Slit lamp view of the corneas of individuals from family GCD-21. A: proband. B: proband's mother. C: proband's brother.

One patient (GCD-18) with mutation of Arg124Leu received a clinical diagnosis of Reis-Bucklers dystrophy (GCD type III) with stromal involvement, based on the presence of multiple opacities in a honeycomb pattern in the sub-epithelial and superficial stromal layers (Fig 3.18). After corneal grafting, histopathological evaluation revealed granular Masson-positive deposits in the stroma, and the patient had a recurrence of opacities in the grafted cornea. These phenotypic features are consistent with those described for Reis-Bucklers dystrophy (GCD type III) in the literature [Haddad *et al.*, 1977; Kuchle *et al.*, 1995, Okada *et al.*, 1998a, Mashima *et al.*, 1999].

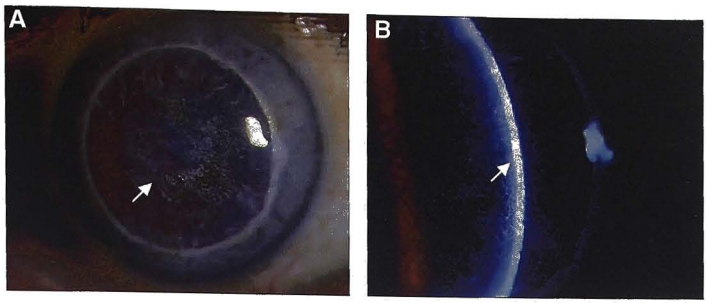

Figure 3.18: Diffuse (A) and slit view (B) of the cornea of patient GCD-18 with mutation of Arg124Leu.

3.1.5 Polymorphisms

Apart from the mutations, we found 12 single nucleotide polymorphisms (11 in LCD and 12 in GCD patients). Of the twelve single nucleotide polymorphisms (Table 3.5), seven were novel and not reported prior to this study. One of the polymorphisms found was a novel missense change of leucine-269 to phenylalanine (Leu269Phe). Significantly, this variant was found in 12/18 patients with the Arg555Trp mutation and was homozygous in individuals who were homozygous for Arg555Trp. This change was also identified in 3% (3/100) unrelated normal individuals as a heterozygous change.

The study on 31 patients with GCD and 29 patients with LCD revealed mutations in 31/31 patients with GCD and 25/29 patients with LCD. Four patients with LCD did not show mutations in coding region. Screening for the mutations may help in diagnosis of the disease in which the clinical features were

ambiguous. Finding mutations with high frequency may help in development of inexpensive PCR–RFLP based diagnostic method.

TABLE 3.4: Clinical and Histopathological features of the patients with GCD.

Patient/ family #	F/H	Sex	Age at Present-ation	Age of Onset	Nature of opacities	Limbus Involve-ment	Surgery	Histo pathology	Mutation
GCD-1	NO	F	47 yrs	4 yrs	Mid- to posterior stromal	No	PK OS	Masson's trichrome positive	Arg555Trp
GCD-2	Yes	F	52 yrs	1 yr	Full thickness of stroma	No	PK not done	-	Arg555Trp
GCD-3	Yes	M	83 yrs	7 yrs	OD failed graft OS clear pk	No	PK OU	Masson's trichrome positive	Arg555Trp
GCD-4	NO	M	35 yrs	15 yrs	OD clear graft OS full thickness	No	PK OU	Masson's trichrome positive	Arg555Trp
GCD-5	Yes	M	57 yrs	14 yrs	OD clear graft OS anterior to mid-stromal	No	PK OD	Masson's trichrome positive	Arg555Trp
GCD-6	Yes	F	71 yrs	6 yrs	Full thickness	No	PK OS	Masson's trichrome positive	Arg555Trp
GCD-7	Yes	F	56 yrs	2 yrs	Full thickness of stroma	No	PK OU	Masson's trichrome positive	Arg555Trp
GCD-8	Yes	M	43 yrs	7 yrs	Full thickness	No	PTK OD	-	Arg555Trp
GCD-9	Yes	M	48 yrs	1 yr	Full thickness	No	PK OD	Masson's	Arg555Trp

								trichrome positive	
GCD-10	Yes	F	45 yrs	6 yrs	Full thickness of stroma	No	PK not done	-	Arg555Trp
GCD-11	Yes	F	20 yrs	1 yr	Anterior 1/3 of stroma	No	PK not done	-	Arg555Trp
GCD-12	No	M	21 yrs	1 yr	Anterior to mid-stromal	No	PK not done	-	Arg555Trp
GCD-13	Yes	F	35 yrs	3 yrs	Full thickness of stroma	No	PK not done	-	Arg555Trp
GCD-15	Yes	F	45 yrs		Full thickness of stroma	No	PK not done	Masson's trichrome positive	Arg555Trp
GCD-16	NO	M	70 yrs	25 yrs	OD clear graft OS anterior 2/3rd of stroma	No	PK OS	Masson's trichrome positive	Arg555Trp
GCD-17	No	M	50 yrs	1 yr	Full thickness of stroma	No	PK not done		Arg555Trp
GCD-19	No	M	75 yrs	2 yrs	Full thickness of stroma (OS) Anterior stromal opacities (OD), spheroidal degeneration	No	PK not done	--	Arg555Trp
GCD-20	Yes	M	73 yrs		Full thickness of stroma	No	PK OD	Masson's trichrome positive	Arg555Trp
GCD-22	No	M	60 yrs	4 mon	Anterior to mid-stromal opacities	No	PK OU	Masson's trichrome positive	Arg555Trp

GCD-23	No	F	38 yrs	10 yrs	Pan-stromal opacities	No	PK OS	Masson's trichrome positive	Arg555Trp
GCD-24	Yes	M	34 yrs	1 yr	Anterior to mid-stromal opacities	No	PK not done	-	Arg555Trp
GCD-25	No	M	19 yrs	3 yrs	Pleomorphic anterior stromal opacities	No	PK not done	-	Arg555Trp
GCD-26	Yes	M	33 yrs		Mid- to posterior stromal opacities	No	PK not done	-	Arg555Trp
GCD-27	No	F	31 yrs	5 yr	Anterior to deep stromal opacities	No	PK not done	-	Arg555Trp
GCD-28	No	F	31 yrs	6 mon	Full thickness of stroma	No	PK OS	Masson's trichrome positive	Arg555Trp
GCD-29	Yes	M	9 yrs	1 yr	Superficial stromal opacities	No	PK not done	-	Arg555Trp
GCD-30	Yes	M	53 yrs	10 yrs	Pan-stromal opacities	No	PK OD	Masson's trichrome positive	Arg555Trp
GCD-31	Yes	F	40 yrs	Since childhood	Sub-epithelial opacities	Yes	PTK	-	Arg555Trp
GCD-32	Yes	F	23 yrs	Since	Sub-epithelial anterior stromal opacities	Yes	Repeat PK	Masson's trichrome positive	Arg555Trp
GCD-21	Yes	F	25 yrs	-	Anterior stromal opacities	No	PK not done	-	Arg124His
GCD-18	Yes	M		25 yrs	Sub-epithelial honeycomb- like	No	PK OD	Masson's trichrome	Arg124Leu

					opacities			positive	

TABLE 3.4: F/H - family history, PK - Penetrating Keratoplasty, PTK - Phototherapeutic Keratectomy, OD – Right eye, OS - Left eye, OU - Both eyes. Families indicated in red color have homozygous and heterozygous individuals.

TABLE 3.5: Polymorphisms identified in *TGFBI* gene.

Location	Polymorphism (codon)	Novel / Reported
Exon 6	c.651C>G (Leu217Leu)	Reported
Exon 7	c.805C>T (Leu269Phe)	Novel
Exon 7	c.816C>T (Asn272Asn)	Novel
Exon 8	c.930C>T (His310His)	Novel
Exon 8	c.981A>G (Val327Val)	Reported
Exon 11	c.1416C>T (Leu472Leu)	Reported
Exon 12	c.1584G>A (Thr528Thr)	Novel
Exon 12	c.1620C>T (Phe540Phe)	Reported
IVS12	g.29683G/A	Reported
IVS13	g.33618A/G	Novel
IVS13	g.33635T/A	Novel
IVS14	g.33836T/C	Novel

TABLE 3.5: Polymorphisms identified are shown according to position in cDNA (GenBank NM_000358.1) or genomic (GenBank NC_000005) DNA. Polymorphisms indicated in blue color are novel.

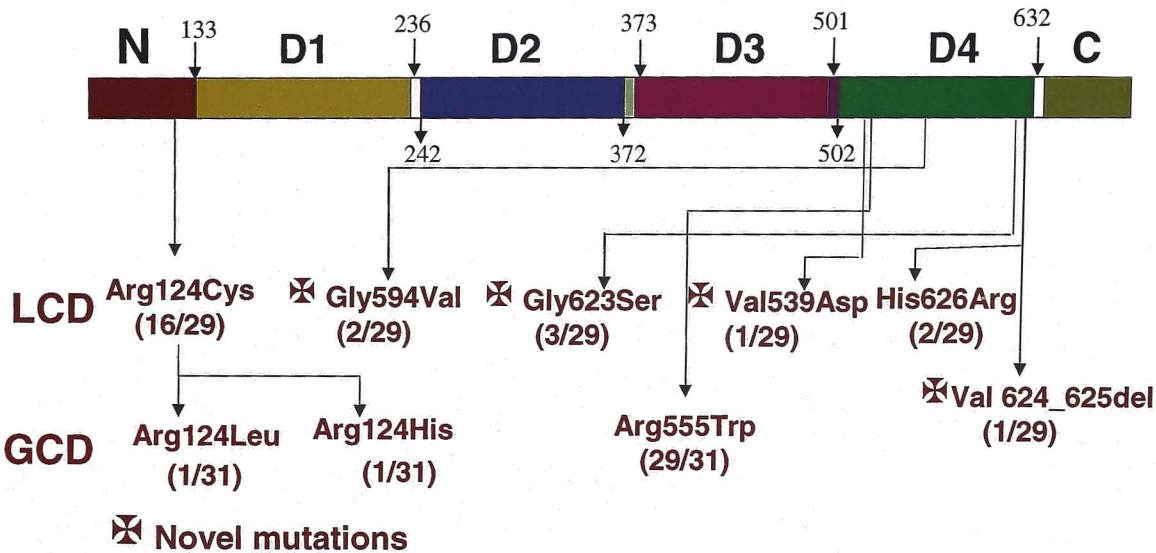

Fig 3.19: Schematic representation of the TGFBI protein showing the four FAS1 domains-DI 133-236, DII 242-372, DIII 373-501 and DIV 502-632. The N-terminal region (1-132) and C-terminal region (633-683) are shown as N&C. The locations of mutations identified in this study are shown. Numbers below each mutation refer to the numbers of patients having the mutation.

3.2 Cloning and expression of *TGFBI* cDNA

3.2.1 Construction of wild type and mutant cDNA clones

Wild type and mutant *TGFBI* cDNAs were cloned after reverse transcription-PCR using specific primers (Fig 3.20) as described in the Chapter 2. The full length (Fig 3.20) sequence of wild type and mutant clones were confirmed by direct sequencing.

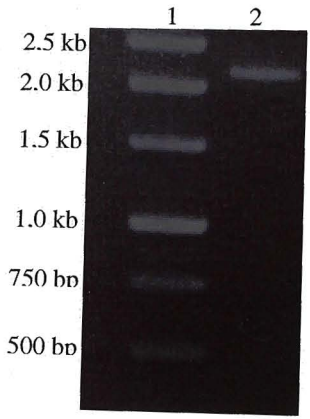

Fig 3.20: PCR amplification of *TGFBI* cDNA. I kb DNA ladder size standard (Lane 1), PCR amplified *TGFBI* cDNA of size 2.092 kb (Lane2).

3.2.2 Constructed clones

The wild type and mutant *TGFBI* cDNAs were cloned into pCMV-HA (pCMV-HA-*TGFBI*-WT-6XHis, pCMV-HA-*TGFBI*-Arg124Cys–6XHis, pCMV-HA-*TGFBI*-Arg124His, pCMV-HA-*TGFBI*-Arg124Leu and pCMV-HA-*TGFBI*-Arg555Trp)

plasmid. pCMV-HA was used to express protein with N-terminal HA tag and C-terminal His tag (the cloning strategy is given in chapter 2). Wild type and mutant *TGFBI* cDNA were cloned in addition, into pcDNA3.1(-) plasmid (Clones pcDNA3.1(-)-*TGFBI*-WT-6XHis, pcDNA3.1(-)-*TGFBI*-Arg124Cys–6XHis, pcDNA3.1(-)-*TGFBI*-Arg124His, pcDNA3.1(-)-*TGFBI*-Arg124Leu and pcDNA3.1(-)-*TGFBI*-Arg555Trp). pcDNA 3.1(-) has the CMV promoter that directs expression of the insert. In addition, the vector contains a neomycin resistance gene for selection of stably transfected cells. The sequence of the insert and insert /vector junctions were confirmed by direct sequencing.

3.2.3 Expression of the wild type and mutant TGFBI cDNA clones in cell lines

Human corneal epithelial (HCE), HeLa and Cos I cells were used for transient expression of the wild type and mutant *TGFBI* cDNA expression plasmids. The transfection procedure was standardized using pEGFP vector, which codes for the enhanced green fluorescent protein (EGFP) expressed from the cytomegalovirus immediate-early promoter (Invitrogen Corporation Ltd, Faraday Avenue, Carlsbad, California, USA). Amounts of plasmid tested were 0.2 μg, 0.5 μg, 1μg, 2 0.μg; volume of lipofectamine reagent was varied from 2 to 4 microliters, and time periods of 12 hrs, 24 hrs, 48 hrs and 72 hrs between transfection and harvest were tested to determine optimum efficiency of transfection. Transfection efficiency was maximal at about 30% of cells expressing green fluorescent protein per field (average from 3 fields) in 2

different wells and was obtained at 0.5 μg of plasmid DNA in 2.0 μl of lipofectamine at 24 hrs post-transfection. pEGFP-transfected cells are shown in Fig 3.21.

The transfection efficiency obtained with pCMV-HA-*TGFBI*-WT-6XHis was higher in HeLa and Cos1 cells as compared to HCE cells on immuno-staining with mouse anti-His antibodies. The immunofluorescence assay using mouse anti–HA antibody did not give any detectable signal with pCMV-HA-*TGFBI*-WT-6XHis transfected cells. Maximum amount of expression of transfected plasmid (estimated as the average number of cells showing fluorescence per field) obtained from pCMV-HA-*TGFBI*-WT-6XHis plasmid was 10/200 or 5% in HeLa and Cos 1 cells and less than 1% in HCE cells (Fig 3.21b). Using optimized parameters, transfections were initially performed with plasmids encoding *TGFBI* wild type, Arg124Cys, and Arg124His proteins in HeLa and Cos1 cells (shown in Figs 3.22 & 3.23). As shown in the figure there was no observable difference in the intracellular localization of the wild type and the two mutant proteins.

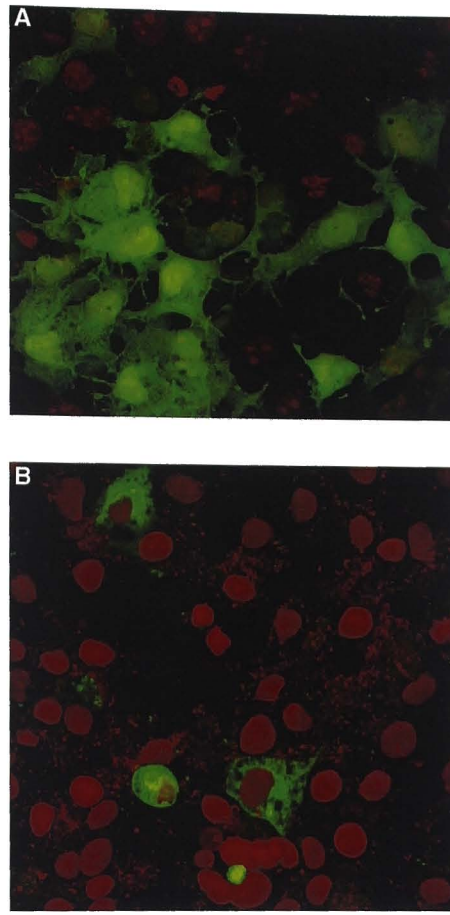

Fig 3.21: A: pEGFP transfected Cos1 cells counterstained with propidium iodide showing green fluorescence in cells expressing EGFP (confocal microscope, excitation wavelength of 488-543nm and emission wavelength of 505-530nm, magnification 400X). B: pCMV-HA-*TGFBI*-WT-6XHis transfected Cos1 cells immuno-stained with anti–His antibody (magnification 400X)

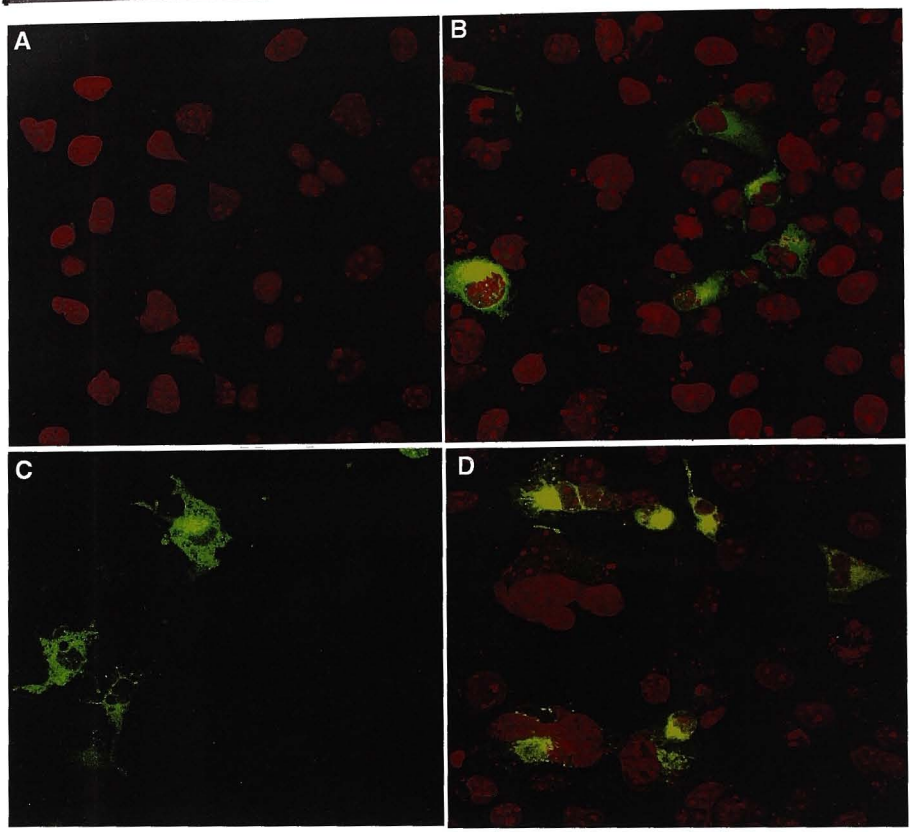

Fig 3.22: Fluorescent confocal microscopic images of the untransfected and transfected Cos1 cells (counterstained with propidium iodide, confocal microscope, excitation wavelength of 488-543 nm and emission wavelength of 505-530nm, magnification 400X) A: untransfected Cos1 cells. B: cells transfected with wild type *TGFBI* clone. C: cells transfected with the *TGFBI*-Arg124Cys mutant clone D: cells transfected with *TGFBI*-Arg124His mutant clone.

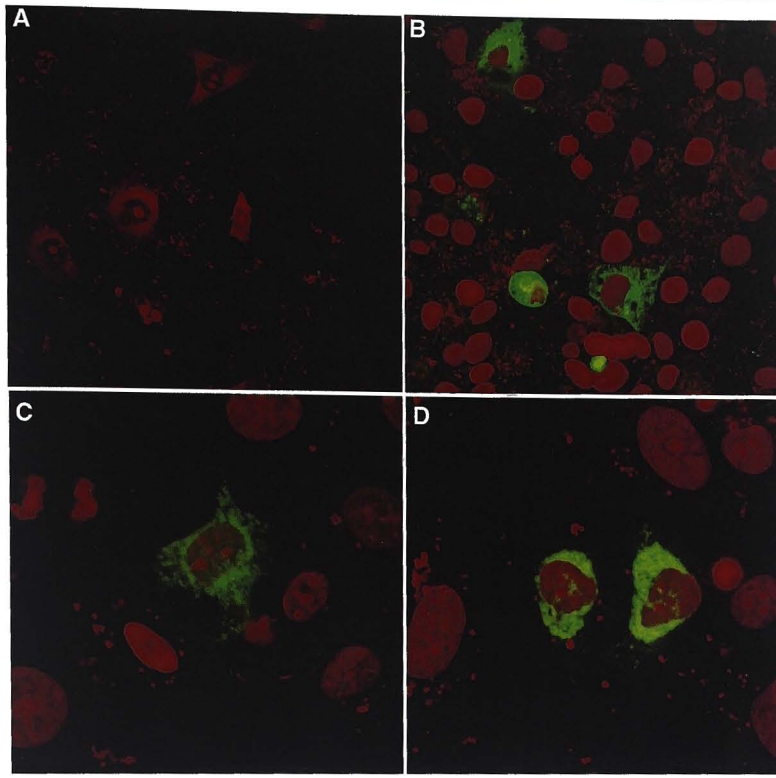

Fig 3.23: Untransfected and transfected Hela cells (counterstained with propidium iodide, confocal microscope, range of excitation wavelength 488-543nm and emission wavelength 505-530nm; (magnification 400X (Un transfected and wild type), 400X3 (Arg124Cys and Arg124His). A: untransfected cells. B: cells transfected with wild type *TGFBI* clone. C: cells transfected with the *TGFBI*-Arg124Cys mutant clone D: cells transfected with *TGFBI*-Arg124His mutant clone

Since detectable expression of the *TGFBI* protein was very low in transfected cells, one possible explanation is that being a known extracellular protein with a secretory signal, most of the protein expressed from the

transfected cDNA was being secreted into the tissue culture medium. The attempt to detect recombinant protein secreted into the medium, Western blotting of protein precipitates of the tissue culture medium was carried out as described in Chapter 2. Tissue culture medium was collected at 12 hrs, 24 hrs, 48 hrs and 72 hrs after transfection. In parallel, lysates of transfected cells were prepared and subjected to Western blotting. We could not detect the protein on Western blots using mouse anti-HA or mouse anti-His antibody in either the medium or the cell extracts suggesting that either the recombinant protein was not being secreted or that it was present in the extracellular medium at very low levels and therefore could not be detected by Western blot.

TGFBI wild type and mutant cDNAs cloned into the pcDNA3.1 plasmid having the neomycin-resistance gene was then carried out to achieve stable expression of the TGFBIp in the transfected cells. This was done in order to get a higher proportion of cells positive for recombinant *TGFBI* expression. The transfection of pcDNA3.1 *(-)-TGFBI*-WT-6XHis, *pcDNA3.1 (-)-TGFBI*-Arg124Cys–6XHis, *pcDNA3.1 (-)-TGFBI*-Arg124His clones into Cos 1 and HeLa cells was followed by selection of cells in medium containing 0.2 mg to 0.8 mg/ml G418. Cells were grown in selective medium for 7 days and then harvested for immunodetection. Despite the selection process, the fraction of cells showing recombinant *TGFBI* expression was similar to the transiently transfected cells. No difference was noted between the wild type and mutant clones.

The experiments carried out to understand the role of the mutants in disease pathogenesis in our study did not give any conclusive information. As we have seen in our experiments we could not detect any difference in the intracellular localization of the transiently expressed wild type and mutant proteins. This is similar to a previous study [Kim et al., 2002] that did not find any significant difference between wild type and mutants in a cell culture system. The inability in detection of the protein in extracellular milieu could be due to the low level of expression of the transfected protein. From our studies, there was no evident intracellular retention or accumulation of mutant proteins in the cell culture systems tested.

Chapter 4

Discussion

4.0 Discussion

This is the first report from India to our knowledge, reporting analysis of a series of 31 patients with GCD and 29 patients with LCD Herein we made an attempt to identify the underlying *TGFBI* gene variations in patients with LCD and GCD and further correlated the genotype with phenotype. In our study 9 mutations were found in 60 families including both GCD and LCD. All except one family showed missense mutations. Till date 1 frameshift [Munier *et al.*, 2002], 1 insertion [Schmitt-Bernard *et al.*,2000] and 5 deletions [Dighiero *et al.*, 2000, Rozzo et al , 1998, Aldave *et al.*, 2006] have been reported in literature. The mutations in LCD are several and involve the N-terminal region and the fourth Fas 1 internal domain of the protein as described in the literature [Kannabiran & Klintworth, 2006; Aldave *et al.*, 2007]. Similar to this, we also identified Arg124Cys involving the N-terminus of the protein, and 5 other mutations-Val539Asp, Gly594Val, Gly623Ser, Val624_V625del and His626Arg, all located in the fourth Fas1 domain of the protein. In comparison to LCD, the mutation spectrum of GCD is less divergent and only 5 mutations in the N-terminal region and 5 mutations in the fourth internal domain of the protein are reported to cause GCD [reviewed by Kannabiran & Klintworth, 2006; Aldave *et al.*, 2007]. In our study we identified mutations of Arg124His and Arg124Leu located in the N-terminal region and Arg555Trp in the fourth Fas 1 domain of the protein.

Among all the mutations identified in our study Arg124Cys (found in 16/29 pts) was the most frequent mutation in LCD and Arg555Trp (found in 29/31) was the predominant one in GCD. This is similar to data obtained on other populations such as those from Japan [Mashima *et al.,* 2000, Fujiki *et al.,* 2000], Hungary [Takacs *et al.,* 2007], Ukraine [Pampukha *et al.,* 2004], and in Western populations [Munier *et al.,* 1997, Korvatska 1998, Afshari *et al.,* 2001, Munier *et al.,* 2002]. In contrast, data from a study on Vietnamese patients with LCD found that mutation of His626Arg may be more frequent [Chau *et al.,* 2003] and from Japan and Korea showing that mutation Arg124His is the most frequent mutation among patients with GCD [Mashima *et al.,* 2000, Fujiki *et al.,* 2000]. In general, the phenotypes of the patients with the mutations at the 2 hotspots of Arg124 and Arg555 were similar to earlier reports. The phenotypes associated with novel mutations Val539Asp, Gly594Val, Gly623Ser, Val624_V625del were distinct from one another. The Val539Asp mutation was associated with typical lattice-like opacities as seen in LCD type I. This adds to the spectrum of mutations reported for typical forms of LCD. Two patients from different families with mutation of Gly594Val showed similar phenotypes involving late onset (6^{th} -7^{th} decade), with mid- to deep stromal, thick lattice opacities. These features describe a variant form of LCD similar to what has been reported with 3 other mutations (Leu527Arg, Asn544Ser and Val631Asp) in the literature [Fujiki *et al.,* 1998; Nakagawa Asahina *et al.,* 2004; Munier *et al.,* 2002]. An atypical phenotype was

also found in association with the mutation Val624_Val625del in the present study. We did not find evidence of clinically detectable lattice lines in this patient This would add to the spectrum of the atypical phenotypes reported for different *TGFBI* mutations including Asp123His [Ha *et al.,* 2003], Arg124Cys [Nakamura *et al.,* 2000, Morishige *et al.,* 2004 and Yoshida *et al.*, 2004 and El-Ashry *et al.*, 2004], Val624Met [Afshari *et al.*, 2004] and Phe547Ser [Takacs *et al.,* 2007].

The 4th novel mutation Gly623Ser identified in the present study was found in both heterozygous and homozygous individuals. In homozygous state, the mutation was associated with a more severe phenotype with earlier onset of disease (2nd decade of life), though there was variability of phenotype between 2 probands. In one heterozygous patient, opacities were mild and the disease was evidently of later onset (6th decade) The earlier onset and more severe phenotype in case of homozygosity for dominant mutations was also reported for Arg124His [Mashima *et al.,* 1998, Fujiki *et al.*, 1998] and Arg555Trp [Okada *et al.,* 1998b] mutations that cause granular dystrophy. In our study, we observed homozygous and heterozygous individuals with Arg555Trp in four families. Similar to previous reports in literature [Okada *et al.,* 1998b], the homozygous individuals having Arg555Trp mutation showed severe phenotypes and an early age of onset [Okada *et al.,* 1998b]. The severe phenotype in individuals with homozygous mutations could be due to a greater amount of mutant protein.

The mutation Arg124His has been associated with combined lattice-granular or Avellino corneal dystrophy [Munier *et al.*, 1997]. The family described by us with mutation of Arg124His showed granular opacities but no signs of lattice-type of opacities. In the present study we identified one family with Arg124Leu showing characteristics of Reis-Bucklers corneal dystrophy with honey-comb shaped Masson's positive opacities that were in the superficial stroma, in agreement with earlier reports [Haddad *et al.*, 1977; Kuchle *et al.*, 1995, Okada *et al.*, 1998b, Mashima *et al.*, 1999].

From our data it is apparent that *TGFBI* associated corneal dystrophies comprise both typical and atypical phenotypes. Further, this study supports the genotype-phenotype correlations derived for the common *TGFBI* mutations causing LCD and GCD in previous studies [Kannabiran & Klintworth, 2006]. Detection of mutations in the majority of patients suggests that mutation analysis of *TGFBI* may help in confirming the diagnosis of the disease where the clinical features are ambiguous.

Very few attempts have been made to elucidate the role of *TGFBI* gene mutations in disease pathogenesis. Takacs *et al.*, [1998] in a study showed the difference in localization of TGFBIp in normal (epithelium) and dystrophic corneas (sub-epithelium). Electrophoretic analysis of protein from deposits showed an additional 42 kDa band in dystrophic patients. Immunohistochemical studies on LCD type I and GCD types I & II by Korvatska and co-workers (1999)

with different antibodies specific for N-terminal and C-terminal regions of the TGFBIp showed the presence of C-terminal fragments in corneal deposits in a cornea with GCD type I, whereas N-terminal fragments were detected in a cornea with LCD type 1. Both types of protein degradation products were found in the cornea having Avellino corneal dystrophy. They hypothesized that the turnover of the protein may differ with each specific mutation [Korvatska *et al*, 1999]. In a subsequent study, Korvatska *et al.*, [2000] showed mutation-specific accumulation of the TGFBIp protein products in corneas of patients with Arg124Cys, Arg124His and Arg124Leu mutations On the other hand, a study on overexpression of TGFBI mutant and wild type proteins in cell-lines did not show any difference in turnover products [Kim *et al.*, 2002b]. The failure to detect differences in protein turnover in cell culture systems [Kim *et al.*, 2002b] in contrast to mutation-specific degradation products in intact corneas of patients with lattice and granular corneal dystrophies [Takacs *et al.*, 1998; Korvatska *et al.*, 1999; Korvatska *et al.*, 2000] could be to the interactions between TGFBIp protein with the other proteins in the milieu of the extracellular matrix of the cornea. It may also indicate that accumulation of degraded or intact mutant protein is a slow process that cannot be visualized in a short term culture system.

The experiments carried out to understand the role of the mutants in disease pathogenesis in our study did not give any conclusive information. As we have seen in our experiments we could not detect any difference in the

intracellular localization of the transiently expressed wild type and mutant proteins. This is similar to a previous study [Kim et al., 2002b] that did not find any significant difference between wild type and mutants in human corneal epithelial cells. The lack of detection of secreted TGFBI protein in tissue culture medium could be due to the low level of expression of the recombinant protein. From our studies, there was no evident intracellular retention or accumulation of mutant proteins in the cell culture systems tested.

Summary

SUMMARY

Chapter 1: Introduction and literature review

This chapter gives a brief description of the structure of the cornea followed by a review of lattice and granular corneal dystrophies. The aspects of these disorders that are discussed include the clinical and histopathological characteristics, as well as the underlying molecular genetic bases and structure, function and interactions of the TGFBI protein in extracellular mileu with other proteins. The background for the present study is followed by statement of the aims and objectives of the study.

Chapter 2: Materials and Methods

This chapter provides the details of methods employed including enrollment of patients and sample collection, principles and procedures of the various molecular genetic techniques, cloning, site-directed mutagenesis, cell culture, transfection and immunoflurorescence assay and Western blotting.

Chapter 3: Mutation screening and genotype-phenotype correlations

This chapter presents the results of molecular genetic analysis of lattice and granular corneal dystrophies, correlations of genotype with phenotype, and

studies on transient expression of the wild type and mutant clones of *TGFBI* by expression in HCE, Cos1, and HeLa cell lines.

Important findings of the present study

Lattice corneal dystrophy

The frequency of the detected mutations in in *TGFBI* gene was 87% in patients with LCD. The mutations identified were located at either a) one of the hotspots at Arg124 or Arg555 or b) in residues in the fourth fasciclin-like domain of the protein. 16 of the 29 families with LCD had mutations at Arg124. 4 novel mutations found in patients with LCD were Val539Asp, Gly594Val, Gly623Ser, and Val624_Val625del. Unusual phenotypes found in association with some of these mutations were presented.

Granular corneal dystrophy

The frequency of the detected mutations in *TGFBI* gene was 100% in patients (from 31 families) with GCD. The mutations identified were located involved only either of the two hotspot residues Arg124 or Arg555 mutations. The predominant mutation was Arg555Trp found in 29/31 probands with GCD. Mutation Arg124His in exon 4 was found in one family, and Arg124Leu, also in exon 4, was found in one family. Arg555Trp was found in homozygous state in 4 families. As compared with patients who had a single Arg555Trp allele who had a milder form of disease, individuals who were homozygous for Arg555Trp

showed childhood-onset disease with dense opacities and severe visual loss. The patients with mutation Arg124His showed a mild phenotype with granular opacities. One patient with mutation Arg124Leu showed features of GCD type III

Experiments involving transient expression of TGFBI wild type and mutant clones in cell culture did not show any detectable differences between wild type and mutant proteins.

References

REFERENCES

Afshari NA, Mullally JE, Afshari MA, Steinert RF, Adamis AP, Azar DT, Talamo JH, Dohlman CH, Dryja TP. 2001. Survey of patients with granular, lattice, Avellino, and Reis-Bucklers corneal dystrophies for mutations in the BIGH3 and gelsolin genes. *Arch Ophthalmolw* 119:16–22

Afshari N, Bahadur RP, Klintworth GK. 2004. Discovery of novel homozygous mutation in the TGFBI (BIGH3) gene (V624M) in a patient with unilateral lattice corneal dystrophy. Invest Ophthalmol Vis Sci 45: E-abstract 1517.

Aitkenhead M, Wang SJ, Nakatsu MN, Mestas J, Heard C, Hughes CC. 2002 Identification of endothelial cell genes expressed in an in vitro model of angiogenesis: induction of ESM-1, (beta)ig-h3, and NrCAM. *Microvasc Res* 63:159-171.

Aldave AJ, Rayner SA, Kim BT, Prechanond A, Yellore VS 2006. Unilateral lattice corneal dystrophy associated with the novel His572del mutation in the TGFBI gene. *Mol Vis* 12:142-146

Aldave AJ, Sonmez B. 2007. Elucidating the molecular genetic basis of the corneal dystrophies: are we there yet? *Arch Ophthalmol.* 125:177-86. Review.

Bae JS, Lee SH, Kim JE, Choi JY, Park RW, Yong Park J, Park HS, Sohn YS, Lee DS, Bae Lee E, Kim IS. 2002. Betaig-h3 supports keratinocyte adhesion, migration, and proliferation through alpha3beta1 integrin. *Biochem Biophys Res Commun* 294:940-948.

Bastiani MJ, Harrelson AL, Snow PM, Goodman CS. 1987 Expression of fasciclin I and II glycoproteins on subsets of axon pathways during neuronal development in the grasshopper. *Cell* 48:745-755.

Behnke H, Thiel HJ. 1965. Ueber die hereditaere Epitheldystrophieder Hornhaut (Typ Meesman-Wilke) in Schleswig-Holstein [On hereditary epithelial dystrophy of the cornea (type Meesmann-Wilke) in Schleswig-Holstein]. *Klin Monatsbl Augenheilkd* 147:662–672.

Berman M, Manseau E, Law M, Aiken D. 1983. Ulceration is correlated with degradation of fibrin and fibronectin at the corneal surface. *Invest Ophthalmol Vis Sci* 24:1358-1366.

Biber, Hugo. 1890. Uber einige seltenere Hornhauterkrankungen. IV. " Die oberflachliche gittrige Keratitis." *Dissertation Zurich*, pp. 35-42.

Billings PC, Whitbeck JC, Adams CS, Abrams WR, Cohen AJ, Engelsberg BN, Howard PS, Rosenbloom. 2002. The transforming growth factor-beta-inducible matrix protein (beta) ig-h3 interacts with fibronectin. *J Biol Chem* 277:28003–28009.

Bucklers, M. (1938) Ber. *dtsch. ophthal. Ges* 52: 441

Chau HM, Ha NT, Cung LX, Thanh TK, Fujiki K, Murakami A, Kanai A. 2003. H626R and R124C mutations of the TGFBI (BIGH3) gene caused lattice corneal dystrophy in Vietnamese people. *Br J Ophthalmol* 87:686–689.

Dighiero P, Drunat S, D'Hermies F, Renard G, Delpech M, Valleix S. 2000. A novel variant of granular corneal dystrophy caused by association of 2 mutations in the TGFBI gene-R124L and DeltaT125-DeltaE126. *Arch Ophthalmol* 118:814–818.

Dimmer. 1899. Uber oberflachliche gitterige Hornhiuttrubung. *Z.Augenheilk' II*: 354-361.

Doran TI, Vidrich A, Sun TT. 1980. Intrinsic and extrinsic regulation of the differentiation of skin, corneal and esophageal epithelial cells. *Cell* 22:17-25.

Dubord PJ, Krachmer JH. 1982. Diagnosis of early lattice corneal dystrophy. *Arch Ophthalmol* 100.788-790

Eifrig DE Jr, Afshari NA, Buchanan HW IV, Bowling BL, Klintworth GK. 2004a Polymorphic corneal amyloidosis: a disorder due to a novel mutation in the transforming growth factor beta-induced (BIGH3) gene. *Ophthalmology* 111 1108–1104.

El-Ashry MF, Abd El-Aziz MM, Ficker LA, Hardcastle AJ, Bhattacharya SS, Ebenezer ND. 2004. BIGH3 mutation in a Bangladeshi family with a variable phenotype of LCDI. *Eye*.18: 723-728.

Endo S, Nguyen TH, Fujiki K, Hotta Y, Nakayasu K, Yamaguchi T, Ishida N, Kanai A. 1999. Leu518Pro mutation of the beta ig-h3 gene causes lattice corneal dystrophy type I. *Am J Ophthalmol* 128:104–106.

Escribano J, Hernando N, Ghosh S, Crabb J, Coca-Prados M 1994. cDNA from human ocular ciliary epithelium homologous to beta ig-h3 is preferentially expressed as an extracellular protein in the corneal epithelium. *J Cell Physiol* 160: 511-21.

Folberg R, Alfonso E, Croxatto JO, Driezen NG, Panjwani N, Laibson PR, Boruchoff SA, Baum J, Malbran ES, Fernandez- Meijide R, Morrison JA Jr, Bernadino VB, Arbizo VV, Albert DM. 1988. Clinically atypical granular corneal dystrophy with pathologic features of lattice-like amyloid deposits. A study of three families. *Ophthalmology* 95:46–51.

Fujiki K, Hotta Y, Nakayasu K, Yokoyama T, Takano T, Yamaguchi T, Kanai A. 1998. A new L527R mutation of the betaIGH3 gene in patients with lattice corneal dystrophy with deep stromal opacities. *Hum Genet* 103:286–289.

Fujiki K, Hotta Y, Nakayasu K, Yamaguchi T, Kato T, Uesugi Y,Ha NT, Endo S, Ishida N, Lu WN, Kanai A. 2000. Six different mutations of TGFBI (betaig-h3,

keratoepithelin) gene found in Japanese corneal dystrophies. *Cornea* 19: 842–845.

Gibson MA, . Hatzinikolas G, Kumaratilake JS, Sandberg LB, Nicholl JK, Sutherland GR, Cleary EG. 1996. Further characterization of proteins associated with elastic fiber microfibrils including the molecular cloning of MAGP-2 (MP25). *J Biol Chem* 271.1096–1103.

Groenouw A. 1890. Knotchenformige Hornhauttrubungen (Noduli corneae). *Arch.Augenheilk* 21:281-289.

Haab. 1899. Die gittrige Keratitis. *Zeitschr. f. Augenheilk* II: 235-246.

Haddad R, Font RL, Fine BS. 1977. Unusual superficial variant of granular dystrophy of the cornea. *Am J Ophthalmol* 83: 213–218.

Hashimoto K, Noshiro M, Ohno S, Kawamoto T, Satakeda H, Akagawa Y, Nakashima K, Okimura A, Ishida H, Okamoto T, Pan H, Shen M, Yan W, Kato Y. 1997. Characterization of a cartilage-derived 66-kDa protein (RGD-CAP/betaig-h3) that binds to collagen. *Biochim Biophys Acta* 1355:303–314.

Hayashi K, Yandell DW. 1993. How sensitive is PCR-SSCP?. *Hum Mutat* 2:338-346.

Hida T, Proia AD, Kigasawa K, Sanfilippo FP, Burchette JL Jr, Akiya S, Klintworth GK. 1987a. Histopathologic and immunochemical features of lattice corneal dystrophy type III. *Am J Ophthalmol* 104:249–254.

Hida T, Tsubota K, Kigasawa K, Murata H, Ogata T, Akiya S. 1987b. Clinical features of a newly recognized type of lattice corneal dystrophy. *Am J Ophthalmol* 104:241–248.

Hirate Y, Okamoto H, Yamasu K. 2003. Structure of the zebrafish fasciclin I-related extracellular matrix protein (betaig-h3) and its characteristic expression during embryogenesis. *Gene Expr Patterns* 3:331-336.

Holland EJ, Daya SM, Stone EM, Folberg R, Dobler AA, Cameron JD, Doughman DJ. 1992. Avellino corneal dystrophy. Clinical manifestations and natural history. *Ophthalmology*. 99.1564-1568

Hourihan RN, O'Sullivan GC, Morgan JG. 2003. Transcriptional gene expression profiles of oesophageal adenocarcinoma and normal oesophageal tissues. *Anticancer Res* 23:161-165.

Jones ST, Zimmerman LE 1961. Histopathologic differentiation of granular, macular and lattice dystrophies of the cornea *Am J Ophthalmol* 51:394-410

Kannabiran C, Klintworth GK 2006. TGFBI gene mutations in corneal dystrophies. *Hum Mutat* 27:615-25. Review.

Kim JE, Kim EH, Han EH, Park RW, Park IH, Jun SH, Kim JC, Young MF, Kim IS. 2000 A TGF-beta-inducible cell adhesion molecule, betaig-h3, is downregulated in melorheostosis and involved in osteogenesis. *J Cell Biochem* 77:169-178.

Kim JE, Jeong HW, Nam JO, Lee BH, Choi JY, Park RW, Park JY, Kim IS. 2002a. Identification of motifs in the fasciclin domains of the transforming growth factor-beta-induced matrix protein betaig-h3 that interact with the alphavbeta5 integrin. *J Biol Chem* 277:46159–46165.

Kim JE, Park RW, Choi JY, Bae YC, Kim KS, Joo CK, Kim IS. 2002b. Molecular properties of wild-type and mutant betaIG-H3 proteins. *Invest Ophthalmol Vis Sci* 43:656-61.

Kim MO, Yun SJ, Kim IS, Sohn S, Lee EH. 2003. Transforming growth factor-beta-inducible gene-h3 beta(ig)-h3) promotes cell adhesion of human astrocytoma cells in vitro: implication of alpha6beta4 integrin. *Neurosci Lett* 336:93–96.

Klintworth GK. 1967. Lattice corneal dystrophy: an inherited variety of amyloidosis restricted to the cornea. *Am J Path* 50: 371–399.

Klintworth GK, Bao W, Afshari NA. 2004. Two mutations in the TGFBI (BIGH3) gene associated with lattice corneal dystrophy in an extensively studied family. *Invest Ophthalmol Vis Sci* 45:1382–1388.

Korvatska E, Munier FL, Djemaï A, Wang MX, Frueh B, Chiou AG, Uffer S, Ballestrazzi E, Braunstein RE, Forster RK, Culbertson WW, Boman H, Zografos L, Schorderet DF. 1998. Mutation hot spots in 5q31-linked corneal dystrophies. *Am J Hum Genet* 62:320-4.

Korvatska E, Munier FL, Chaubert P, Wang MX, Mashima Y, Yamada M, Uffer S, Zografos L, Schorderet DF. 1999. On the role of kerato-epithelin in the pathogenesis of 5q31-linked corneal dystrophies. *Invest Ophthalmol Vis Sci* 40:2213–2219.

Korvatska E, Henry H, Mashima Y, Yamada M, Bachmann C,Munier FL, Schorderet DF. 2000. Amyloid and non-amyloid forms of 5q31-linked corneal dystrophy resulting from kerato-epithelin mutations at Arg-124 are associated with abnormal turnover of the protein. *J Biol Chem* 275: 11465–11469.

Kuchle M, Green WR, Volcker HE, Barraquer J. 1995. Reevaluation of corneal dystrophies of Bowman's layer and the anterior stroma (Reis-Bucklers and Thiel-Behnke types): a light and electron microscopic study of eight corneas and a review of the literature. *Cornea* 14:333–354.

Kuwahara Y, Akiya S, Obazawa H. 1967 Electron microscopic study on granular dystrophy, macular dystrophy and gelatinous drop-like dystrophy of the cornea *Nippon Ganka Kiyo*. 18.434-435

Laule A, Cable MK, Hoffman CE, Hanna C. 1978 Endothelial cell population changes of human cornea during life. *Arch Ophthalmol* 96:2031-2035.

LeBaron RG, Bezverkov KI, Zimber MP, Pavelec R, Skonier J, Purchio AF 1995. Beta IG-H3, a novel secretory protein inducible by transforming growth factor-beta, is present in normal skin and promotes the adhesion and spreading of dermal fibroblasts in vitro *J Invest Dermatol.* 104.844-849

Lee BH, Bae JS, Park RW, Kim JE, Park JY, Kim IS. 2006. betaig-h3 triggers signaling pathways mediating adhesion and migration of vascular smooth muscle cells through alphavbeta5 integrin. *Exp Mol Med* 38:153-161.

Matsuo N, Fujiwara H, Ofuchi Y. 1967. Electron and light microscopic observations of a case of Groenouw's nodular corneal dystrophy. *Nippon Ganka Kiyo* 18:436-447.

Mashima Y, Konishi M, Nakamura Y, Imamura Y, Yamada M, Ogata T, Kudoh J, Shimizu N. 1998. Severe form of juvenile corneal stromal dystrophy with homozygous R124H mutation in the keratoepithelin gene in five Japanese patients. *Br J Ophthalmol* 82:1280–1284.

Mashima Y, Nakamura Y, Noda K, Konishi M, Yamada M, Kudoh J, Shimizu N. 1999. A novel mutation at codon 124 (R124L) in the BIGH3 gene is associated with a superficial variant of granular corneal dystrophy. *Arch Ophthalmol* 117:90–1793.

Mashima Y, Yamamoto S, Inoue Y, Yamada M, Konishi M, Watanabe H, Maeda N, Shimomura Y, Kinoshita S 2000. Association of autosomal dominantly

inherited corneal dystrophies with BIGH3 gene mutations in *Japan. Am J Ophthalmol* 130:516–517.

Mc Tigue JW, Fine BS 1964. The stromal lesion in lattice dystrophy of the cornea. a light and electron microscopic study. *Invest Ophthalmol.* 3:355-365.

Meratoja J.1973. Genetic aspects of familial amyloidosis with corneal lattice dystrophy and cranial neuropathy. *Clin Genet* 4:173-185.

Meallet MA, Affeldt JA, McFarland TJ, Appukuttan B, Read R, Stout JT, Rao NA. 2004. An unusual clinical phenotype of Avellino corneal dystrophy associated with an Arg124His beta iG-H3 mutation in an African-American woman. *Am J Ophthalmol.* 37:765-767.

Morishige N, Chikama T, Ishimura Y, Nishida T, Takahashi M, Mashima Y. 2004. Unusual phenotype of an individual with the R124C mutation in the TGFBI gene. *Arch Ophthalmol* 122:1224-1227.

Munier FL, Korvatska E, Djemai A, Le Paslier D, Zografos L, Pescia G, Schorderet DF. 1997. Kerato-epithelin mutations in four 5q31-linked corneal dystrophies. *Nat Genet* 15:247–251.

Munier FL, Frueh BE, Othenin-Girard P, Uffer S, Cousin P, Wang MX, Heon E, Black GC, Blasi MA, Balestrazzi E, Lorenz B, Escoto R, Barraquer R, Hoeltzenbein M, Gloor B, Fossarello M, Singh AD, Arsenijevic Y, Zografos L, Schorderet DF. 2002. BIGH3 mutation spectrum in corneal dystrophies. *Invest Ophthalmol Vis Sci* 43:949–954.

Mutch JR. 1944. Hereditary Corneal Dystrophy. *Br J Ophthalmol* 28:49-86.

Nakagawa Asahina S, Fujiki K, Enomoto Y, Murakami A, Kanai A. 2004. [Case of late onset and isolated lattice corneal dystrophy with Asn544Ser (N544S)

mutation of transforming growth factor beta-induced (TGFBI, BIGH3) gene] *Nippon Ganka Gakkai Zasshi* 108.618–620.

Nakamura T, Nishida K, Dota A, Adachi W, Yamamoto S, Maeda N, Okada M, Kinoshita S 2000 Gelatino-lattice corneal dystrophy. clinical features and mutational analysis. *Am J Ophthalmol* 129:665-6.

Nam JO, Kim JE, Jeong HW, Lee SJ, Lee BH, Choi JY, Park RW, Park JY, Kim IS. 2003. Identification of the alphavbeta3 integrin-interacting motif of betaig-h3 and its anti-angiogenic effect *J Biol Chem.* 278:25902-25909.

Nayak SK, Binder PS. 1984. The growth of endothelium from human corneal rims in tissue culture. *Invest Ophthalmol Vis Sci* 25:1213-1216.

Nishida K, Kawasaki S, Kinoshita S. 1998. Clusterin may be essential for maintaining ocular surface epithelium as a non-keratinizing epithelium *Adv Exp Med Biol* 438:629-635.

Ohno S, Noshiro M, Makihira S, Kawamoto T, Shen M, Yan W, Kawashima-Ohya Y, Fujimoto K, Tanne K, Kato Y. 1999. RGD-CAP ((beta) ig-h3) enhances the spreading of chondrocytes and fibroblasts via integrin alpha (1) beta (1). *Biochim Biophys Acta* 1451:196-205.

Okada M, Yamamoto S, Tsujikawa M, Watanabe H, Inoue Y, Maeda N, Shimomura Y, Nishida K, Quantock AJ, Kinoshita S, Tano Y. 1998a. Two distinct kerato-epithelin mutations in Reis-Bucklers corneal dystrophy. *Am J Ophthalmol* 126:535–542.

Okada M, Yamamoto S, Watanabe H, Inoue Y, Tsujikawa M, Maeda N, Shimomura Y, Nishida K, Kinoshita S, Tano Y 1998b. Granular corneal dystrophy with homozygous mutations in the kerato-epithelin gene. *Am J Ophthalmol* 126:169–176.

Pampukha VM, Drozhyna GI, Livshits LA. 2004. TGFBI gene mutation analysis in families with hereditary corneal dystrophies from Ukraine. *Ophthalmologica* 218. 411– 414.

Park SW, Bae JS, Kim KS, Park SH, Lee BH, Choi JY, Park JY, Ha SW, Kim YL,Kwon TH, Kim IS, Park RW. 2004. Beta ig-h3 promotes renal proximal tubular epithelial cell adhesion, migration and proliferation through the interaction with alpha3beta1 integrin. *Exp Mol Med* 36:211-219

Pfister RR. 1973. The normal surface of corneal epithelium: a scanning electron microscopic study. *Invest Ophthalmol Vis Sci* 12:654-68

Rawe IM, Zhan Q, Burrows R, Bennett K, Cintron C. 1997. Beta-ig. Molecular cloning and in situ hybridization in corneal tissues. *Invest Ophthalmol Vis Sci.* 38:893-900.

Reis W. Familiare, fleckige Hornhautentartung. 1917. *Dtsch Med Wochenschr* 43: 575

Rosenwasser GO, Sucheski BM, Rosa N, Pastena B, Sebastiani A, Sassani JW, Perry HD. 1993. Phenotypic variation in combined granular-lattice (Avellino) corneal dystrophy *Arch Ophthalmol* 111:1546–1552.

Rozzo C, Fossarello M, Galleri G, Sole G, Serru A, Orzalesi N, Serra A, Pirastu M. 1998. A common beta ig-h3 gene mutation (delta f540) in a large cohort of Sardinian Reis Bucklers corneal dystrophy patients. Mutation in Brief] 180. Online. *Hum Mutat* 12:215–216.

Sambrook J, Fritsch EF, Maniatis T. 1989. Molecular cloning. A laboratory manual. 2nd ed. New York, Cold Spring Harbor Laboratory Press.

Sasaki H, Kobayashi Y, Nakashima Y, Moriyama S, Yukiue H, Kaji M, Kiriyama M,Fukai I, Yamakawa Y, Fujii Y. 2002. Beta IGH3, a TGF-beta inducible gene, is overexpressed in lung cancer. *Jpn J Clin Oncol* 32:85-89.

Schorderet DF, Menasche M, Morand S, Bonnel S, Buchillier V, Marchant D, Auderset K, Bonny C, Abitbol M, Munier FL. 2000. Genomic characterization and embryonic expression of the mouse Bigh3 (Tgfbi) gene. *Biochem Biophys Res Commun* 274.267–274.

Schmitt-Bernard CF, Guittard C, Arnaud B, Demaille J, Argiles A, Claustres M, Tuffery-Giraud S. 2000. BIGH3 exon 14 mutations lead to intermediate type I/IIIA of lattice corneal dystrophies. *Invest Ophthalmol Vis Sci* 41:1302–1308

Seitelberger F, nemetz UR. 1961. A contribution to the problem of lattice dystrophy of the cornea. *Graefes Arch Clin Exp Ophthalmol* 164 102-111

Skonier J, Neubauer M, Madisen L, Bennett K, Plowman GD, Purchio AF. 1992. cDNA cloning and sequence analysis of beta ig-h3, a novel gene induced in a human adenocarcinoma cell line after treatment with transforming growth factor-beta. *DNA Cell Biol* 11:511–522.

Skonier J, Bennett K, Rothwell V, Kosowski S, Plowman G, Wallace P, Edelhoff S, Disteche C, Neubauer M, Marquardt H, Rodgers J, Purchio AF. 1994. beta ig-h3: a transforming growth factor-beta-responsive gene encoding a secreted protein that inhibits cell attachment in vitro and suppresses the growth of CHO cells in nude mice. *DNA Cell Biol* 13:571–584

Small KW, Mullen L, Barletta J, Graham K, Glasgow B, Stern G, Yee R. 1996. Mapping of Reis-Bücklers' corneal dystrophy to chromosome 5q. *Am J Ophthalmol* 121:384-390.

gene mutations in Japanese patients with corneal dystrophy. *Cornea* 19(Suppl):S21–S23.

Yee RW, Sullivan LS, Lai HT, Stock EL, Lu Y, Khan MN, Blanton SH, Daiger SP. 1997. Linkage mapping of Thiel-Behnke corneal dystrophy (CDB2) to chromosome 10q23–q24. *Genomics* 46. 152–154.

Yoshida S, Yoshida A, Nakao S, Emori A, Nakamura T, Fujisawa K, Kumano Y, Ishibashi T. 2004. Lattice corneal dystrophy type I without typical lattice lines: role of mutational analysis. *Am J Ophthalmol* 137:586–588.

Yu J, Zou LH, He JC, Liu NP, Zhang W, Lu L, Sun XG, Dong DS, Wu YY, Yin XT. 2003 [Analysis of mutation of BIGH3 gene in Chinese patients with corneal dystrophies]. *Zhonghua Yan Ke Za Zhi* 39:582-586.

Yuan C, Yang MC, Zins EJ, Boehlke CS, Huang AJ. 2004. Identification of the promoter region of the human betaIGH3 gene. *Mol Vis* 10:351-360.

Appendix

List of Antibodies used:

Anti-HA antibody-monoclonal antibody (Santa Cruz, California, cat # sc- 7392)

Anti–6XHistidine antibody–monoclonal antibody (Calbiochem cat # OB05)

Anti-human *BIG-H3* antibody–monoclonal mouse IgG1 (R&D systems, Cat # MAB2935).

ABBREVIATIONS

µg	: Microgram
µl	: Microlitre
µM	Micromolar
A	: Adenine
APS	. Ammonium persulfate
bp	. Base pair
BSA	. Bovine serum albumin
C	: Cytosine
c.DNA	: Complementary DNA
Cos 1	. African green monkey kidney cells
Del	· Deletion
DM	: Descemet's membrane
DMEM	: Dulbecco's modified Eagles medium
DMSO	: Dimethylsulphoxide
DNA	: Deoxyribonucleic acid
dNTPs	: Deoxy nucleoside triphosphates
EDTA	: Ethylene diamine tetraacetic acid
EGFP	· Enhanced green fluorescence protein
FBS	: Fetal bovine serum
fs	: Frameshift
G	: Guanine

GCD	: Granular corneal dystrophy
HA	: Hemagglutinin
IF	: Immunofluorescence
Ins	: Insertion
KDa	: Kilo Dalton
LCD	: Lattice corneal dystrophy
MCS	: Multiple cloning sites
MEM	: Minimal essential medium
ml	. Millilitre
nm	: Nanometer
OD	: Optical density
PAS	. Periodic acid-Schiff
PAGE	: Polyacrylamide gel electrophoresis
PBS	: Phosphate buffered saline
PCR	. Polymerase chain reaction
PI	: Propidium iodide
PMSF	: Phenylmethylsulfonylfluoride
RE	: Restriction enzyme
RFLP	: Restriction fragment length polymorphism
RNA	: Ribonucleicacid
RNase A	: ribonuclease A
rpm	: Revolutions per minute
SDS	: Sodium dodecylsulfate

SNP	Single nucleotide polymorphism
SSCP	Single strand conformation polymorphism
T	: Thymine
TBE	. Tris borate EDTA
TCA	: Tri-chloro acetic acid
TEMED	: Tetramethylethylenediamine
TGFBI	: Transforming growth factor beta induced gene
TAE	: Tris Acetic acid EDTA
VA	: Visual acuity

Publications

MUTATION IN BRIEF

Mutational Screening of the RB1 Gene in Indian Patients with Retinoblastoma Reveals Eight Novel and Several Recurrent Mutations

Velamakanni Saroj Kiran [1], Chitra Kannabiran [1]*, Kalyana Chakravarthi[1], Geeta K. Vemuganti [2], and Santosh G. Honavar[3]

[1] Kallam Anji Reddy Molecular Genetics Laboratory, [2] Ophthalmic Pathology Service, [3] Ocular Oncology Service, Prof Brien Holden Eye Research Centre, L V Prasad Eye Institute, L V Prasad Marg, Banjara Hills, Hyderabad 500 034, India

*Correspondence to: Chitra Kannabiran, Dept of Molecular Genetics, L V Prasad Eye Institute, L V Prasad Marg, Banjara Hills, Hyderabad 500 034, India, E-mail chitra@lvpei org

Grant sponsors. Indian Council of Medical Research, Council for Scientific and Industrial Research

Communicated by Nobuyoshi Shimizu

Retinoblastoma is the most common primary intraocular malignancy in children, caused by inactivation of the RB1 gene on chromosome 13. We carried out a mutational screen of the exons and promoter of the RB1 gene in Indian patients with retinoblastoma in order to determine the range of mutations giving rise to disease. Forty-seven patients were screened for mutations in all exons and promoter of the RB1 gene by single strand conformation polymorphism followed by sequencing. Tumors were available from 27 patients (12 bilateral and 15 unilateral retinoblastoma) while only peripheral blood was available from 20 patients, all with bilateral disease. Mutations were found in 22 patients, 9 from the analysis of tumors and 13 from peripheral blood. Eight novel mutations were identified, including 4 single base changes, 2 small deletions and 1 duplication. These are g.64365T>G (Tyr325Ter), g.78131G>A (Trp515Ter), g.150061G>T (Glu587Ter), g.170383C>G (S834X), g.41924A>C (IVS3–2A>C), g.150064ins4, g.160792del22, and g.76940del14 (IVS15 del +20-33). Almost all mutations produced nonsense codons or frameshifts. Recurrent mutations, especially at CpG sites were seen predominantly. Detectable mutations in exons were found in 46% of patients tested. Large deletions, epigenetic changes as well as mutations in non-coding regions may be the cause of disease in the remainder of patients. Knowledge of the full range of mutations can aid in the design of screening tests for individuals at risk. © 2003 Wiley-Liss, Inc

KEY WORDS RB1, mutation screening, retinoblastoma, Indian

INTRODUCTION

Retinoblastoma (MIM# 180200), a malignancy of retinal precursor cells usually occurring in children below the age of 5 years, is brought about by inactivation of the RB1 gene on chromosome 13q14 (Friend et al , 1986) One mutant allele of the RB1 gene is required for hereditary transmission of disease, while the development of malignancy requires the mutation of the second allele at the cellular level (Knudson, 1971) The hereditary form is

Received 15 May 2003, accepted revised manuscript 16 July 2003

DOI: 10.1002/humu.9181

inherited as an autosomal dominant trait, mostly manifests bilaterally and with high penetrance In the non-hereditary form of disease, which is unilateral, mutational inactivation of both alleles of RB1 is somatic. About 12% of unilateral cases are hereditary (Vogel, 1979) Most RB1 gene mutations occur de-novo, and are new mutations arising in the germline or during embryonic development Thus siblings and offspring of all individuals with bilateral and some with unilateral disease may be at risk of developing the disease, even in the absence of a family history. Identification of mutations in the RB1 gene in individuals with retinoblastoma has been recognized as a valuable adjunct to the management of the disease since it enables the unequivocal identification of carriers and accurate risk evaluation for relatives (Noorani et al , 1996; Smith and O'Brien, 1996). It is important for counseling of individuals with hereditary disease in general since such individuals may have affected offspring and have an increased likelihood of second malignancies

Retinoblastoma is one of the most common types of malignant tumors occurring in children below the age of 5 yrs in India (Pratap et al., 1973; Das et al , 1994), although no population-based prevalence data are available The ratio of unilateral·bilateral disease is 60 40 with familial disease occurring in ~4-5% or less of patients (Honavar S , unpublished data) The major features of the disease as it occurs in India, noted in clinicopathologic studies include a relatively high frequency of infiltration/invasion of tumor into surrounding tissues, found in 56% of patients, and a higher mean age at presentation (Sahu et al , 1998) than reported in Western countries (Gupta et al., 2002), both of these features are possibly due to a delay in seeking treatment We analyzed the RB1 gene for mutations within the exons and splice junctions as well as the promoter in Indian patients with retinoblastoma in order to determine the range of mutations occurring in these patients

We screened for mutations within exons and splice junctions as well as the promoter of the RB1 gene among 47 patients, 32 with bilateral and 15 with unilateral retinoblastoma, using peripheral blood (20 patients) and tumors (27 patients). By means of single-strand conformation polymorphism (SSCP) analysis followed by sequencing, mutations were identified in 22 patients (46%) Eight mutations identified in this study are novel.

PATIENTS AND METHODS

Patients and sample collection

Peripheral blood samples were collected from 47 unrelated probands with retinoblastoma and where family history was present, from family members as well after obtaining informed consent. All except two patients recruited for this study had sporadic disease The two patients with familial disease had affected siblings with the parents being normal. The follow-up period from the start of the study was too short to know of the occurrence of second malignancy in any of the patients The study protocol adhered to the tenets of the Declaration of Helsinki and the research was done after prior approval by the institutitonal review board of the L.V. Prasad Eye Institute. Fresh tissue was obtained from tumors of patients (27) who underwent enucleation. Retinoblastoma was diagnosed according to standard clinical and histopathological criteria. DNA was isolated from blood leukocytes and tumors and used for PCR amplification

PCR amplification

Primers and the PCR conditions used for individual exons were as described previously (Ata-ur-Rasheed et al , 2002) The primers used for amplification of the RB1 promoter were as follows. the upstream primer was as described (Lohmann et al , 1994), starting at position 1377 of the RB1 gene. The sequence of this primer was: 5' GCGAATTCCCAAAAGGCCAGCAAGTGTCT 3' The downstream primer was designed so as to include all sequences upstream of the first exon, and starts at position 2060 of RB1. The sequence of the reverse primer was. 5' GGGGGTTTTGGGCGGCAT 3'. PCR amplification of the promoter was carried out at an annealing temperature of 61°C with other parameters being the same as for all exons

SSCP

PCR products that were greater than 300 bp in size were digested so as to produce smaller fragments that were within the range of mutation detection by SSCP For SSCP screening, the PCR product for the RB1 promoter was digested with *Cfr101* so as to produce a fragment of 256 bp containing the proximal promoter sequence upstream of exon 1 including the Sp1, ATF and p53 binding sites.

PCR products were mixed with an equal volume of formamide, denatured by heating at 95° C for 5 minutes followed by immediate chilling in ice-salt mixture (temperature, −18°C) Essentially SSCP was performed by separation of denatured PCR products on 20x16 cm acrylamide gels (8% acrylamide, 39 1 acrylamide bis) with 5% glycerol electrophoresed in 1XTBE (Tris-borate EDTA) buffer at 4°C and at room temperature for 8-16 hrs Gels were fixed in 10% ethanol·0.5% acetic acid, washed in deionized water and stained in 0 2% silver nitrate They were then washed, developed in 1 5% sodium hydroxide 0 4% formaldehyde until bands were visible at the desired intensity and photographed in a UVIDoc gel documentation system (UVITec, Cambridge, England) Fragments showing altered mobility relative to controls were sequenced directly

Sequencing

PCR products were purified on Microcon-PCR filter units (Millipore Corpororation, USA), and directly sequenced bidirectionally using PCR primers on an automated sequencer Sequences were compared to published RB1 gene sequence (Genbank accession no L11910 1)

RESULTS AND DISCUSSION

From previous studies that have characterized mutations in the RB1 gene (Harbour, 1998), the predominant types of mutations in retinoblastoma are small mutations affecting the coding sequence We therefore looked for mutations in all the exons, splice junctions, and the promoter We screened a total of 47 patients (Table 1), 32 with bilateral and 15 with unilateral retinoblastoma Tumor tissue was available from of 27 patients (12 bilateral and 15 unilateral)

Table 1: Details of Patients and Samples Studied

Source of DNA	No. of patients		Total no.	Mutations found
	Bilateral	Unilateral		
Tumor	12	15	27	9
Blood leukocytes	20	-	20	13

The method of SSCP was standardized by using PCR fragments containing known mutations in the RB1 gene, including point mutations (5) and small length alterations (2) previously identified by direct sequencing (Ata-ur-Rasheed et al., 2002). Our present analysis of all exons and promoter in 47 unrelated patients revealed mutations in 22 (46%) Out of 27 tumors analyzed, mutations were found in nine patients, five with unilateral, and four with bilateral disease (Table 1). Analysis of leukocyte DNA of these 9 patients revealed the presence of the mutation identified in tumor DNA in all four patients with bilateral disease indicating that they were all germline mutations, and the absence of the corresponding mutations in all five with unilateral disease indicating that these mutations were somatic In addition, 13 mutations were found in 20 patients with bilateral disease upon screening of peripheral blood alone. In two patients, DNA from tumors did not produce any amplification products for several of the exons (data not shown) suggesting the presence of large homozygous deletions at the RB1 locus

Details of mutations and polymorphisms identified are shown in Table 2 To our knowledge, 8 mutations and 1 polymorphism (Table 2 and data reviewed but not shown) identified in this study are novel (RB1 gene mutation database website Available at http //www d-lohmann de/Rb/mutations html)

Among these, four nonsense mutations, g 64365T>G (Tyr325Ter), g 78131G>A (Trp515Ter), g 150061G>T (Glu587Ter) and g 170383C>G (Ser834X), and were identified and these are shown in Table 2 A novel splice-site mutation g 41924A>C (IVS3–2A>C), was found in the splice acceptor site of intron 3 resulting in an AG>CG heterozygous change Such an alteration may possibly lead to skipping of exon 4, which would result in an in-frame deletion. If it results in the retention of the intron it would produce a frameshift Analysis of RNA, which is not available to us at the present time, is required to distinguish these possibilities.

Other novel mutations identified include small length alterations found in three patients One patient (RB65, Table 1) had a duplication of 4 bp in exon 18 (g 150064ins4). This duplication creates a nonsense codon within exon 18. Small deletions were found in 2 patients. Of particular interest is a 14 bp deletion in intron 15 (g.76940del14;IVS15 del +20-33) extending from +18 to +32 of the intron (RB72). The effect of this deletion within intron 15 is not clear although it is probably oncogenic since no other mutations were found in this patient

Furthermore, a deletion of an overlapping region to the one described here was reported in a previous study (Liu et al , 1995). It is possible that the deleted sequence includes the splicing branchpoint of the intron although no perfect match for the branchpoint consensus is found in the region of the deletion A 22 bp deletion in exon 21, g 160792del22, was found in one patient (RB74), this would be expected to result in frameshift in exon 21.

Recurrent mutations were identified that involved C>T changes at arginine codons including (Table 2) Arg255Ter (g 69695C>T) and Arg445Ter (g 76430C>T) Mutations at splice donor sites of introns 12 and 14, g 70330G>A and g 76488T>Cwere also to recur (Table 2 and Ata-ur-Rasheed et al , 2002).

Table 2: RB1 Gene Alterations Identified

Location	Patient no.	Age at diagnosis/sex	Laterality	Mutation	Identified in	Putative consequence
Exon 8	RB25#	12 yrs/F	Unilateral	g 59695C>T	Tumor	Arg255X; termination
Exon 8	RB56	2 yrs/M	Bilateral	g.59695C>T	Blood	Arg255X; termination
Exon 10	RB27	2 yrs/M	Unilateral	g 64348C>T	Tumor	Arg320X; termination
Exon 10	RB40#	2 yrs/F	Unilateral	g 64365T>G*	Tumor	Tyr325X; termination
Exon 14	RB26	1 yr/M	Bilateral	g.76430C>T	Tumor	Arg445X; termination
Exon 14	RB34	4 mths/M	Bilateral	g.76430C>T	Tumor	Arg445X; termination
Exon 15	RB60	11 mths/M	Bilateral	g 76898C>T	Blood	Arg467X; termination
Exon 16	RB44	1 yr/M	Bilateral	g.77073T>G	Blood	Tyr498X; termination
Exon 17	RB58	1 yr/M	Bilateral	g 78238C>T	Blood	Arg552X; termination
Exon 17	RB59	1 yr/M	Bilateral	**g.78131G>A***	Blood	Trp515X, termination
Exon 17	RB63	7 yrs/M	Unilateral	g 78250C>T	Tumor	Arg556X, termination
Exon 18	RB54#	3 mths/F	Bilateral	**g.150061G>T***	Tumor	Glu587X; termination
Exon 18	RB65	2 yrs/F	Bilateral	**g.150064ins4***	Blood	frameshift
Exon 19	RB55	9 yrs/M	Bilateral	g 153284C>T	Blood	Gln631X; termination
Exon 21	RB74	4 yrs/F	Bilateral	**g.160792del22***	Blood	frameshift
Exon 24	RB57	1 mth/F	Bilateral	**g.170383C>G***	Blood	Ser834X; termination
IVS 3	RB66	3 yrs/M	Bilateral	**g.41924A>C***	Blood	AG>CG; exon skipping
IVS12	RB23@	2 yrs./M	Bilateral	g 70330G>A	Blood	GT>AT; exon skipping
IVS 12	RB29	3 yrs/F	Unilateral	g 70330G>A	Tumor	GT>AT; exon skipping
IVS 12	RB73	5 yrs/M	Bilateral	g.73752G>A	Blood	AG>AA; exon skipping
IVS 14	RB62	1 yr/M	Bilateral	g 76488T>C	Tumor	GT>GC;exon skipping
IVS 15	RB72	3 yrs/F	Bilateral	**g.76940del14***	Blood	del+20-33; exon skipping
IVS 25	RB35 RB39	2 yrs/M 4 yrs/M	Bilateral Unilateral	**g.173882T>C***	Blood Tumor	Polymorphism
IVS 25	RB36	5 yrs/M	Bilateral	g 174351T>A	Blood	Polymorphism

Mutations are designated according to their position in the genomic sequence of RB1 (GenBank accession no. L11910.1). @RB23 has familial disease with one affected sibling and unaffected parents *Novel changes identified in this study. # These patients had mutations that were heterozygous in tumors.

With the exception of 2 patients who had mutations involving splice acceptor sites of introns 3 and 12, which would be expected to lead possibly to in-frame deletions, all other mutations produced premature termination codons (see Table 2) We did not correlate these genotypes with clinical and histological features since previous studies that have attempted to correlate the position of nonsense mutations with disease parameters such as age at diagnosis or number of tumor foci have essentially found no correlation (Lohmann et al., 1996).

The sensitivity of SSCP in general may not be high enough to detect all changes, and more efficient techniques such as DHPLC may provide a better estimate of the frequency of small mutations in the patient population studied. Our earlier analysis of RB1 mutations using direct sequencing of all exons (Ata-ur-Rasheed et

al , 2002) revealed mutations in 7 of 14 patients The frequency of detection of mutations within RB1 exons and flanking sequences in retinoblastoma has varied between 20% and 70% (see below, Liu et al , 1995, Blanquet et al, 1995, Lohmann et al., 1996, Alonso et al , 2001) A comparison of data obtained in the present study with the frequency and types of small mutations in the RB1 gene reported for patients from some other populations is shown in Table 3 It is evident that while the frequency of detection varies over a wide range, the pattern of mutations is very similar across various populations studied, the most predominant category (70-80%) from all studies being nonsense and frameshift mutations (Table 3) Splice site mutations account for most of the remaining cases, with a very small number of missense or inframe mutations Many of the splice mutations would also be expected to lead to frameshifts

Table 3: Frequency and Distribution of Small Mutations in the Coding Sequences of the RB1 Gene Reported from Different Countries

Patient population from	Reference	Screening method(s)	Frequency of detection@	% nonsense/ frameshift mutations	% missense & inframe mutations	% splice site/intron mutations
Japan	Shimizu et al , 1994	SSCP	58%	86	0	14
UK	Liu et al , 1995	SSCP	48%	74	8	17
France	Blanquet et al , 1995	DGGE	20%*	76	13	11
Germany	Lohmann et al , 1996	SSCP, HDA, sequencing	68%	88	0	11
Spain	Alonso et al , 2001	Sequencing	67%	69	0	31
China	Choy et al., 2002	SSCP	38%*	64	12	24
India	Ata-ur-Rasheed et al., 2002, this study	Sequencing, SSCP	47%	70	0	28

Shown above are the data reported for small mutations in the RB1 gene detectable by PCR-based analysis of exons and splice sites on various populations @Frequency is given as %age of patients having detectable mutations % of each type of mutation is the fraction of the total number of mutation (percentages were rounded off and hence may not add up to 100%) *These studies included sporadic unilateral retinoblastoma in a screen for constitutional mutations

The absence of detectable mutations in a proportion of patients in our study could be explained in part by the presence of large deletions, either hetero- or homozygous A combination of approaches including quantitative PCR and sequencing have been found to identify mutations in almost 90% of patients (Richter et al , 2003) Other phenomena such as mosaicism, epigenetic alterations or a possible inactivation of RB1 through mutation of non-coding sequences may also be invoked to explain the cause of disease in the remainder of patients

These studies provide a detailed molecular genetic analysis of retinoblastoma in an Indian population for which few studies have been done so far. Data suggest that the mutational spectrum obtained is essentially similar to that obtained in other populations and that more sensitive and multiple approaches to mutation screening will be required to determine the basis of disease in all patients These data may contribute to the design and implementation of screening strategies for patients in the future

REFERENCES

Alonso, J, Garcia-Miguel, P, Abelairas, J, Mendiola M, Sarret E, Vendrell MT, Navajas A, Pestana A 2001 Spectrum of germline RB1 gene mutations in Spanish retinoblastoma patients phenotype and molecular epidemiological implications *Hum Mutat* 17 412-422

Ata-ur-Rasheed, M, Vemuganti, GK, Honavar, SG, Ahmed, N, Hasnain, SE, Kannabiran, C. 2002 Mutational analysis of the RB1 gene in Indian patients with retinoblastoma *Ophthal Genet* 23, 121-128

Blanquet, V, Turleau, C, Gross-Morand MS, Senamaud-Beaufort, C, Doz, F, Besmond, C. 1995. Spectrum of germline mutations in the RB1 gene· a study of 232 patients with hereditary and non-hereditary retinoblastoma. *Hum Mol Genet* 4 383-388

Choy KW, Pang, CP, Yu CB, Wong, HL, Ng, JS, Fan, DS, Lo, KW, Chai, JT, et al Loss of heterozygosity and mutations are the major mechanisms of RB1 gene inactivation in Chinese with sporadic retinoblastoma *Hum Mutat* 2002, Online Mutations in Brief #548

Das, S, Chakraborty, AK, Mukherjee, K, Kundu, BK and Haldar, KK. 1994. Profile of malignant lesions amongst children in North Bengal *Indian Pediatrics* 31·1281-1285.

Friend SH, Bernards R, Rogelj S, Weinberg RA, Rapaport JM, Albert DM, Dryja TP 1986. A human DNA segment with properties of the gene that predisposes to retinoblastoma and osteosarcoma. Nature, 323 643-646

Gupta, R, Hazari A, Vemuganti GK, Honavar SG, Histopathologic risk factors in retinoblastoma Presented at the Annual Meeting of the American Academy of Ophthalmology, Orlando, Fl, USA, October 2002)

Harbour, JW 1998. Overview of RB gene mutations in patients with retinoblastoma. Implications for clinical genetic screening. *Ophthalmology* 105. 1442-47

Knudson, A. 1971. Mutation and cancer.statistical study of retinoblastoma. *Proc Natl Acad Sci USA* 68:820-823

Liu, Z, Song, Y, Bia, B, Cowell, JK. Germline mutations in the RB1 gene in patients with hereditary retinoblastoma. 1995. *Genes, Chromosomes & Cancer* 14 277-284.

Lohmann, DR, Brandt, B, Hopping, W, Passarge, E, Horsthemke, B 1994 Distinct RB1 gene mutations with low penetrance in hereditary retinoblastoma. *Hum Genet* 94·349-354.

Lohmann, DR, Brandt, B, Hopping, W, Passarge, E. and Horsthemke, B 1996 The Spectrum of RB1 Germ-Line Mutations in Hereditary Retinoblastoma *Am J Hum Genet* 58.940-949

Noorani, HZ, Khan, HN, Gallie, BL, Detsky, AS 1996 Cost comparison of molecular versus conventional screening of relatives at risk for retinoblastoma. *Am J Hum Genet* 59: 301-7

Pratap, VK, Singh, S, Agarwal, BM and Jain, PC 1973. Malignancy in Infancy and Childhood. *Indian Pediatrics* 10 729-733.

Richter S, Vandezande K, Chen N, Zhang K, Sutherland J, Anderson J, Han L, Panton R, Branco P, and Gallie B. 2003. Sensitive and efficient detection of RB1 gene mutations enhances care for families with retinoblastoma. *Am J Hum Genet* 72 253-269

Sahu, S, Banavali, DK, Pai, SK, Nair CN, Kurkure PA, Motwani SA, Advani SH. 1998 Retinoblastoma. problems and perspectives from India *Pediatr Hematol Oncol* 15 501-8.

Shimizu, T, Toguchida, J, Kato, MV, Kaneko, A, Ishizaki, K, Sasaki, MS. 1994 Detection of mutations of the RB1 gene in retinoblastoma patients by using exon-by-exon PCR-SSCP analysis *Am J Hum Genet* 54· 793-800.

Smith, BJ, O'Brien, J M 1996 The genetics of retinoblastoma and current diagnostic testing. *J Pediatr Ophthalmol Strabismus* 33· 120-123.

Vogel, F 1979. Genetics of Retinoblastoma *Hum Genet* 52:1-54

GFBI Gene Mutations Causing Lattice and Granular corneal Dystrophies in Indian Patients

S. V. V. Kalyana Chakravarthi,[1] Chitra Kannabiran,[1] Mittanamalli S. Sridhar,[2] and Geeta K. Vemuganti[3]

Purpose. To identify mutations in the *TGFBI* gene in Indian patients with lattice corneal dystrophy (LCD) or granular corneal dystrophy (GCD) and to look for genotype–phenotype correlations.

Methods. Thirty-seven unrelated patients were studied, 18 with LCD and 19 with GCD The diagnosis of LCD or GCD was made on the basis of clinical and/or histopathological evaluation Exons and flanking intron sequences of the *TGFBI* gene were amplified by PCR with specific primers PCR products were screened by the method of single-strand conformation polymorphism followed by sequencing Mutations were confirmed by screening at least 100 unrelated normal control subjects

Results. Mutations were identified in 14 of 18 patients with LCD and in all 19 patients with GCD In LCD, three novel heterozygous mutations found were glycine-594-valine (Gly594Val) in 2 of 18 patients, valine-539-aspartic acid (Val539Asp) in 1 patient, and deletion of valine 624, valine 625 (Val624-Val625del) in 1 patient In addition, mutation of arginine 124-to-cysteine (Arg124Cys) was found in 8 of 18 patients and histidine 626-to-arginine (His626Arg) in 2 of 18 patients Atypical clinical features for LCD were noted in patients with the Gly594Val and Val624-Val625del mutations In GCD, 18 patients with GCD type I had a mutation of arginine 555 to-tryptophan (Arg555Trp) and 1 patient with GCD type III (Reis-Bucklers dystrophy), had the Arg124Leu mutation Seven novel single-nucleotide polymorphisms (SNPs) were also found, of which a change of leucine 269 to phenylalanine (Leu269Phe) was found in 12 of 18 patients with the Arg555Trp mutation

Conclusions. Arg124Cys and Arg555Trp appear to be the predominant mutations causing LCD and GCD, respectively, in the population studied The novel mutations identified in this study are associated with distinct phenotypes (*Invest Ophthalmol Vis Sci.* 2005,46 121–125) DOI 10 1167/iovs 04-0440

Corneal dystrophies involve the formation of corneal opacities that are most often characterized by bilateral, inherited, noninflammatory, and progressive lesions The opacities are caused by progressive accumulation of deposits in the cornea resulting in loss of transparency and visual impairment Lattice corneal dystrophy (LCD) and granular corneal dystrophy (GCD) are autosomal dominant dystrophies of the corneal stroma caused by mutations in the *TGFBI* gene (*TGI BI* or *BIGH3*, transforming growth factor-β induced) on chromosome 5 at q31 [1,2] The protein product of the *TGFBI* gene, keratoepithelin, is an extracellular matrix protein expressed in many tissues, as well as in the corneal epithelium [3,4] Its function in the cornea is not understood as yet, although it has been found to affect the adhesion of different types of cells in vitro [5] In the cornea, it presumably contributes to the structure of the extracellular matrix

LCD (OMIM 122200, On-line Mendelian Inheritance in Man, http //www ncbi nlm nih gov/Omim/ provided in the public domain by the National Center for Biotechnology Information [NCBI], Bethesda, MD) is a primary, usually bilateral, corneal amyloidosis characterized by refractile lines that are in the form of a fine, branching network Histologically, the deposits in LCD stain positively with Congo red and are birefringent under polarized light LCD has at least four different subtypes (reviewed in Ref 6) LCD type I[7] is an autosomal dominant, bilaterally symmetrical corneal disorder that is characterized by numerous translucent fine lattice lines that are associated with white dots and faint haze in the superficial and middle layers of the central stroma. LCD type III[8] is a late-onset disease of autosomal recessive inheritance that appears with decreased vision in the fifth to seventh decades of life Asymmetrical findings are common Lattice lines extend up to the limbus, are thicker, and are more easily seen with direct illumination than those in LCD type I LCD type IIIA differs from type III in the presence of erosions and an autosomal dominant inheritance pattern [9] Recently, LCD type IV has been described, with deep stromal opacities and late onset of disease [6]

GCD type I (OMIM 121900) is characterized by small, discrete, sharply demarcated grayish white opacities in the anterior central stroma resembling bread crumbs or snowflakes [10] Histologically, the corneal deposits stain positively with Masson trichrome and are nonamyloid [11] As the condition advances, individual lesions increase in size and number and may coalesce, extending into the deeper and more peripheral stroma GCD type II (Avellino corneal dystrophy, OMIM 607541), shares features of lattice and granular dystrophies and has both granular and amyloid types of deposits [12] It is clinically similar to GCD type I GCD type III is a superficial variant of GCD[13] (Reis-Bucklers dystrophy, OMIM 608470) and the deposits are morphologically similar to those in GCD type I, but are present mainly in the Bowman's layer and beneath the epithelium

Phenotype-specific mutations have been characterized in the *TGFBI* gene Most patients have mutations at mutational hot spots corresponding to arginine 124 and arginine 555 of the keratoepithelin protein These include the arginine 124-to-cysteine (Arg124Cys) mutation in LCD type I, arginine 555-to-tryptophan (Arg555Trp) in GCD type I, arginine 124-to-histidine (Arg124His) in Avellino corneal dystrophy,[2,14] and arginine124-to-leucine (Arg124Leu) in Reis-Bucklers corneal dystrophy [15] In addition to these common mutations, muta-

From the [1]Kallam Anji Reddy Molecular Genetics Laboratory, the [2]Cornea and Anterior Segment Service, and the [3]Ophthalmic Pathology Service, L V Prasad Eye Institute, Hyderabad, India

Supported by the Hyderabad Eye Research Foundation, and the Department of Biotechnology, Government of India SVVKC was supported by a fellowship from the Council for Scientific and Industrial Research

Submitted for publication April 19, 2004, revised September 2, 2004, accepted September 10, 2004

Disclosure **S.V.V.K. Chakravarthi**, None, **C. Kannabiran**, None, **M.S. Sridhar**, None, **G.K. Vemuganti**, None

The publication costs of this article were defrayed in part by page charge payment This article must therefore be marked "*advertisement*" in accordance with 18 U S C §1734 solely to indicate this fact

Corresponding author Chitra Kannabiran, Kallam Anji Reddy Molecular Genetics Laboratory, L V Prasad Eye Institute, L V Prasad Marg, Banjara Hills, Hyderabad 500 034, India, chitra@lvpei org

TABLE 1. Details of *TGFBI* Gene Mutations and Phenotypes of Probands with LCD or GCD

Probands (*n*)	Mutation in *TGFBI*		Restriction Site Change	Clinical Features	Histopatholo Features
	Amino Acid	cDNA			
8	Arg124Cys	c 417C→T	*Cpo*I−	Anterior-to-mid stromal lattice lines	Amyloid (4)†
2	His626Arg	c 1924A→G	—	Anterior to-deep stromal lattice lines	Amyloid (1)
1	Val539Asp*	c 1663T→A	*Taa*I−	Anterior and mid-stromal lattice lines	Amyloid
2	Gly594Val*	c 1828G→T	*Hmc*II+	Posterior stromal, thick lattice lines, late onset	NA
1	Val624, Val625del*	c 1917-22del	*Ava*II−	Anterior stromal opacities and scarring, no clinically evident lattice lines	Amyloid in anterio stroma
4	None identified	—	—	Anterior to mid stromal lattice lines	Amyloid
18	Arg555Trp	c 1710C→T	*Bst*XI+	Granular opacities in anterior third to full stroma	Masson +ve (9)
1	Arg124Leu	c 418G→T	*Cpo*I−	Subepithelial and stromal opacities with recurrence after grafting	Masson +ve deposi

The first column shows the number of patients with each of the mutations Restriction sites created (+) or destroyed (−) as a result mutation are shown NA, data not available

* Novel mutations

† Number of patients for whom data were available In those without a number, data were available for all

tional heterogeneity exists, particularly in different forms of lattice dystrophy [16]

We screened the *TGFBI* gene for mutations in Indian patients with LCD and GCD to determine the range of mutations underlying these diseases and to characterize the associated phenotypes LCD and GCD account for approximately 15% to 25% of all patients with corneal dystrophy requiring corneal grafts in our institution, a tertiary-care referral center in southern India [17] No genetic studies have been reported so far on lattice and granular dystrophies in Indians We report the results of our study on 37 unrelated patients (18 with LCD, 19 with GCD)

Materials and Methods

The study protocol adhered to the tenets of the Declaration of Helsinki Corneal dystrophies were diagnosed by clinical and/or histopathological evaluation, and clinical examination was performed by slit lamp biomicroscopy Histopathological data were available for 11 patients with LCD and 10 patients with GCD who underwent corneal transplantation For histopathology, corneal sections were processed by standard methods and stained with Congo red or Masson trichrome The presence of amyloid was confirmed by birefringence under polarized light Blood samples were collected from patients and available family members after obtaining informed consent and approval of the study by the Institutional Review Board of the L V Prasad Eye Institute Among the patients studied, 7 with LCD and 13 with GCD had a family history of disease, and all patients were bilaterally affected None of the patients had any systemic manifestations The control population consisted of 100 unrelated individuals who had no history of the diseases studied

Genomic DNA was isolated from blood leukocytes by standard procedures [18] Individual exons of the *TGFBI* gene were amplified with primers designed by us, specific for flanking intron sequences (primer sequences available on request) PCR amplified products of all 17 exons were screened for sequence changes by the method of single strand conformation polymorphism (SSCP), as previously described [19] Fragments showing altered mobility relative to control subjects were sequenced bidirectionally Sequencing of purified PCR products was performed (BigDye Terminator Kit on a model 310 Prism sequencer, Applied Biosystems, Inc [ABI], Foster City, CA) Sequences were compared with the published sequence of *TGFBI* (GenBank accession no for genomic sequence, AY149344, mRNA sequence- NM_000358, version NM_000358 1, http //www ncbi nlm nih gov/Genbank, provided in the public domain by the National Center for Biotechnology Information, Bethesda, MD) All samples that were negative for mutations on screening by SSCP, were sequenced directly in all exons identify mutations At least 100 normal unrelated control individuals well as family members were screened for identified mutations t confirm pathogenicity PCR restriction fragment length polymorphism (RFLP) was used to test for the presence of various mutations unrelated control subjects and family members Restriction sit changes are detailed in Table 1 PCR products of normal and mutan DNAs were digested with the relevant restriction enzyme and resolve on polyacrylamide or agarose gels DNA was visualized by staining with ethidium bromide

Results

Details of mutations and phenotypic features of patients are summarized in Table 1.

Mutations

Five mutations, of which three are novel, were identified in 14 patients with a diagnosis of LCD Eight patients had a mutation of arginine 124 to cysteine (Arg124Cys), two patients had a mutation of histidine 626 to arginine (His626Arg), one patient had a mutation of valine 539 to aspartic acid (Val539Asp), two patients had a mutation of glycine 594 to valine (Gly594Val), and one patient had an in-frame deletion of two amino acids, valine 624 and valine 625 (Val624-Val625del) All the mutations detected were heterozygous in probands and were absent in 100 unrelated unaffected individuals No mutations were identifiable after sequencing of all exons of *TGFBI* in the remaining four patients Eighteen patients with a diagnosis of GCD type I had a mutation of arginine 555 to tryptophan (Arg555Trp), and one patient with a diagnosis of GCD type III (or Reis-Bucklers dystrophy) had a mutation of arginine 124 to leucine (Arg124Leu) Pedigrees with segregation of novel mutations in available family members are shown in Figure 1

Clinical and Histopathological Features of Patients

LCD. Clinical and histopathological features of patients bearing the three novel mutations identified in this study are described in the following sections.

Val539Asp. The slit lamp photograph of the cornea of the proband is shown in Figure 2A The opacities were in the form of lattice lines in the anterior stroma. Cosegregation analysis of

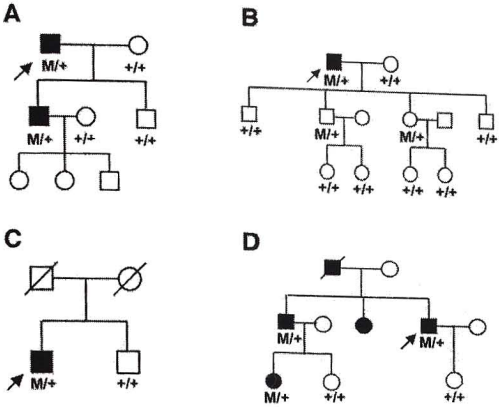

FIGURE 1. Pedigrees of patients having novel mutations in *TGFBI*, showing segregation of mutations and disease status of individuals examined (A) Val539Asp, (B) Gly594Val, (C) Gly594Val, and (D) Val624-Val625del Only parts of the pedigree containing individuals tested are shown M, mutant allele, +, wild type allele Probands are marked by an *arrow* at the *lower left* of the symbol Cosegregation was checked by PCR-RFLP (restriction enzymes used for each mutation are in Table 1)

the mutation in this pedigree, shown in Figure 1A, revealed that his older son, aged 34 years, affected but asymptomatic, was heterozygous for the mutation

Gly594Val Two unrelated patients with this mutation had opacities in the posterior stroma on clinical examination They presented with late-onset disease, in the sixth and seventh decades of life, and thick lattice lines (Figs 2B–D) extending into the corneoscleral limbus No histopathological data were available for these patients Cosegregation analysis of the available members of the families of the two probands is shown in Figures 1B and 1C As shown in Figure 1B, two offspring of the proband who were aged 44 and 40 years carried the mutation but showed no signs of disease on slit lamp examination

Val624-Val625del One patient had this mutation and showed manifestations that are atypical of LCD (Figs 3A, 3B) He had diffuse corneal opacities with no clear lattice lines He

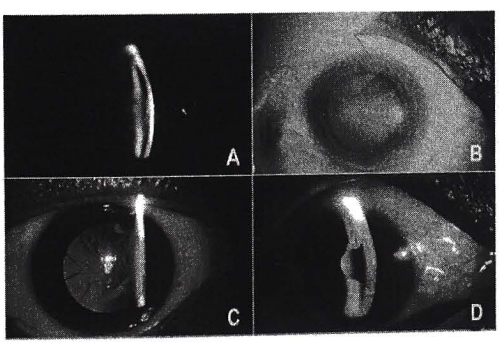

FIGURE 2. Slit view of patient with mutation Val539Asp showing lattice lines on indirect illumination (A) Diffuse (B) and retroillumi nated (C) slit lamp views of patient with Gly594Val showing thick lattice lines with intervening opacity (D) Slit lamp view of second patient with Gly594Val showing lattice lines

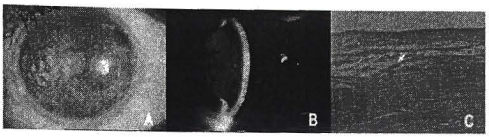

FIGURE 3. Diffuse slit lamp view of the patient with deletion of Val624-Val625 (A) showing opacities Note the associated spheroidal degeneration Narrow slit view of the cornea in the same patient (B) Congo red stained section (C) when seen under polarized filters showed birefringence in the subepithelial region (*arrow*) Magnifica tion × 400

complained of progressive loss of vision and photophobia during his 20s and at the age of 30 years, underwent corneal grafting The diagnosis of LCD was based on the histopathol ogy of the corneal button, which showed amyloid deposits in the anterior stroma (Fig 3C) The deposits were negative for Masson trichrome His father and two siblings were reported to be similarly affected in their 20s The brother of the proband, who was also examined in our institution, had scarring and deposits in the superficial stroma He was diagnosed to have corneal dystrophy of an unspecified type After a corneal graft at the age of 30 years, histopathology revealed amyloid depos its in the Bowman's layer and anterior stroma The pedigree was analyzed for cosegregation of the mutation with disease, and details are shown in Figure 1D

GCD. Eighteen patients with granular dystrophy had the Arg555Trp mutation and presented with features of type I GCD, with granular opacities, the extent of which ranged from the anterior third to the full thickness of the stroma (summarized in Table 1)

One patient with the Arg124Leu mutation, received a clin ical diagnosis of Reis-Bucklers dystrophy (GCD type III) with stromal involvement, based on the presence of multiple opacities in a honeycomb pattern in the subepithelial and superficial stromal layers (Figs 4A, 4B) Disease had its onset during the second decade The patient underwent corneal transplantation in both eyes with recurrence of the opacities within a few years of surgery Histopathological evaluation revealed granular Masson positive deposits in the stroma

Polymorphisms Identified in *TGFBI*

In addition to the mutations just described, we identified several single nucleotide polymorphisms (SNPs) in the *TGFBI* gene Details are shown in Table 2 Eight exonic polymorphisms, of which four are novel, and four intronic polymorphisms, three novel, were identified Among the exonic polymorphisms, seven were located at the third base position of the respective codons and did not result in a codon change

The remaining exonic polymorphism, located in exon 7, consists of a C→T variation at cDNA position 852, and results

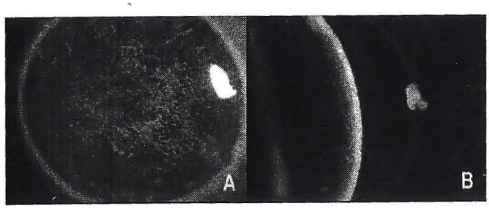

FIGURE 4. Diffuse (A) and slit (B) views of proband with Arg124Leu mutation showing multiple opacities in subepithelial and anterior stro mal regions

TABLE 2. SNPs in the *TGFBI* Gene

Location	Polymorphism (codon)	Novel/Reported
Exon 6	c 698C→G (Leu217Leu)	Reported (20)
Exon 7	c 852C→T (Leu269Phe)	Novel
Exon 7	c 863C→T (Asn272Asn)	Novel
Exon 8	c 977C→T (His310His)	Novel
Exon 8	c 1028A→G (Val327Val)	Reported (14)
Exon 11	c 1463C→T (Leu472Leu)	Reported (14)
Exon 12	c 1631G→A (Thr528Thr)	Novel
Exon 12	c 1667C→T (Phe540Phe)	Reported (14)
IVS12	g 29683G/A	Reported (14)
IVS13	g 33618A/G	Novel
IVS13	g 33635T/A	Novel
IVS14	g 33836T/C	Novel

Polymorphisms identified are shown according to position in cDNA or genomic DNA Codons involved are given in parentheses In column 3, the numbers indicate the first published report of the polymorphism IVS, intervening sequence

in a change of CTT (coding for leucine 269) to TTT (phenylalanine) This change was heterozygous in 12 of 18 patients with GCD type I and in 3 of 100 unrelated normal control subjects It cosegregated with the Arg555Trp mutation in some affected families and in one family (not included in this series), affected members were homozygous for both the Arg555Trp mutation and the Leu269Phe variant (data not shown), suggesting that the two sequence changes may be in *cis* This polymorphism was absent in the patients that we studied who had LCD and Reis-Bucklers dystrophy

DISCUSSION

Our study of 37 patients of Indian origin with LCD and GCD, shows that the predominant mutations causing these diseases in the patient cohort screened were Arg124Cys (found in 8/18 patients with LCD) and Arg555Trp (found in 18/19 patients with GCD) Although these two mutations have been found to be the major causes of LCD and GCD respectively in different ethnic groups,[21] population-specific variations in the prevalence of different mutations in *TGFBI* have been documented For example, GCD type II (Avellino corneal dystrophy) caused by the Arg124His mutation, is the most common type of GCD in Japan[22] and His626Arg may be more frequent than Arg124Cys among Vietnamese patients with LCD [23]

We observed a broad correspondence similar to that reported in earlier studies, between mutations at arginine 124 and arginine 555 residues in *TGFBI* and their associated phenotypes [2,14] In addition, our study demonstrates further mutational heterogeneity in *TGFBI* and brings to light unusual phenotypes of *TGFBI*-linked corneal dystrophies (Table 1)

The three novel mutations identified in this study were each associated with different phenotypes of LCD All three mutations involve the fourth fasciclin-like domain in which most pathogenic alterations in *TGFBI* have been found The two missense changes at valine 539 and glycine 594, as well as the in-frame deletion at valine residues 624 and 625, involve highly conserved residues, conserved among fasciclin-like domains of several proteins (NCBI Conserved Domain Database, available in the public domain at http //www.ncbi nlm nih gov/entrez/query fcgi?db=cdd)

For the Gly594Val mutation, the clinical features in both probands (Table 1) were late onset of disease and the presence of deep stromal opacities that extended up to the limbus These manifestations are similar to those reported for two other mutations—namely, Leu527Arg[24] and Val631Asp[21]—and have been classified as LCD type IV [6] The Gly594Val mutation, to our knowledge, represents the third mutation causi form of LCD Cosegregation analysis in the family m revealed that two offspring of one of the patients (Fig carried the mutation but did not manifest disease It is p that the mutation carriers in this family may manifest dis a more advanced age or that this mutation has incom penetrance. The high degree of conservation of the resi mutated, as well as the absence of the change in 100 unrel control subjects support the conclusion that it is patho

The novel deletion of Val624-Val625 occurred in a pa having diffuse corneal opacities with no clinically evident tice type pattern and amyloid deposits in the stroma (Fig. 3 nonlattice pattern of corneal opacification has also been served in association with the Arg124Cys mutation,[25] raising the idea that factors such as advanced stage dise ageing, environmental factors, or modifier genes contribut the phenotype In addition, a nonlattice phenotype resul from a mutation in *TGFBI* was reported in a family polymorphic corneal amyloidosis.[26] These data together large the range of phenotypic variability associated with *TG* gene mutations and suggest that the lattice and nonlattice t of stromal amyloidoses showing autosomal dominant inh tance may be part of a spectrum of phenotypes of the s disease

An interesting novel polymorphism identified in this s is a change of leucine269 to phenylalanine (Leu269Phe) thirds of the patients with GCD (12/18) with the Arg555 mutation were heterozygous for Leu269Phe as were 3% normal control subjects Analysis of a larger cohort of fa with GCD is necessary to determine whether the Leu269 polymorphism is in linkage disequilibrium with the Arg555 mutation in this population To examine the possibility common origin of the Arg555Trp allele in patients with Arg555Trp and Leu269Phe changes, we looked at the ha types of the other SNPs that we identified in the *TGFBI* ge as well as of flanking microsatellite markers We found t there was more than one haplotype in this group of 12 patie (data not shown) The small number of patients with G studied did not permit a conclusion as to whether there significant difference in the frequency of any haplotype tween patients and control subjects

No mutations were identified in four patients diagno with LCD clinically and histopathologically (Table 1). I possible that mutations in these cases lie within the introns promoter of the *TGFBI* gene.

The keratoepithelin protein has four internal repeat mains, the FAS1 domains with homology to fasciclin-1, insect cell-adhesion molecule.[27] Most of the mutations so reported lie in the fourth fasciclin-like domain Structural m eling of the fourth FAS1 domain in *TGFBI* has predicted t the mutations in this domain possibly disrupt the structure leading to misfolding of the protein.[28] Mutant keratoepith especially for the Arg124 mutations, appears to undergo normal processing and /or turnover, resulting in the accu lation of mutant protein or fragments thereof [29,30] It may speculated that the mutants within FAS1 domain 4 also foll a similar route. Leucine 269 is present in the second F domain of keratoepithelin (NCBI Conserved Domain D base). Because no pathogenic alterations have been found this region, it is possible that sequence variations, especi replacement of one hydrophobic residue with another, as the case of Leu269Phe, are tolerated Knowledge of the tions of the different domains of keratoepithelin may eve ally provide insight into the pathogenesis of the different fo of *TGFBI*-linked corneal dystrophies.

References

1 Stone EM, Mathers WD, Rosewasser GO, et al Three autosomal dominant corneal dystrophies map to chromosome 5q *Nat Genet* 1994,6 47-51

2 Munier FL, Korvatska E, Djemai A, et al Keratoepithelin mutations in four 5q31-linked corneal dystrophies *Nat Genet* 1997,15 247-251

3 Skonier J, Neubauer M, Madisen L, et al cDNA cloning and sequence analysis of beta ig h3, a novel gene induced in a human adenocarcinoma cell line after treatment with transforming growth-beta *DNA Cell Biol* 1992,11 511-522

4 Escribano J, Hernando N, Ghosh S, Crabb J, Coca Prados M cDNA from human ocular ciliary epithelium homologous to beta ig h3 is preferentially expressed as an extracellular protein in the corneal epithelium *J Cell Physiol* 1994,160 511-521

5 Skonier J, Bennett K, Rothwell V, et al Beta ig-h3 a transforming growth factor beta responsive gene encoding a secreted protein that inhibits cell attachment in vitro and suppresses the growth of CHO cells in nude mice *DNA Cell Biol* 1994,13 571-584

6 Klintworth GK Advances in the molecular genetics of corneal dystrophies *Am J Ophthalmol* 1999,128 747-754

7 Klintworth GK Lattice corneal dystrophy an inherited variety of amyloidosis restricted to the cornea *Am J Pathol* 1967,50 371-399

8 Hida TK, Tsubota K, Kigasawa K, Murata H, Ogata T Akiya S Clinical features of a newly recognized type of lattice corneal dystrophy *Am J Ophthalmol* 1987,104 241-248

9 Stock EL, Feder RS, O Grady RB, Sugar J, Roth SI Lattice corneal dystrophy type IIIA clinical and histopathological correlations *Arch Ophthalmol* 1991,109 351-358

10 Brav A Familial nodular degeneration of the cornea *Arch Ophthalmol* 1935,14 985-986

11 Garner A Histochemistry of corneal granular dystrophy *Br J Ophthalmol* 1969,53 799-807

12 Folberg R, Alfonso E, Croxatto JO, et al Clinically atypical granular corneal dystrophy with pathologic features of lattice like amyloid deposits a study of these families *Ophthalmology* 1988,95 46-51

13 Haddad R Font RL, Fine BS Unusual superficial variant of granular dystrophy of the cornea *Am J Ophthalmol* 1977,83 213-218

14 Korvatska E, Munier FL, Djemai A, et al Mutation hot spots in 5q31 linked corneal dystrophies *Am J Hum Genet* 1998,62 320-324

15 Mashima Y, Nakamura Y, Noda K, et al A novel mutation at codon 124 (R124L) in the *TGFBI* gene is associated with a superficial variant of granular corneal dystrophy *Arch Ophthalmol* 1999, 117 90-93

16 Klintworth GK The molecular genetics of the corneal dystrophies current status *Front Bioscience* 2003 8 687-713

17 Pandrowala H, Bansal A Vemuganti GK, Rao GN Frequency distribution, and outcome of keratoplasty for corneal dystrophies at a tertiary eye care center in South India *Cornea* 2004,23 541-546

18 Sambrook J, Fritsch EF, Maniatis T *Molecular Cloning a Laboratory Manual* 2nd ed Vol 2 Cold Spring Harbor, NY Cold Spring Harbor Press, 1989 9 17-9 18

19 Kiran VS, Kannabiran C, Chakravarthi K Vemuganti GK, Honavar SG Mutational screening of the RB1 gene in Indian patients with retinoblastoma reveals 8 novel and several recurrent mutations *Hum Mutat* 2003,22 339

20 Schmitt Bernard CF, Guittard C, Arnaud B, et al *BIGH3* exon 14 mutations lead to intermediate type I/IIIA of lattice corneal dystrophies *Invest Ophthalmol Vis Sci* 2000,41 1302-1308

21 Munier FL, Frueh BE, Othenin Girard P, et al *BIGH3* mutation spectrum in corneal dystrophies *Invest Ophthalmol Vis Sci* 2002, 43 949-954

22 Mashima Y, Yamamoto S, Inoue Y, et al Association of autosomal dominantly inherited corneal dystrophies with *BIGH3* gene mutations in Japan *Am J Ophthalmol* 2000,130 516-517

23 Chau HM, Ha NT Cung LX, et al H626R and R124C mutations of the BIGH3 (*TGFBI*) gene caused lattice corneal dystrophy in Vietnamese people *Br J Ophthalmol* 2003 87 686-689

24 Fujiki K, Hotta Y, Nakayasu K, et al A new L527R mutation of the betaIGH3 gene in patients with lattice corneal dystrophy with deep stromal opacities *Hum Genet* 1998,103 286-289

25 Yoshida S, Yoshida A, Nakao S, et al Lattice corneal dystrophy type I without typical lattice lines role of mutational analysis *Am J Ophthalmol* 2004,586-588

26 Eifrig DE, Afshari NA, Buchanan HW IV, Bowling BL, Klintworth GK Polymorphic corneal amyloidosis a disorder due to a novel mutation in the transforming growth factor beta induced (*BIGH3*) gene *Ophthalmology* 2004,111 1108-1114

27 Zinn K, McAllister L, Goodman CS Sequence analysis and neuronal expression of fasciclin I in grasshopper and Drosophila *Cell* 1988,53 577-587

28 Clout NJ, Hohenester E Model of the FAS1 domain 4 of the corneal protein βig h3 gives a clearer view of the corneal dystrophies *Mol Vis* 2003,9 440-448

29 Korvatska E, Henry H, Mashima Y, et al Amyloid and non amyloid forms of 5q31-linked corneal dystrophy resulting from keratoepithelin mutations at arg-124 are associated with abnormal turnover of protein *J Biol Chem* 2000,275 11465-11469

30 Hedegaard CJ, Thogersen IB, Enghild IJ et al Transforming growth factor beta induced protein accumulation in granular corneal dystrophy type III (Reis Bucklers) identification by mass spectrometry in 15 year old two-dimensional protein gels *Mol Vis* 2003,9 355-359

SECTION EDITOR JANEY L WIGGS, MD PhD

Genotype-Phenotype Correlation in 2 Indian Families With Severe Granular Corneal Dystrophy

Chitra Kannabiran, PhD, Mittanamalli S Sridhar, MD, S Kalyana Chakravarthi, MSc, Geeta K Vemuganti, MD, Meena Lakshmipathi, MD

Objectives: To determine genotypes in 2 Indian families with severe granular corneal dystrophy, to document clinical and histopathologic features, and to attempt a genotype-phenotype correlation

Methods: Mutation analysis of exon 12 of the *TGFBI* gene was carried out in 9 individuals from 2 families

Results: A C→T mutation at residue 1710 of *TGFBI* complementary DNA, corresponding to an Arg555Trp mutation in keratoepithelin, was found in affected members of both families In 5 patients, this mutation was homozygous, and it was heterozygous in the other 4 Clinical examination revealed a severe form of granular corneal dystrophy with early onset and superficial lesions in the homozygous individuals and a milder phenotype in the heterozygous individuals Histopathologic evaluation of corneal specimens from 2 homozygous patients confirmed the presence of superficial granular deposits

Conclusions: To our knowledge, this is the first molecular and clinical characterization of severe granular corneal dystrophy in India Genotype-phenotype correlation and comparison with earlier reports on this entity highlight the uniform expressivity of the Arg555Trp allele in homozygous individuals

Clinical Relevance: Homozygous granular corneal dystrophy has a severe phenotype and can be recognized based on clinical and histopathologic features, especially in association with consanguinity or inbreeding

Arch Ophthalmol 2005,123 1127-1133

GRANULAR CORNEAL DYSTROPHY (Online Mendelian Inheritance in Man 121900) is an autosomal dominant disorder characterized by small white, sharply demarcated spots that resemble bread crumbs in the cornea beneath the Bowman layer The opacities vary in shape but usually fall into 3 basic morphologic types of drop, crumb, and ring shapes [1,2] The overall pattern of deposition is radial or disk shaped, or it may be in the form of a Christmas tree [1] Initially, the region of the corneal stroma between the opacities remains clear Vision is usually not affected in the early stage of the disease, but some patients may have mild photophobia from light scattering by the corneal lesions In a subset of patients, erosive episodes are more common As the condition advances, individual lesions increase in size and number and may coalesce They frequently extend into deeper and more peripheral stroma However, 2 to 3 mm of the peripheral cornea usually remains free of deposits With more advanced disease, the intervening cornea develops a diffuse hazy appearance Although the lesions can involve the Bowman layer and result in superficial irregularities, recurrent erosions are unusual Visual impairment is rare before the fifth decade of life and usually develops secondary to the opacification of the intervening stroma Corneal sensation is variably affected

Atypical more severe and early-onset forms of granular corneal dystrophy have been reported, in which onset of visual loss occurs within the first to second decades of life and repeated corneal grafts are often necessary [3,5] These phenotypes have been linked to homozygous mutations in the dominant disease gene [3,6]

Granular corneal dystrophy arises as a result of mutations in the *TGFBI* (transforming growth factor β induced) gene on chromosome 5q31,[7] the protein product of which is known as keratoepithelin Keratoepithelin is expressed in the cor-

Author Affiliations Kallam Anji Reddy Molecular Genetics Laboratory (Dr Kannabiran and Mr Chakravarthi) and Ophthalmic Pathology Service (Dr Vemuganti), Professor Brien Holden Eye Research Centre, and Cornea and Anterior Segment Service (Drs Sridhar and Lakshmipathi), L V Prasad Eye Institute, Hyderabad, India

Financial Disclosure None

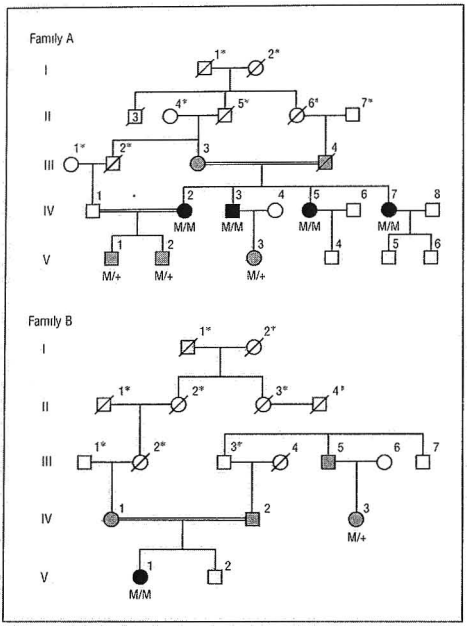

Figure 1. Pedigrees of the families studied Clear circles and squares indicate unaffected women and men respectively, dark symbols, severely affected shaded symbols, mildly affected, asterisk disease status unknown, double line, consanguineous spouses, M/M, homozygous mutant allele (Arg555Trp), and M/+, heterozygous mutant allele The number '3" in the first symbol in generation II designates 3 male siblings

nea and many other tissues, is up-regulated by transforming growth factor β, and is an extracellular matrix protein, possibly mediating cell-cell adhesion [8 10] Specific mutations in the *TGFBI* gene are responsible for different types of granular and lattice types of corneal dystrophies [7] These mutations lead to the formation of insoluble deposits within the cornea that are recognized by their characteristic histopathologic staining properties, which are distinctive for granular and lattice types of dystrophies In granular corneal dystrophy, the cornea shows hyaline deposits that are nonamyloid in nature and stain positively with Masson trichrome Ultrastructurally, the deposits appear as rhomboid-shaped crystals Three subtypes of granular corneal dystrophy are distinguished based on clinical and histopathologic features [11] Granular corneal dystrophy type I, originally described by Groenouw, is predominantly due to a mutation that results in an Arg555Trp substitution [12] We present herein the clinical and genetic analyses of individuals from 2 Indian families with multiple affected members having granular corneal dystrophy Consanguinity was present in both families There were 2 severities of manifestation in the families Individuals with the more severe phenotype were homozygous for the Arg555Trp mutation, while those with a milder phenotype resembling the "typical" form of granular corneal dystrophy were heterozygous for the Arg555Trp mutation

Molecular genetic analyses were performed in 7 individuals (patients IV 2, IV 3, IV 5, IV 7, V 1, V 2, and V 3) from family A and in 2 individuals (patients V 1 and IV 3) from family B (**Figure 1**) The study was approved by the institutional review board, and blood samples were collected from subjects after obtaining informed consent Genomic DNA was isolated from leukocytes by standard procedures [13] Exon 12 of the *IGFBI* gene was amplified from 50 ng of genomic DNA by polymerase chain reaction (PCR) using specific primers (thermal cycler P1C200, MJ Research, Inc, Watertown, Mass) Sequences of the primers were 5'TCAGCGTGGTGAGGTATTTAAGG 3' (forward) and 5'GGGCCCTGAGGGATCACTAC 3' (reverse)

Cycling conditions included an initial denaturation at 94°C for 1 minute, followed by 34 cycles of denaturation at 94°C fo 45 seconds, annealing at 58°C for 30 seconds, and extension at 72°C for 45 seconds The amplified products were purified on Amicon columns (Millipore, Billerica, Mass) and directly sequenced on the ABI310 genetic analyzer (Applied Biosystems, Foster City, Calif) using PCR primers Sequences wer compared with those of healthy control samples and with th genomic sequence of *TGFBI* (GenBank accession No AY149344 version AY149344 1)

The presence of the Arg555Trp mutation, located in exo 12, was tested by digestion with the enzyme *Bst*XI Polymerase chain-reaction products of exon 12 were digested with *Bst*XI, and the digested fragments were resolved on agarose gels DN from healthy individuals was not cut by the enzyme and showe a band corresponding to a fragment of 259 base pairs (bp), which was the full-length PCR product In addition to the 259-bp fragment, the presence of a heterozygous mutation yielded 2 fragments of 182 and 77 bp, while the homozygous mutation resulted in 2 fragments of 182 and 77 bp In addition, 100 healthy unrelated control subjects were screened for the sequence changes identified in patients by digestion with *Bst*XI

FAMILY A

Patient IV·2

A 40-year-old woman (the proband) was an offspring o a consanguineous marriage. She had had complaints o defective vision since childhood Her vision had worsened in the last 4 years She had recurrent episodes o watering and photophobia in both eyes On examination, she had a visual acuity of counting fingers in both the eyes Corneal examination revealed coarse reticulate subepithelial opacities in both eyes, with spheroidal degeneration involving the central cornea The opacities spared the limbus but were close to it (**Figure 2**A) Details of the anterior chamber and lens were not visualized She underwent phototherapeutic keratectomy in the right eye (Zyoptic; Bausch & Lomb, Rochester, NY) After the epithelial defect healed, she had a visual acuity of 20/125 OU and midstromal granular opacities and haze She underwent debridement of the lesions in the left eye

Patient IV.3

A 37-year-old man, the brother of the proband, had had white opacities in both eyes since childhood He com-

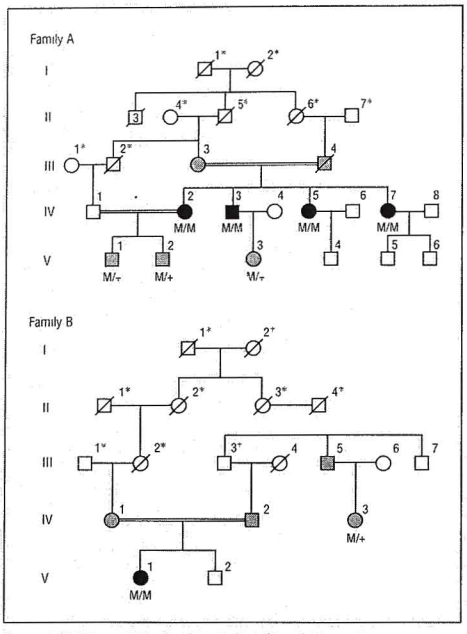

Figure 1. Pedigrees of the families studied Clear circles and squares indicate unaffected women and men, respectively dark symbols, severely affected, shaded symbols, mildly affected, asterisk, disease status unknown, double line, consanguineous spouses, M/M, homozygous mutant allele (Arg555Trp), and M/+, heterozygous mutant allele The number "3' in the first symbol in generation II designates 3 male siblings

nea and many other tissues, is up-regulated by transforming growth factor β, and is an extracellular matrix protein, possibly mediating cell-cell adhesion [8 10] Specific mutations in the *TGFBI* gene are responsible for different types of granular and lattice types of corneal dystrophies [7] These mutations lead to the formation of insoluble deposits within the cornea that are recognized by their characteristic histopathologic staining properties, which are distinctive for granular and lattice types of dystrophies In granular corneal dystrophy, the cornea shows hyaline deposits that are nonamyloid in nature and stain positively with Masson trichrome Ultrastructurally, the deposits appear as rhomboid-shaped crystals Three subtypes of granular corneal dystrophy are distinguished based on clinical and histopathologic features [11] Granular corneal dystrophy type I, originally described by Groenouw, is predominantly due to a mutation that results in an Arg555Trp substitution [12] We present herein the clinical and genetic analyses of individuals from 2 Indian families with multiple affected members having granular corneal dystrophy Consanguinity was present in both families There were 2 severities of manifestation in the families Individuals with the more severe phenotype were homozygous for the Arg555Trp mutation, while those with a milder phenotype resembling the "typical" form of granular corneal dystrophy were heterozygous for the Arg555Trp mutation

METHODS

Molecular genetic analyses were performed in 7 individuals (patients IV 2, IV 3, IV 5, IV 7, V 1, V 2, and V 3) from family A and in 2 individuals (patients V 1 and IV 3) from family B (**Figure 1**) The study was approved by the institutional review board, and blood samples were collected from subjects after obtaining informed consent Genomic DNA was isolated from leukocytes by standard procedures [13] Exon 12 of the *IGFBI* gene was amplified from 50 ng of genomic DNA by polymerase chain reaction (PCR) using specific primers (thermal cycler PTC200, MJ Research, Inc, Watertown, Mass) Sequences of the primers were 5'TCAGCGTGGTGAGGTATTTAAGG 3' (forward) and 5'GGGCCCTGAGGGATCACTAC 3' (reverse)

Cycling conditions included an initial denaturation at 94°C for 1 minute, followed by 34 cycles of denaturation at 94°C for 45 seconds, annealing at 58°C for 30 seconds, and extension at 72°C for 45 seconds The amplified products were purified on Amicon columns (Millipore, Billerica, Mass) and directly sequenced on the ABI310 genetic analyzer (Applied Biosystems, Foster City, Calif) using PCR primers Sequences were compared with those of healthy control samples and with the genomic sequence of *TGFBI* (GenBank accession No AY149344, version AY149344 1)

The presence of the Arg555Trp mutation, located in exon 12, was tested by digestion with the enzyme *Bst*XI Polymerase chain reaction products of exon 12 were digested with *Bst*XI, and the digested fragments were resolved on agarose gels DNA from healthy individuals was not cut by the enzyme and showed a band corresponding to a fragment of 259 base pairs (bp), which was the full-length PCR product In addition to the 259-bp fragment, the presence of a heterozygous mutation yielded 2 fragments of 182 and 77 bp, while the homozygous mutation resulted in 2 fragments of 182 and 77 bp In addition, 100 healthy unrelated control subjects were screened for the sequence changes identified in patients by digestion with *Bst*XI

REPORT OF CASES

FAMILY A

Patient IV:2

A 40-year-old woman (the proband) was an offspring of a consanguineous marriage She had had complaints of defective vision since childhood Her vision had worsened in the last 4 years She had recurrent episodes of watering and photophobia in both eyes On examination, she had a visual acuity of counting fingers in both the eyes Corneal examination revealed coarse reticulate subepithelial opacities in both eyes, with spheroidal degeneration involving the central cornea The opacities spared the limbus but were close to it (**Figure 2**A) Details of the anterior chamber and lens were not visualized She underwent phototherapeutic keratectomy in the right eye (Zyoptic, Bausch & Lomb, Rochester, NY) After the epithelial defect healed, she had a visual acuity of 20/125 OU and midstromal granular opacities and haze She underwent debridement of the lesions in the left eye

Patient IV:3

A 37-year-old man, the brother of the proband, had had white opacities in both eyes since childhood. He com-

plained that the opacities were gradually increasing He gave a history suggestive of having undergone lamellar corneal grafting in the left eye 17 years earlier On examination, he had a visual acuity of counting fingers at 1 m OD and at 2 m OS Corneal examination revealed coarse reticulate subepithelial opacities and some midstromal granular opacities He underwent superficial keratectomy in the left eye and debridement in the right eye The keratectomy specimen was submitted for histopathologic examination One week after surgery, his visual acuity was 20/80 OD and 20/40 OS, and there were midstromal granular opacities and scarring

Patient IV·5

Patient IV 5, a sister of the proband who was 31 years old, complained of having had white opacities in both eyes since she was 11 years old, which were progressively increasing, with occasional pain and watering She had a best-corrected visual acuity of 20/120 OU Corneal examination revealed coarse reticulate subepithelial lesions The cornea between the lesions showed deep stromal granular opacities She underwent superficial keratectomy in the right eye and debridement in the left eye The keratectomy specimen was submitted for histopathologic examination Following surgery, her visual acuity was 20/60 OD and 20/125 OS, and deep stromal opacities remained

Patient IV:7

Another sister of the proband (patient IV 7), age 25 years, had had diminution of vision in both eyes since childhood She had undergone surgery in the right eye 10 years previously On examination, her visual acuity was 20/100 OD and 20/125 OS, the right eye had a failed graft, with reticulate subepithelial opacities In the left eye, similar opacities were seen that were subepithelial and involving the anterior stroma These opacities spared the peripheral 1 mm of the limbus She underwent debridement of the lesions in the left eye Her visual acuity improved to 20/60 OS There was anterior stromal haze, with granular deposits in the stroma

Patients V.1, V.2, and V:3

A 21-year-old man (patient V 1) complained of occasional eye watering He had a visual acuity of 20/20 to 20/25 OU On examination, anterior to midstromal discrete granular opacities were seen (Figure 2B), with a clear limbus

An 18-year-old man (patient V 2) had a visual acuity of 20/20 OU Anterior to midstromal discrete opacities were seen (Figure 2C) The limbus was free of opacities

A 14-year-old girl (patient V 3) had a visual acuity of 20/20 OU, with anterior to midstromal opacities The limbus was clear

FAMILY B

Patient V:1

A 23-year-old woman, an offspring of a consanguineous marriage, had had complaints of diminution of vision in both eyes since she was 8 years of age She also had complaints of light sensitivity She gave a history of having undergone corneal grafting in both eyes about 10 years earlier Her medical history was unremarkable She had a visual acuity of counting fingers at 1 5 m OU, which could not be improved further Anterior segment evaluation in both eyes showed confluent subepithelial opacities involving the entire graft, extending into the posterior cornea (**Figure 3**A) She underwent penetrating keratoplasty in the right eye Five months after surgery, she had a visual acuity of 20/40 OD At her recent follow-up, the graft was clear, and she had an intraocular pressure of 14 mm Hg (Figure 3B) The corneal button was subjected to routine histopathologic evaluation

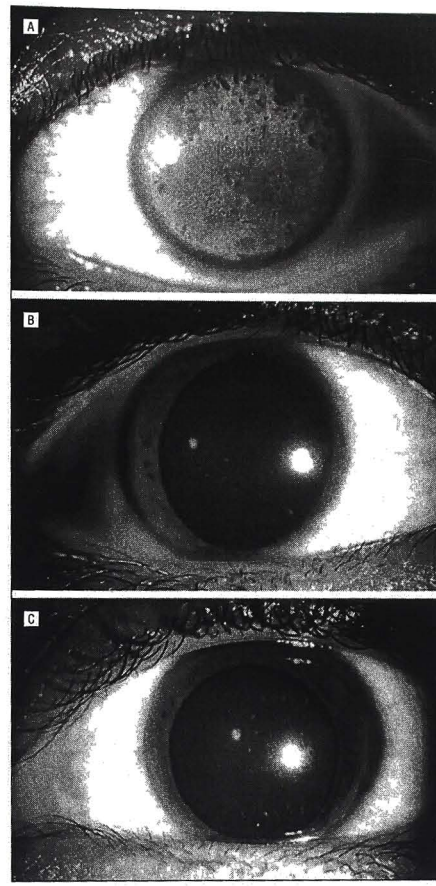

Figure 2. Diffuse slitlamp views from patients in family A A, Right eye of patient IV 2, age 40 years, showing dense subepithelial lesions B, Left eye of patient V 1 age 21 years, showing granular deposits C Left eye of patient V 2 age 18 years showing granular deposits

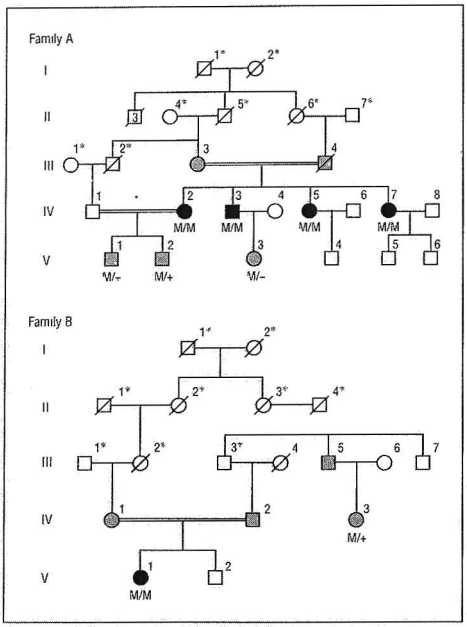

Figure 1 Pedigrees of the families studied Clear circles and squares indicate unaffected women and men respectively, dark symbols, severely affected shaded symbols, mildly affected, asterisk, disease status unknown, double line consanguineous spouses, M/M, homozygous mutant allele (Arg555Trp), and M/+, heterozygous mutant allele The number "3" in the first symbol in generation II designates 3 male siblings

nea and many other tissues, is up-regulated by transforming growth factor β, and is an extracellular matrix protein, possibly mediating cell-cell adhesion [8 10] Specific mutations in the *TGFBI* gene are responsible for different types of granular and lattice types of corneal dystrophies [7] These mutations lead to the formation of insoluble deposits within the cornea that are recognized by their characteristic histopathologic staining properties, which are distinctive for granular and lattice types of dystrophies In granular corneal dystrophy, the cornea shows hyaline deposits that are nonamyloid in nature and stain positively with Masson trichrome Ultrastructurally, the deposits appear as rhomboid-shaped crystals Three subtypes of granular corneal dystrophy are distinguished based on clinical and histopathologic features [11] Granular corneal dystrophy type I, originally described by Groenouw, is predominantly due to a mutation that results in an Arg555Trp substitution [12] We present herein the clinical and genetic analyses of individuals from 2 Indian families with multiple affected members having granular corneal dystrophy Consanguinity was present in both families There were 2 severities of manifestation in the families Individuals with the more severe phenotype were homozygous for the Arg555Trp mutation, while those with a milder phenotype resembling the "typical" form of granular corneal dystrophy were heterozygous for the Arg555Trp mutation

METHODS

Molecular genetic analyses were performed in 7 individuals (patients IV 2, IV 3, IV 5, IV 7, V 1, V 2, and V 3) from family A and in 2 individuals (patients V 1 and IV 3) from family B (**Figure 1**) The study was approved by the institutional review board, and blood samples were collected from subjects after obtaining informed consent Genomic DNA was isolated from leukocytes by standard procedures [13] Exon 12 of the *IGFBI* gene was amplified from 50 ng of genomic DNA by polymerase chain reaction (PCR) using specific primers (thermal cycler PTC200, MJ Research, Inc, Watertown, Mass) Sequences of the primers were 5′TCAGCGTGGTGAGGTATTTAAGG 3′ (forward) and 5′GGGCCCTGAGGGATCACTAC 3′ (reverse)

Cycling conditions included an initial denaturation at 94°C for 1 minute, followed by 34 cycles of denaturation at 94°C for 45 seconds, annealing at 58°C for 30 seconds, and extension at 72°C for 45 seconds The amplified products were purified on Amicon columns (Millipore, Billerica, Mass) and directly sequenced on the ABI310 genetic analyzer (Applied Biosystems, Foster City, Calif) using PCR primers Sequences were compared with those of healthy control samples and with the genomic sequence of *TGFBI* (GenBank accession No AY149344, version AY149344 1)

The presence of the Arg555Trp mutation, located in exon 12, was tested by digestion with the enzyme *Bst*XI Polymerase chain reaction products of exon 12 were digested with *Bst*XI, and the digested fragments were resolved on agarose gels DNA from healthy individuals was not cut by the enzyme and showed a band corresponding to a fragment of 259 base pairs (bp), which was the full-length PCR product In addition to the 259-bp fragment, the presence of a heterozygous mutation yielded 2 fragments of 182 and 77 bp, while the homozygous mutation resulted in 2 fragments of 182 and 77 bp In addition, 100 healthy unrelated control subjects were screened for the sequence changes identified in patients by digestion with *Bst*XI

REPORT OF CASES

FAMILY A

Patient IV·2

A 40-year-old woman (the proband) was an offspring of a consanguineous marriage. She had had complaints of defective vision since childhood Her vision had worsened in the last 4 years She had recurrent episodes of watering and photophobia in both eyes. On examination, she had a visual acuity of counting fingers in both the eyes Corneal examination revealed coarse reticulate subepithelial opacities in both eyes, with spheroidal degeneration involving the central cornea The opacities spared the limbus but were close to it (**Figure 2**A) Details of the anterior chamber and lens were not visualized She underwent phototherapeutic keratectomy in the right eye (Zyoptic, Bausch & Lomb, Rochester, NY) After the epithelial defect healed, she had a visual acuity of 20/125 OU and midstromal granular opacities and haze She underwent debridement of the lesions in the left eye

Patient IV:3

A 37-year-old man, the brother of the proband, had had white opacities in both eyes since childhood He com-

plained that the opacities were gradually increasing He gave a history suggestive of having undergone lamellar corneal grafting in the left eye 17 years earlier On examination, he had a visual acuity of counting fingers at 1 m OD and at 2 m OS Corneal examination revealed coarse reticulate subepithelial opacities and some midstromal granular opacities He underwent superficial keratectomy in the left eye and debridement in the right eye The keratectomy specimen was submitted for histopathologic examination One week after surgery, his visual acuity was 20/80 OD and 20/40 OS, and there were midstromal granular opacities and scarring

Patient IV.5

Patient IV 5, a sister of the proband who was 31 years old, complained of having had white opacities in both eyes since she was 11 years old, which were progressively increasing, with occasional pain and watering She had a best-corrected visual acuity of 20/120 OU Corneal examination revealed coarse reticulate subepithelial lesions The cornea between the lesions showed deep stromal granular opacities She underwent superficial keratectomy in the right eye and debridement in the left eye The keratectomy specimen was submitted for histopathologic examination Following surgery, her visual acuity was 20/60 OD and 20/125 OS, and deep stromal opacities remained

Patient IV.7

Another sister of the proband (patient IV·7), age 25 years, had had diminution of vision in both eyes since childhood She had undergone surgery in the right eye 10 years previously On examination, her visual acuity was 20/100 OD and 20/125 OS, the right eye had a failed graft, with reticulate subepithelial opacities In the left eye, similar opacities were seen that were subepithelial and involving the anterior stroma These opacities spared the peripheral 1 mm of the limbus She underwent debridement of the lesions in the left eye Her visual acuity improved to 20/60 OS There was anterior stromal haze, with granular deposits in the stroma

Patients V.1, V:2, and V.3

A 21-year-old man (patient V 1) complained of occasional eye watering He had a visual acuity of 20/20 to 20/25 OU On examination, anterior to midstromal discrete granular opacities were seen (Figure 2B), with a clear limbus

An 18-year-old man (patient V 2) had a visual acuity of 20/20 OU Anterior to midstromal discrete opacities were seen (Figure 2C) The limbus was free of opacities

A 14-year-old girl (patient V 3) had a visual acuity of 20/20 OU, with anterior to midstromal opacities The limbus was clear

FAMILY B

Patient V·1

A 23-year-old woman, an offspring of a consanguineous marriage, had had complaints of diminution of vision in both eyes since she was 8 years of age She also had complaints of light sensitivity She gave a history of having undergone corneal grafting in both eyes about 10 years earlier Her medical history was unremarkable She had a visual acuity of counting fingers at 1 5 m OU, which could not be improved further Anterior segment evaluation in both eyes showed confluent subepithelial opacities involving the entire graft, extending into the posterior cornea (**Figure 3**A) She underwent penetrating keratoplasty in the right eye Five months after surgery, she had a visual acuity of 20/40 OD At her recent follow-up, the graft was clear, and she had an intraocular pressure of 14 mm Hg (Figure 3B) The corneal button was subjected to routine histopathologic evaluation

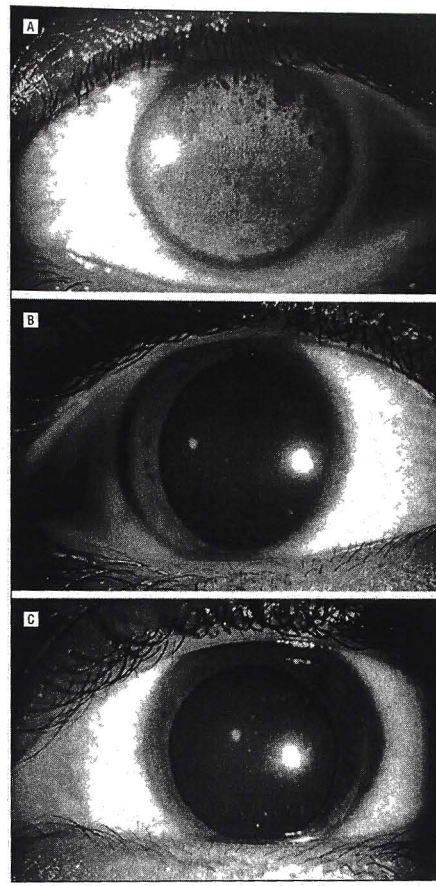

Figure 2 Diffuse slitlamp views from patients in family A A, Right eye of patient IV 2 age 40 years, showing dense subepithelial lesions B, Left eye of patient V 1, age 21 years showing granular deposits C, Left eye of patient V 2, age 18 years showing granular deposits

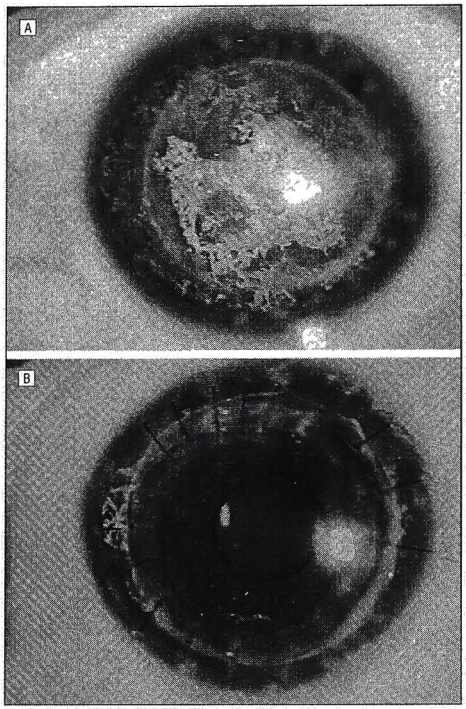

Figure 3. Diffuse slitlamp views from patient in family B. A, Right eye of patient V-1, age 23 years, showing granular opacities involving the graft. Note that the lesions are beyond the graft, reaching close to the limbus. B, Same eye following a repeated penetrating keratoplasty. Note the clear graft, with lesions beyond the graft.

Patient IV:3

A 41-year-old woman had had complaints of diminution of vision in both eyes since age 1½ years. Her visual acuity was 20/25 OU. Anterior segment evaluation revealed discrete opacities involving the anterior to midstroma in both eyes. The results of the rest of the ocular examination were normal.

RESULTS

Because the Arg555Trp mutation is a predominant cause of granular corneal dystrophy, we screened for the presence of this mutation in 9 members of the 2 families (Figure 1). All individuals were tested by digestion of the PCR-amplified product of exon 12 with *Bst*XI as described in the "Methods" section. A homozygous C→T transition (at residue 1710 of *TGFBI* complementary DNA) corresponding to the Arg555Trp mutation was found in patients IV-2, IV-3, IV-5, and IV-7 from family A and in patient V-1 from family B. This change was heterozygous in patients V-1, V-2, and V-3 from family A and in patient IV-3 from family B. To confirm that the observed patterns of *Bst*XI restriction digests corresponded to homozygous and heterozygous mutations, a representative sample of each these patterns was subjected to direct sequencing (data not shown).

The clinical features of all patients are summarized in the **Table**. Patients with the homozygous Arg555Trp mutation had early-onset disease that manifested during childhood, severe visual loss, and a dense reticulate pattern of opacities on slitlamp examination that was superficial (Figures 2A and 3A). In family A (Figure 1), this included 4 siblings, who were the offspring of first cousins. Two of these (patients IV-3 and IV-7), who had corneal grafts, had a rapid recurrence of disease, with opacities redeveloping within 2 and 10 years of surgery, respectively. Their mother was reportedly affected, although we did not examine her. No information is available about the father, who was deceased. The children of these homozygous individuals are obligate heterozygotes. Three of the offspring were studied, namely, patients V-1, V-2, and V-3. As shown in the Table, although they had discrete granular opacities on slitlamp examination, they were asymptomatic (the oldest patient examined in this generation was 21 years old) and had visual acuities of 20/20 OU. The opacities were located in the anterior and midstroma, in contrast to the predominantly subepithelial opacities seen in the homozygous parents. In family B (Figure 1), patient V-1 was homozygous, she was the offspring of a consanguineous marriage. Her parents were reportedly affected, although they were not examined at our institution. The features of her disease were similar to those of the homozygous members of family A (Table). Patient IV-3 (Figure 1, family B) displayed a milder phenotype that was consistent with the typical form of granular corneal dystrophy.

Histopathologic examination of the keratectomy specimens from patients IV-3 and IV-5 of family A showed similar features. The epithelium was made up of 2 to 5 layers of cells, with areas of attenuation and absent Bowman layers. There were eosinophilic, patchy to confluent, irregular deposits seen in the subepithelial regions, causing attenuation of the overlying epithelium (**Figure 4**A). The deposits appeared bright red with Masson trichrome staining (Figure 4B).

The keratoplasty specimen from patient V-1 (family B) showed an intact epithelium with patchy, irregular deposits that were abundant in the subepithelial stroma, with some deposits in the deep stroma. The deposits stained bright red with Masson trichrome, consistent with granular corneal dystrophy (Figure 4C).

COMMENT

Homozygosity for dominant disease genes is a rare occurrence, found in some communities where inbreeding is prevalent. Most dominant disease genes show partial dominance, resulting in an increased severity of disease manifestation in homozygotes, sometimes affecting other tissues or organs. There are few examples of true dominance, in which there are no differences in phenotype between homozygotes and heterozygotes for the disease gene. A prominent example of true dominance is Huntington disease.[14] A similar phenomenon has been observed in vitreous amyloidosis,[15] arising from a muta-

Table. Clinical Features and Mutation Status of Patients With Granular Corneal Dystrophy

Patient No.	Age at Onset	Nature of Opacity	Location of Lesions	Prior Surgery*	VA at Presentation	Surgical Procedure	VA After Surgery	Final Clinical Picture	Mutation Status
Family A									
IV:2	First to second decades	Coarse reticulate	Subepithelial	None	CF OU	PTK	20/125 OU	Central corneal haze	Homozygous
IV:3	First to second decades	Coarse reticulate	Subepithelial, anterior stroma	LK (left eye)	CF OU	Debridement (right eye), SK (left eye)	20/80 OD 20/40 OS	Corneal haze	Homozygous
IV:5	First to second decades	Coarse reticulate	Subepithelial, anterior stroma	None	20/120 OU	SK (right eye) debridement (left eye)	20/60 OD, 20/125 OS	Slight corneal haze, midstromal deposits	Homozygous
IV:7	First to second decades	Coarse reticulate	Subepithelial	PK (right eye)	20/100 OD, 20/125 OS	Debridement (left eye)	20/60 OS	Failed graft (right eye), corneal haze (left eye)	Homozygous
V:1	Asymptomatic at 21 y	Discrete granular	Anterior to midstroma	None	20/20-20/25 OU	None			Heterozygous
V:2	Asymptomatic at 18 y	Discrete granular	Anterior to midstroma	None	20/20 OU	None			Heterozygous
V:3	Asymptomatic at 14 y	Discrete granular	Anterior to midstroma	None	20/20 OU	None			Heterozygous
Family B									
V:1	First to second decades	Confluent	Subepithelial, anterior stroma	PK (both eyes)	CF OU	PK repeated (right eye)	20/40 OD	Clear graft	Homozygous
IV:3	40 y	Discrete granular	Anterior to midstroma	None	20/25 OU	None			Heterozygous

Abbreviations CF, counting fingers LK lamellar keratoplasty PK, penetrating keratoplasty PTK, phototherapeutic keratectomy, SK, superficial keratectomy, VA, visual acuity

*Before the patient was seen at our institution

tion in the transthyretin gene, and in retinitis pigmentosa, caused by a mutation in the rhodopsin gene [16] At the other extreme is an instance of a homozygous missense mutation in the myocilin gene in a family with primary open-angle glaucoma, which resulted in a normal phenotype, whereas heterozygotes for the same mutation were affected [17] The presence of a phenotype only in heterozygotes has been attributed to a dominant negative effect of the heterozygous mutant allele

We report herein for the first time, to our knowledge, the clinical, histopathologic, and genetic analyses of a severe form of granular corneal dystrophy in India Our data from 2 families support the view that there is a "dosage" effect of the mutant protein in homozygotes for the Arg555Trp mutation in keratoepithelin Compared with heterozygotes from the same family, individuals homozygous for the mutation displayed a severe phenotype Despite the ubiquitous expression pattern of the *TGFBI* gene, homozygotes had no obvious manifestations in other organs

Severe forms of granular corneal dystrophy have been documented in previous studies Before knowledge of the genetic defect underlying granular corneal dystrophy, the severe phenotype was proposed to be due to homozygosity, as suggested by pedigree data [3 5 18 19] Such a phenotype has subsequently been linked to homozygous mutations of *TGFBI*, including Arg555Trp[6] and Arg124His [20 21] The characteristics of the severe form of disease in all patients described in these earlier reports are early onset (in the first to second decades of life), rapid recurrence after surgery, and multiple surgical procedures [4 6] Notably, deposits are predominantly located in the superficial cornea, with most lesions at the level of Bowman layer,[4 6] leading to the term *superficial juvenile granular dystrophy* [4] These features are similar to those of the homozygous patients in our study (Table and Figure 4) The superficial confluent nature of the deposits may be suggestive of Reis-Bucklers corneal dystrophy,[4 22] but the clinical appearance of Reis-Bucklers corneal dystrophy, which consists of fine opacities that show a geographic pattern, is different from that of the patients in our study Another unusual feature that we observed was that lesions extended close to the limbus in the homozygous individuals (Figure 2A), compared with the typical form of granular corneal dystrophy

Superficial keratectomy, phototherapeutic keratectomy, and simple debridement are alternative modes of treatment of this condition In both families, the deposits recurred after penetrating keratoplasty and lamellar keratoplasty (Table) Sajjadi and Javadi[4] reported deeper recurrence after penetrating keratoplasty in patients with superficial juvenile granular corneal dystrophy

The increased dosage effect due to homozygosity for the mutant *TGFBI* allele may explain an increased severity of disease, yet it is not clear why the deposits showed an altered distribution Typical granular corneal dystrophy resulting from a heterozygous Arg555Trp mutation shows granular deposits primarily in the stroma Keratoepithelin is present mainly in the corneal epithelium and Bowman layer but is also seen in the stromal interlamellar regions and at the Descemet membrane [23 24] However, *TGFBI* messenger RNA is expressed primarily in the epithelium of the normal adult cornea, during corneal

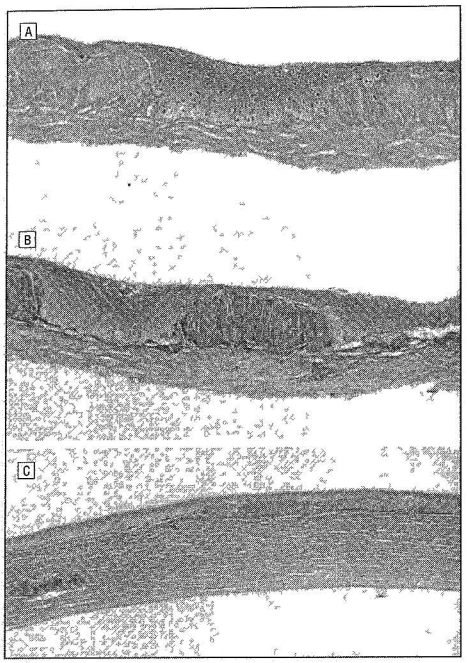

Figure 4. Patient IV 5 in family A (A and B) A, Corneal section from the keratectomy specimen shows reddish crystalline subepithelial deposits, causing attenuation of the overlying epithelium (hematoxylin-eosin, original magnification ×400) B, Deposits appeared bright red on staining with Masson trichrome (original magnification, ×400) C, Corneal button section from patient V 1 in family B shows confluent bright red deposits in the subepithelial stroma, with some deposits in the deep posterior stroma (Masson trichrome, original magnification ×100)

development and wound healing, it is expressed in all regions of the cornea [25] Mutant keratoepithelin is presumably a component of the corneal deposits found in granular and lattice dystrophies, as indicated by immunohistochemical studies [24,26] Although, to our knowledge, there have been no studies on the Arg555Trp-induced changes in the keratoepithelin protein, it can be speculated from investigation of the Arg124Leu mutation that the nonamyloid types of deposits do not result from abnormal proteolysis of keratoepithelin but may be associated with a change in protein stability[27] or abnormal interactions of keratoepithelin The predominantly epithelial location of deposits in homozygous individuals may suggest that the wild-type allele of *TGFBI* has a protective or alleviating effect and that its absence, as in the case of a homozygous Arg555Trp mutant, promotes the deposition of other proteins of epithelial origin along with mutant keratoepithelin

Whatever the exact pathogenesis of the homozygous form of granular corneal dystrophy, the resulting phenotype in terms of visual prognosis and pattern of corneal deposits appears distinctive in its severity, as observed in our patients and in previously described patients from different populations [4-6] We suggest that the severe phenotype of the disease described herein is distinguishable from the typical heterozygous form of granular corneal dystrophy The presence of these clinical features suggests possible underlying homozygosity, especially among patients from communities where inbreeding is prevalent Our data further establish that there is a consistent genotype-phenotype correlation among homozygous individuals with granular corneal dystrophy across different populations

Submitted for Publication: September 29, 2003, final revision received September 28, 2004, accepted September 30, 2004

Correspondence. Chitra Kannabiran, PhD, Kallam Anji Reddy Molecular Genetics Laboratory, Professor Brien Holden Eye Research Centre, L V Prasad Eye Institute, L V Prasad Marg, Banjara Hills, Hyderabad 500 034, India (chitra@lvpei org)

Funding/Support: This work was supported by the Hyderabad Eye Research Foundation, L V Prasad Eye Institute, and by a fellowship from the Council of Scientific & Industrial Research, New Delhi, India (Mr Chakravarthi), and by grant BT/PRPR3573/Med/12/157 from the Department of Biotechnology, Government of India (Dr Kannabiron).

REFERENCES

1 Mannis MJ, DeSousa LB Gross RH The stromal dystrophies In Krachmer JH Mannis MJ, Holland EJ eds *Cornea* Vol 2 St Louis Mo Mosby Publications, 1997 1043-1062
2 Weidle EG, Lisch W Various forms of opacities in granular corneal dystrophy *Klin Monatsbl Augenheilkd* 1984,185 167-173
3 Moller HU, Ridgway AE Granular corneal dystrophy Groenouw type I a report of a probable homozygous patient *Acta Ophthalmol (Copenh)* 1990,68 97-101
4 Sajjadi SH Javadi MA Superficial juvenile granular dystrophy *Ophthalmology* 1992 99 95-102
5 Diaper CJ Severe granular dystrophy a pedigree with presumed homozygotes *Eye* 1994,8(pt 4) 448-452
6 Okada M Yamamoto S, Watanabe H, et al Granular corneal dystrophy with homozygous mutations in the kerato-epithelin gene *Am J Ophthalmol* 1998, 126 169-176
7 Munier FL, Korvatska E, Djemai A, et al Kerato-epithelin mutations in four 5q31-linked corneal dystrophies *Nat Genet* 1997,15.247-251
8 Skonier J, Neubauer M, Madisen L, Bennett K, Plowman GD, Purchio AF cDNA cloning and sequence analysis of beta ig-h3, a novel gene induced in a human adenocarcinoma cell line after treatment with transforming growth factor-β *DNA Cell Biol* 1992 11 511-522
9 Skonier J, Bennett K, Rothwell V et al beta ig-h3 A transforming growth factor-β–responsive gene encoding a secreted protein that inhibits cell attachment in vitro and suppresses the growth of CHO cells in nude mice *DNA Cell Biol* 1994, 13:571-584
10 LeBaron RG Bezverkov KI Zimber MP, Pavelec R, Skonier J, Purchio AF βig-h3, A novel secretory protein inducible by transforming growth factor-β is present in normal skin and promotes the adhesion and spreading of dermal fibroblasts in vitro *J Invest Dermatol* 1995,104 844-849
11 Klintworth GK Advances in the molecular genetics of corneal dystrophies *Am J Ophthalmol* 1999,128 747-754
12 Munier FL, Frueh BE, Othenin-Girard P, et al *BIGH3* mutation spectrum in corneal dystrophies *Invest Ophthalmol Vis Sci* 2002,43 949-954
13 Sambrook J, Fritsch EF, Maniatis T *Molecular Cloning A Laboratory Manual* 2nd ed Vol 2 Cold Spring Harbor, NY Cold Spring Harbor Press 1989
14 Wexler NS, Young AB, Tanzi RE et al Homozygotes for Huntington s disease *Nature* 1987,326 194-197
15 Sandgren O, Holmgren G, Lundgren E Vitreous amyloidosis associated with homozygosity for the transthyretin methionine-30 gene *Arch Ophthalmol* 1990, 108 1584-1586
16 Reig CM, Trujillo JM, Martinez-Gimeno MM et al Homozygous and heterozygous Gly-188-Arg mutation of the rhodopsin gene in a family with autosomal dominant retinitis pigmentosa *Ophthalmic Genet* 2000,21 79-87

17 Morissette J Clepet C, Moisan S, et al Homozygotes carrying an autosomal dominant *TIGR* mutation do not manifest glaucoma *Nat Genet* 1998 19 319-321
18 Haddad R Font RL, Fine BS Unusual superficial variant of granular corneal dystrophy of the cornea *Am J Ophthalmol* 1977 83 213-218
19 Rodrigues MM, Gaster RN Pratt MV Unusual superficial confluent form of granular corneal dystrophy *Ophthalmology* 1983,90 1507-1511
20 Mashima Y, Konishi M, Nakamura Y, et al Severe form of juvenile corneal stromal dystrophy with homozygous R124H mutation in the keratoepithelin gene in five Japanese patients *Br J Ophthalmol* 1998,82 1280-1284
21 Fujiki K, Hotta Y, Nakayasu K, Kanai A Homozygotic patient with beta ig h3 gene mutation in granular dystrophy *Cornea* 1998,17 288-292
22 Mashima Y, Nakamura Y, Noda K, et al A novel mutation at codon 124 (R124L) in the *TGFBI* gene is associated with a superficial variant of granular corneal dystrophy *Arch Ophthalmol* 1999,117 90 93
23 Takacs L, Csutak A Balazs E, Berta A Immunohistochemical detection of βIG H3 in scarring human corneas *Graefes Arch Clin Exp Ophthalmol* 1999 237 529 534
24 Streeten BW Qi Y Klintworth GK Eagle RC Jr Strauss JA Bennett K Immunolocalization of βig-h3 protein in 5q31-linked corneal dystrophies and normal corneas *Arch Ophthalmol* 1999 117 67-75
25 Rawe IM, Zhan Q, Burrows R, Bennett K Cintron C Beta ig Molecular cloning and in situ hybridization in corneal tissues *Invest Ophthalmol Vis Sci* 1997 38 893-900
26 Korvatska E, Munier FL Chaubert P, et al On the role of kerato-epithelin in the pathogenesis of 5q31 linked corneal dystrophies *Invest Ophthalmol Vis Sci* 1999 40 2213-2219
27 Korvatska E Henry H Mashima Y et al Amyloid and non-amyloid forms of 5q31-linked corneal dystrophy from kerato epithelin mutations at Arg 124 are associated with abnormal turnover of protein *J Biol Chem* 2000 275 11465 11469

Archives Web Quiz Winner

April 2005 Web Quiz Winner

Congratulations to the winner of our April quiz, Steven M Friedlander, MD, FACS, Nevada Retina Associates, Reno, Nev The correct answer to our April challenge was central retinal vein occlusion due to an intraocular nematode For a complete discussion of this case, see the Photo Essays section in the May ARCHIVES (Greven CM Central retinal vein occlusion secondary to an intraocular nematode *Arch Ophthalmol* 2005,123 704)

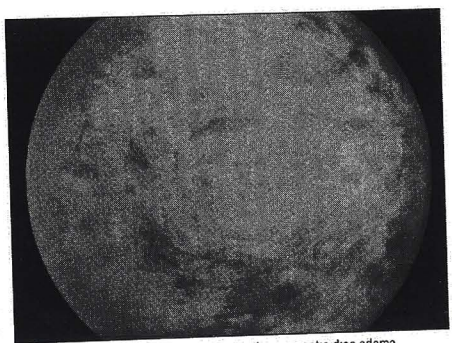

Figure 1. Right eye at initial examination showing optic disc edema hemorrhagic retinopathy, and distended veins

Be sure to visit the *Archives of Ophthalmology* Web site (http //www archophthalmol com) and try your hand at our Clinical Challenge Interactive Quiz We invite visitors to make a diagnosis based on selected information from a case report or other feature scheduled to be published in the following month's print edition of the ARCHIVES The first visitor to e-mail our Web editors with the correct answer will be recognized in the print journal and on our Web site and will also be able to choose one of the following books published by AMA Press *Clinical Eye Atlas, Clinical Retina*, or *Users' Guides to the Medical Literature*

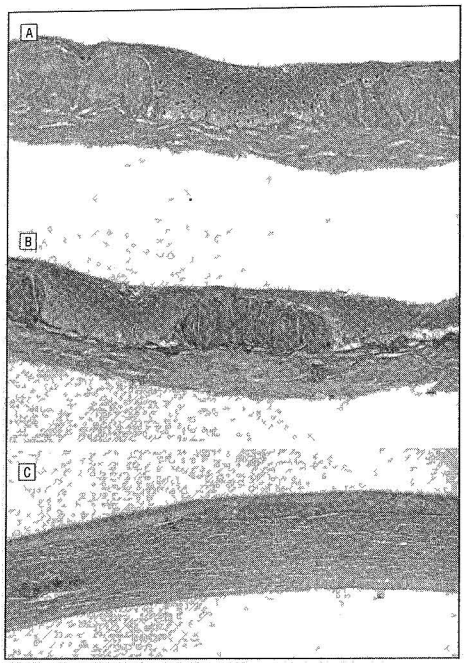

Figure 4. Patient IV 5 in family A (A and B) A Corneal section from the keratectomy specimen shows reddish crystalline subepithelial deposits causing attenuation of the overlying epithelium (hematoxylin eosin original magnification ×400) B, Deposits appeared bright red on staining with Masson trichrome (original magnification, ×400) C, Corneal button section from patient V 1 in family B shows confluent bright red deposits in the subepithelial stroma, with some deposits in the deep posterior stroma (Masson trichrome, original magnification ×100)

development and wound healing, it is expressed in all regions of the cornea [25] Mutant keratoepithelin is presumably a component of the corneal deposits found in granular and lattice dystrophies, as indicated by immunohistochemical studies [24 26] Although, to our knowledge, there have been no studies on the Arg555Trp-induced changes in the keratoepithelin protein, it can be speculated from investigation of the Arg124Leu mutation that the nonamyloid types of deposits do not result from abnormal proteolysis of keratoepithelin but may be associated with a change in protein stability[27] or abnormal interactions of keratoepithelin The predominantly epithelial location of deposits in homozygous individuals may suggest that the wild-type allele of *TGFBI* has a protective or alleviating effect and that its absence, as in the case of a homozygous Arg555Trp mutant, promotes the deposition of other proteins of epithelial origin along with mutant keratoepithelin

Whatever the exact pathogenesis of the homozygous form of granular corneal dystrophy, the resulting phenotype in terms of visual prognosis and pattern of corneal deposits appears distinctive in its severity, as observed in our patients and in previously described patients from different populations [4 6] We suggest that the severe phenotype of the disease described herein is distinguishable from the typical heterozygous form of granular corneal dystrophy The presence of these clinical features suggests possible underlying homozygosity, especially among patients from communities where inbreeding is prevalent Our data further establish that there is a consistent genotype-phenotype correlation among homozygous individuals with granular corneal dystrophy across different populations

Submitted for Publication. September 29, 2003, final revision received September 28, 2004, accepted September 30, 2004

Correspondence. Chitra Kannabiran, PhD, Kallam Anji Reddy Molecular Genetics Laboratory, Professor Brien Holden Eye Research Centre, L V Prasad Eye Institute, L V Prasad Marg, Banjara Hills, Hyderabad 500 034, India (chitra@lvpei org)

Funding/Support: This work was supported by the Hyderabad Eye Research Foundation, L V Prasad Eye Institute, and by a fellowship from the Council of Scientific & Industrial Research, New Delhi, India (Mr Chakravarthi), and by grant BT/PRPR3573/Med/12/157 from the Department of Biotechnology, Government of India (Dr Kannabiron)

REFERENCES

1 Mannis MJ DeSousa LB Gross RH The stromal dystrophies In Krachmer JH, Mannis MJ, Holland EJ eds *Cornea* Vol 2 St Louis Mo Mosby Publications 1997 1043-1062
2 Weidle EG, Lisch W Various forms of opacities in granular corneal dystrophy *Klin Monatsbl Augenheilkd* 1984,185 167-173
3 Moller HU, Ridgway AE Granular corneal dystrophy Groenouw type I a report of a probable homozygous patient *Acta Ophthalmol (Copenh)* 1990,68 97 101
4 Sajjadi SH, Javadi MA Superficial juvenile granular dystrophy *Ophthalmology* 1992,99 95-102
5 Diaper CJ Severe granular dystrophy a pedigree with presumed homozygotes *Eye* 1994 8(pt 4) 448-452
6 Okada M, Yamamoto S, Watanabe H, et al Granular corneal dystrophy with homozygous mutations in the kerato-epithelin gene *Am J Ophthalmol* 1998 126 169-176
7 Munier FL, Korvatska E Djemai A, et al Kerato-epithelin mutations in four 5q31-linked corneal dystrophies *Nat Genet* 1997,15 247-251
8 Skonier J, Neubauer M, Madisen L, Bennett K, Plowman GD, Purchio AF cDNA cloning and sequence analysis of beta ig-h3, a novel gene induced in a human adenocarcinoma cell line after treatment with transforming growth factor-β *DNA Cell Biol* 1992,11 511-522
9 Skonier J, Bennett K Rothwell V, et al beta ig-h3 A transforming growth factor-β–responsive gene encoding a secreted protein that inhibits cell attachment in vitro and suppresses the growth of CHO cells in nude mice *DNA Cell Biol* 1994 13 571-584
10 LeBaron RG Bezverkov KI, Zimber MP, Pavelec R, Skonier J Purchio AF βig-h3 A novel secretory protein inducible by transforming growth factor-β, is present in normal skin and promotes the adhesion and spreading of dermal fibroblasts in vitro *J Invest Dermatol* 1995,104 844-849
11 Klintworth GK Advances in the molecular genetics of corneal dystrophies *Am J Ophthalmol* 1999,128 747-754
12 Munier FL, Frueh BE, Othenin-Girard P, et al *BIGH3* mutation spectrum in corneal dystrophies *Invest Ophthalmol Vis Sci* 2002,43 949-954
13 Sambrook J, Fritsch EF, Maniatis T *Molecular Cloning A Laboratory Manual* 2nd ed Vol 2 Cold Spring Harbor, NY Cold Spring Harbor Press 1989
14 Wexler NS Young AB, Tanzi RE et al Homozygotes for Huntington s disease *Nature* 1987,326 194-197
15 Sandgren O, Holmgren G, Lundgren E Vitreous amyloidosis associated with homozygosity for the transthyretin methionine-30 gene *Arch Ophthalmol* 1990, 108 1584-1586
16 Reig CM, Trujillo JM, Martinez-Gimeno MM, et al Homozygous and heterozygous Gly-188-Arg mutation of the rhodopsin gene in a family with autosomal dominant retinitis pigmentosa *Ophthalmic Genet* 2000,21 79-87

17 Morissette J Clepet C, Moisan S, et al Homozygotes carrying an autosomal dominant *TIGR* mutation do not manifest glaucoma *Nat Genet* 1998 19 319 321
18 Haddad R Font RL, Fine BS Unusual superficial variant of granular corneal dystrophy of the cornea *Am J Ophthalmol* 1977 83 213-218
19 Rodrigues MM, Gaster RN Pratt MV Unusual superficial confluent form of granular corneal dystrophy *Ophthalmology* 1983,90 1507-1511
20 Mashima Y, Konishi M, Nakamura Y, et al Severe form of juvenile corneal stromal dystrophy with homozygous R124H mutation in the keratoepithelin gene in five Japanese patients *Br J Ophthalmol* 1998 82 1280-1284
21 Fujiki K, Hotta Y Nakayasu K, Kanai A Homozygotic patient with beta ig-h3 gene mutation in granular dystrophy *Cornea* 1998,17 288 292
22 Mashima Y, Nakamura Y, Noda K, et al A novel mutation at codon 124 (R124L) in the *TGFBI* gene is associated with a superficial variant of granular corneal dystrophy *Arch Ophthalmol* 1999,117 90-93
23 Takacs L Csutak A Balazs E Berta A Immunohistochemical detection of βIG-H3 in scarring human corneas *Graefes Arch Clin Exp Ophthalmol* 1999 237 529 534
24 Streeten BW Qi Y Klintworth GK Eagle RC Jr Strauss JA, Bennett K Immunolocalization of βig h3 protein in 5q31-linked corneal dystrophies and normal corneas *Arch Ophthalmol* 1999,117 67-75
25 Rawe IM, Zhan Q Burrows R, Bennett K Cintron C Beta ig Molecular cloning and in situ hybridization in corneal tissues *Invest Ophthalmol Vis Sci* 1997 38 893-900
26 Korvatska E Munier FL Chaubert P et al On the role of kerato epithelin in the pathogenesis of 5q31 linked corneal dystrophies *Invest Ophthalmol Vis Sci* 1999 40 2213 2219
27 Korvatska E Henry H Mashima Y et al Amyloid and non amyloid forms of 5q31-linked corneal dystrophy from kerato epithelin mutations at Arg-124 are associated with abnormal turnover of protein *J Biol Chem* 2000 275 11465 11469

ARCHIVES Web Quiz Winner

April 2005 Web Quiz Winner

Congratulations to the winner of our April quiz, Steven M Friedlander, MD, FACS, Nevada Retina Associates, Reno, Nev The correct answer to our April challenge was central retinal vein occlusion due to an intraocular nematode For a complete discussion of this case, see the Photo Essays section in the May ARCHIVES (Greven CM Central retinal vein occlusion secondary to an intraocular nematode *Arch Ophthalmol* 2005,123 704)

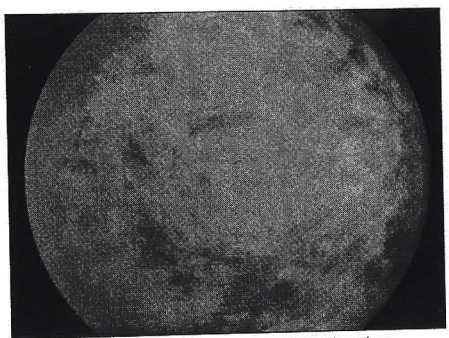

Figure 1. Right eye at initial examination showing optic disc edema hemorrhagic retinopathy, and distended veins

Be sure to visit the *Archives of Ophthalmology* Web site (http //www archophthalmol com) and try your hand at our Clinical Challenge Interactive Quiz We invite visitors to make a diagnosis based on selected information from a case report or other feature scheduled to be published in the following month's print edition of the ARCHIVES The first visitor to e-mail our Web editors with the correct answer will be recognized in the print journal and on our Web site and will also be able to choose one of the following books published by AMA Press *Clinical Eye Atlas, Clinical Retina*, or *Users' Guides to the Medical Literature*